Preliminary Reports, Memoranda and Technical Notes of the Materials Research Council Summer Conference

La Jolla, California

Volume II

July 1981

Sponsored by
Defense Advanced Research Projects Agency
ARPA Order No. 4000

Department of ~~Mechanical~~ Materials and Metallurgical Engineering

PRELIMINARY REPORTS, MEMORANDA AND TECHNICAL NOTES

of the

MATERIALS RESEARCH COUNCIL SUMMER CONFERENCE

La Jolla, California

July 1981

VOLUME II

DARPA Order Number: 4000
Program Code Number: P1D10
Contractor: The Regents of The University of Michigan
Effective Date of Contract: 10 June 81
Amount of Contract: $349,980
Contract Number: MDA903-80-C-0505
Principal Investigator: Professor Maurice J. Sinnott
Department of Chemical Engineering
The University of Michigan
Ann Arbor, Michigan 48109
(313)764-4314

The views and conclusions contained in this document are those of the authors and should not be interpreted as necessarily representing the official policies, either expressed or implied, of the Defense Advanced Research Projects Agency or the U.S. Government.

TABLE OF CONTENTS

Foreword

This collection of papers does not constitute a formal reporting of the activities of the DARPA Materials Research Council Summer Conference. Each report, memoranda or technical note is a draft of the author or authors and is their work alone. The Steering Committee, in conjunction with the authors, will decide how this material can best be presented as a formal report to DARPA.

Steering Committee

Professor Henry Ehrenreich
Secretary of the Steering Committee
Pierce Hall
Harvard University
Cambridge, MA 02138

Professor Robert L. Coble
Materials Science Department
Massachusetts Institute of Technology
Cambridge, MA 02139

Dean Daniel C. Drucker
College of Engineering
University of Illinois
Urbana, IL 61801

Professor Anthony G. Evans
University of California
Lawrence Berkeley Laboratories
1 Cyclotron Road
Berkeley, CA 94720

Professor Paul L. Richards
Department of Physics
University of California
Berkeley, CA 94720

Professor Amnon Yariv
Electrical Engineering Department
California Institute of Technology
Pasadena, CA 91125

Project Director

Professor Maurice J. Sinnott
Department of Chemical Engineering
The University of Michgigan
Ann Arbor, MI 48109

Members

Professor Nico Bloembergen
Div. of Eng. & Appl. Physics
231 Pierce Hall
Harvard University
Cambridge, MA 02138

Professor Bernard Budiansky
Division of Applied Sciences
Pierce Hall
Harvard University
Cambridge, MA 02139

Professor Roland M. Cannon
Materials Science Department
Room 13-4026
Massachusetts Institute of Technology
Cambridge, MA 02139

Professor Brice Carnahan
Department of Chemical Engineering
The University of Michigan
Ann Arbor, MI 48109

Professor Morris Cohen
Dept. of Mat. Sci. & Engineering
Room 13-5046
Massachusetts Institute of Technology
Cambridge, MA 02139

Professor Leslie E. Cross
Electrical Engineering
Pennsylvania State University
251A Materials Research Labs.
University Park, PA 16801

Professor Anthony H. Francis
Department of Chemistry
3028 Chemistry Building
University of Michigan
Ann Arbor, MI 48109

Dr. John J. Gilman
Manager, Corp. Res.
Standard Oil Company (Indiana)
AMOCO Research Center
P.O. Box 400
Naperville, IL 60540

Professor Robert Gomer
James Franck Institute
University of Chicago
Chicago, IL 60637

Professor Robert E. Green
Materials Science Engineering
Johns Hopkins University
Baltimore, MD 21218

Professor Alan J. Heeger
Department of Physics/El
University of Pennsylvania
Philadelphia, PA 19104

Professor John P. Hirth
Metallurgical Engineering Dept.
Ohio State University
Columbus, OH 43201

Professor Edward E. Hucke
Materials & Metallurgical Engineering Dept.
The University of Michigan
Ann Arbor, MI 48109

Professor John W. Hutchinson
Div. of Applied Sciences
316 Pierce Hall
Harvard University
Cambridge, MA 02138

Professor Gordon S. Kino
Ginzton Laboratory
Stanford University
Stanford, CA 94305

Professor Walter Kohn
Institute for Theoretical Physics
University of California
Santa Barbara, CA 93106

Professor James A. Krumhansl
Department of Physics
Clark Hall
Cornell University
Ithaca, NY 14850

John L. Margrave, Vice President
Rice University
316 Lovett Hall
Houston, TX 77001

Dr. Robert Mehrabian
National Bureau of Standards
Washington, DC 20234

Professor Frank A. McClintock
Dept. of Mechanical Engineering
Room 1-304
Massachusetts Institute of Technology
Cambridge, MA 02139

Professor Thomas C. McGill
M.S. 116-81
California Institute of Technology
Pasadena, CA 91125

Professor Elliott W. Montroll
Institute for Physical Science
and Technology
University of Maryland
College Park, MD 20740

Professor Howard Reiss
Department of Chemistry
University of California
Los Angeles, CA 90024

Professor James R. Rice
Division of Applied Science
Room 224, Pierce Hall
Harvard University
Cambridge, MA 02138

Professor Frans Spaepen
Division of Applied Science
207A Pierce Hall
Harvard University
Cambridge, MA 02138

Dr. C. Martin Stickley
BDM Corporation
7915 Jones Branch Drive
McLean, VA 22102

Dr. Robb M. Thomson
National Bureau of Standards
Center for Materials Science
Washington, DC 20234

Dr. George H. Vineyard
Brookhaven National Laboratory
Upton, Long Island, NY 11973

Professor J. C. Williams
Metallurgy & Materials Science
Carnegie-Mellon University
Pittsburgh, PA 15213

Professor Mark S. Wrighton
Department of Chemistry
Room 6-335
Massachusetts Institute of Technology
Cambridge, MA 02139

HIGH STRAIN-RATE POWDER TECHNOLOGY

A. G. Evans, R. M. Cannon and E. E. Hucke

INTRODUCTION

A meeting concerned with the processing of powder materials under high strain-rate conditions was held on July 9-10. The primary intent was to examine the potential of high strain-rate methods for fabricating materials with substantially improved mechanical performance. There has been substantial prior effort devoted toward understanding the behavior and fabrication of metals under shock loading, and the major focus here (with some exceptions) is on non-metallic materials. Three categories of material fabrication were explored in this context: shock activation of ceramic powders, shock consolidation of ceramic and metal/ceramic powders, combustion wave propagation in refractory metal, non-metal powder mixtures. No attempts were made to cover shock synthesis.

The meeting was devoted largely to a discussion of the phenomena accompanying the high rate, large amplitude deformation of powders. The intent was to establish scientific and technological goals pertinent to a program on high strain-rate methods for fabricating mechanically superior materials. Several presentations describing the status of the technology formed the basis of the discussion.

BACKGROUND

The first presentation consisted of a brief summary of a recent NMAB report by the Committee Chairman, V. Linse of Battelle. The committee described the high strain-rate area as one of opportunity for exploring the fabrication of materials with unique microstructures, including new ceramics and ceramic/metal systems. In particular, analysis of a substantial research and development effort in the U.S.S.R. during the last decade has suggested that some success has been realized in that country. A substantial U.S. effort on high strain-rate effects was recommended, with particular emphasis upon the development of a sound fundamental comprehension of the issues.

A series of presentations by researchers from Lawrence Livermore National Lab. described research advances and opportunities in the shock wave compaction and combustion wave synthesis of materials. M. Wilkins described the development of computer methods of analyzing both the propagation of shock waves in powder systems and the material consolidation near the shock front. Relatively simple constitutive relations have, thus far, been used to predict compaction. The motivation for the computer studies has been the prediction of the compaction pressure and of the geometric conditions needed to avoid rarefraction waves of large amplitude (which cause cracking). Numerical studies of material consolidation, involving more complex material models, could be instituted when a demand is perceived. It is not yet clear that adequate constitutive equations exist to justify a full numerical study.

W. Gourdin of LLNL described some experimental studies of shock wave compaction in ceramics. The experiments using a long rod configuration suggested that a narrow range of shock conditions exist which permit complete consolidation without cracking. More typically, a porous compact or a cracked fully dense body is produced. The consensus based on work at LLNL and elsewhere was that this range would be much wider for geometries, such as thin walled tubes or plates, in which the rarefaction waves are less damaging. Identification of optimum shock conditions could be aided by computer simulation with the appropriate equations of state. Most studies had been conducted on AlN, a material that exhibits more substantial "plasticity" than typical covalent solids. Examples of consolidated microstructures indicated small, (<1 μm), heavily dislocated grains embedded within amorphous zones containing small crystallites. The microstructures presented were quite different from those obtained with more conventional consolidation techniques. However, the influence of the unique microstructural characteristics (such as heavily dislocated grains) on the essential mechanical properties (hardness, toughness and fracture strength) have not yet been ascertained. The presence of the amorphous material indicated the development of surface melting during the shock treatment and/or the existence of appreciable impurities in the powder.

The work performed at Sandia on the shock treatment of non-metallic powders was reported by R. Graham. Compelling

evidence was presented that the passage of a shock wave through a powder compact (under conditions which did not induce consolidation) introduces a variety of point, line and area defects. These defects increase the catalytic activity of the material by two orders of magnitude. It has also been conjectured that the defects could be a cause of enhanced sinterability. Additionally, it was noted that shock waves can produce considerable comminution, particularly of coarse powders and very fine agglomerates. Transmission electron microscopy evidence of both dislocations and planar (stacking fault) defects in TiO_2 was consistent with the Livermore observations of shock induced defects in AlN. Considerable plastic deformation of the powder thus appears to be demonstrated. Evidence of point defect creation was associated with enhanced ESR activity and more tenuously with the observation of small, faceted voids in certain shocked TiO_2 grains. The origin of the ESR activity is uncertain but probably results from electronic defects rather than new vacancies or interstitials. The shock induced defects, coupled with the particle comminution and deagglomeration have been demonstrated in several instances (e.g., Al_2O_3) to enhance sinterability (vis-a-vis the initial, unshocked powder). However, shock enhancement of sinterability in powder with good intrinsic sintering characteristics has not yet been established.

The substantial experimental studies of shock compaction performed at Battelle were summarized by V. Linse. A considerable variety of materials has been compacted, including covalent

solids (SiC, Sialon, B_4C), ceramic/metal systems and unique ceramic/ceramic combinations. The ability to compact to near full density has been experimentally substantiated at Battelle for most material systems of interest. For many of these, the effects of subsequent hot isostatic pressing has also been explored. However, again, the mechanical performance of the compacted bodies has not yet been assessed. Evidence of particle fragmentation in the brittle covalent solids and of subsequent void formation (spherodization of the cracks) during hot isostatic pressing indicated that the conditions needed to achieve fully consolidated, mechanically sound covalent solids have not yet been identified. Similarly, the extent of the bonding at the ceramic and metal interfaces created by shock compaction (vital to the development of high toughness) is subject to uncertainty.

Holt of LLNL gave a background discussion of a group of rapid combustion processes known collectively in the U.S.S.R. literature as "self-propagating high temperature synthesis (SHS) or sometimes "gasless combustion". The combustion is carried out in a pre-compacted powder body utilizing the heat of reaction of at least one component of the body to sustain the reaction while forming at least one additional condensed phase. Reactant combinations are chosen so that intentional gas phase products of combustion are not formed. Reaction fronts progress at typical rates of several centimeters per sec, but are not in the range of rates involved with explosives.

During the past decade a relatively large scale research and development program involving at least 30 institutions and >130 professionals in the U.S.S.R. has produced >150 technical papers and technical press releases. In 1978 an SHS scientific council was created and plans innitiated to build a "large R & D facility." At the second "All Union Conference on Technological Combustion" about 40% of the program was concerned with SHS materials and theory. Notably missing from the literature are significant details on the properties of SHS bodies or applications (e.g., cutting) as would be expected if applications have materialized.

The Russian work is aimed at technological goals and the literature claims without detailed comparison the following advantages over conventional methods:

1) A wide variety (>200) of refractory compounds (carbides, nitrides, silicides, borides, etc) can be made, including some "new phases."
2) Overall cost advantages resulting from an energy saving, the elimination of "furnaces," and the relatively rapid reaction rate.
3) Product purity stemming from the high reaction temperatures.

The Russian literature hints at producing near net shapes of quality ceramics, but gives no specific examples. The major thrust appears at this time directed toward synthesis of materials for later comminution and consolidation by powder techniques.

Experimential results and modelling of seven "new" combustion processes have been presented. They are 1): Solid phase combustion 2) Fast combustion in the condensed phase, 3) Filtering combustion, 4) Combustion in liquid N_2, 5) Spinning combustion, 6) Self-oscillating combustion and, 7) Repeated combustion.

In view of the extensive Russian effort LLNL is carrying out an exploratory program to confirm some of the results and explore possible areas where SHS could be applied. Holt showed movies where a pressed compact of powdered T_i and carbon was ignited by a W filament on one end with subsequent rapid progogation of the combustion front along the sample. He obtained a result very much like that described in the Russian literature. Observation of a volume increase at the combustion front and liberation of large amounts of fumes indicated that the reaction was not gasless. The coherent bar that was produced showed substantial porosity in a very coarse grained TiC of unknown stoichiometry. Additional work planned at LLNL will center on TiC, TiB_2, and AlN.

SCIENTIFIC ISSUES

Shock Activated Sintering

Enhanced sinterability of ceramic powders "activated" by shock waves has been reported by a number of investigators, although the enhancement mechanisms have not been satisfactorily identified. It has been suggested that shock activation may permit the sintering of materials which cannot otherwise be

sintered without additives (or very high pressures): notably simple covalent compounds such as SiC and Si_3N_4. The comminution and defect creation associated with shock wave propagation through ceramic powders can undoubtedly contribute to improved sinterability. However, any advantages of shock activation must be assessed in terms of the properties and processing costs associated with the final sintered microstructure, relative to the best microstructures that can be generated by conventional sintering or hot pressing. Such comparisons must be a major objective of studies concerned with the merits of shock activation. In addition, in order to understand the applicability of shock activation to 'difficult to sinter' materials, it is necessary to better understand the underlying causes of the enhanced sinterability.

Several possible sources of enhanced sintering following shock wave treatment have been conjectured. Comminution can affect the sintering in several ways. Small initial particle sizes increase the initial sintering rate and encourage densification in the presence of environments that permit material transport by evaporation/condensation (e.g., SiC and Al_2O_3 in vacuum). However, small particles can also be obtained by chemical methods or other grinding methods in most instances. Small particle size generation is not, therefore, a unique feature of shock comminution. Shock comminution could also modify several powder characteristics that influence sintering, such as particle shapes, particle size distributions, reduced agglomeration, superior powder handling characteristics, and

resulting compact densities. However, it is important to correlate such effects with resultant microstructures and properties. For example, a higher compact density associated with the shock induced particle size distribution may enhance the initial sintering rate; but the benefit may be counteracted by a more rapid grain growth rate in the final stage since grain growth rates are directly related to the particle size distribution.

The defects introduced by shock can be conjectured to enhance sintering in several ways; none of which have yet been demonstrated. Large vacancy or interstitial concentrations could enhance the lattice diffusion rates at the expense of non-densifying matter transport processes (such as surface diffusion and evaporation/condensation). However, a vacancy volume (or equivalent interstitial content) equal to the initial void volume in the compact (~30-50%) would be required to permit the enhanced diffusivity to be retained throughout the sintering cycle. Such high defect densities are impossible. Additionally, point defect annihilation at the high density of dislocations also introduced during the shock process (in fact, the vacancies are probably created by non-conservative dislocation motion), would probably occur at temperatures below the sintering temperature. Further, it is highly unlikely that this point defect annihilation would occur in the biased manner required for appreciable densification.

The high density of dislocations is a more likely source of enhanced sinterability. The dislocations could be of

sufficient density that pipe diffusion may become a significant material transport process, thereby circumventing the deleterious effects of surface diffusion or evaporation/condensation. Additionally, the climb and glide of the dislocations, subject to the stresses induced around the interparticle necks, could be a source of strain that benefits the densification process. It is plausible that enough dislocations are generated during the shock loading (i.e., $>10^{11}$ cm^{-2}) that the strain from their annihilation could contribute to densification, if properly biased. However, enhanced densification in the time-temperature range at which the strain relaxation occurs has not yet been examined. A theoretical study of these dislocation effects could be readily instituted should superior sintered bodies created by shock activation be demonstrated.

Finally, it can be argued that shock compaction may lead to "activated" surfaces which enhance sinterability. Such surfaces could include high concentrations of steps, kinks, point defects, and emerging dislocations and a low frequency of inherently low energy surface orientations. Although such features may stimulate catalytic activity, most (except perhaps orientation effects) would anneal out before significant sintering commences.

Of the variously proposed mechanisms of enhancing sinterability, size reduction and effects on size distributions are the most likely to be important. It is unclear that shock can sufficiently comminute particles that the small sizes

achieved by other methods could be duplicated (e.g., 10 nm achieved by gas or liquid phase precipitation, or 0.1 μm by attrition milling). However, such particles could offer the advantage of a low degree of agglomeration and much less contamination. Impurities from milling media or surface active reactants from precipitation are examples of chemical problems with the competing methods of fine powder preparation. The high dislocation densities may also be important in some cases.

There is presently no evidence that the benefits of shock activation could sufficiently increase the densification rate of covalent materials that the sintering problems associated with such materials could be circumvented. The poor sinterability of covalent materials is thought to be primarily a result of rapid coarsening, because of a combination of relatively rapid surface diffusion and vapor transport (aggrevated by low driving forces, i.e., high ratios of γ_b/γ_s). A careful study, over a range of starting particle sizes may be required to determine the existence of significant benefits.

Finally, it is suggested that shock activation may be most conveniently performed by partial compaction of a powder (i.e. to ~80% density) followed by sintering. This approach would be of most benefit with materials that are subject to neck growth by surface diffusion or evaporation/condensation at low and intermediate temperatures (e.g. Al_2O_3 and SiC), because partial consolidation could permit a fine scale microstructure to be retained into the final stages of sintering. An enhanced

potential for creating fully dense, fine scale microstructures could then ensue.

Shock Wave Consolidation

Shock consolidation would appear to be experimentally demonstrated for pure metals (e.g., Cu, W), oxides (e.g., Al_2O_3, UO_2, BeO), and hard covalents (e.g., BN or C in the cubic or wurtzitic form) and the macroscopic cracking eliminated, for some geometric arrangements. Significant local densification, but with some macroscopic cracking has been achieved for a larger number of materials. Thus, it appears that virtually any metallic or ceramic material could be consolidated, without macroscopic cracking, if sufficient engineering effort were devoted to the problem. However, some caution is warranted for the hard, brittle ceramics, because many of the densification claims have not been duplicated and the materials have not been thoroughly characterized. In general the pressure needed to achieve consolidation increases with the compressive yield stress (or hardness) of the material and there is often only a narrow range of pressures at which consolidation without cracking can be obtained.

The microstructures which result from shock compaction can be quite variable. Fully dense, but mechanically weak, Cu has been obtained. Grain refinement after shock compaction and hot isostatic pressing has been observed in UO_2 and BeO (presumably indicating recrystallization). Extremely high dislocation densities (perhaps approaching $10^{12}/cm^2$) have been identified in

in Al_2O_3 powder and in AlN. Local melting has occurred in both metals (Al) and refractory covalent ceramics (AlN). Evidently, there can be appreciable local heating as a result of the compaction of porous materials, and the varied microstructures in AlN suggest that significant temperature gradients may exist.

The optimistic view would be that, with sufficient work, most materials could be densified with shock compaction and that a range of microstructures could be obtained. It remains, therefore, to study the material combinations and the shock conditions what might permit the creation of mechanically superior materials. Since it appears to be relatively straightforward to produce crack free regions of shock induced, fully dense materials (especially by employing hollow, cylindrical compaction geometries), the mechanical properties of these dense regions could be evaluated using small scale mechanical tests (i.e., overload indentation tests to establish the flow stress and fracture toughness, and small discs to determine the biaxial failure strength). The material systems which exhibit potential mechanical superiority could then be ascertained in a relatively straightforward manner. Such measurements would provide direction for futher exploration of high toughness/hardness systems.

Shock compaction may offer singular advantages in several situations, such as the fabrication of materials which are unsinterable without additives, materials which are unstable except at high pressure, two phase materials which are otherwise reactive. It is often unclear whether shock compaction offers

obvious advantages over high pressure static techniques in which temperature and pressure can be independently controlled. Three advantages which may be suggested are: larger samples with higher attainable pressures, much shorter times at temperature, and significantly more local shear strain.

In addition, shock compaction, in combination with subsequent thermal or thermo-mechanical treatments, offers opportunities to achieve exceptional microstructures and properties, but may also have exceptional problems. For example, very high dislocation densities and/or fine grain sizes can be obtained in ceramics. Hence, if flaw free samples can be produced, a superior hardness, strength, and perhaps even K_{IC} for the softer ceramics (e.g., halides, MgO, UO_2, and perhaps AlN) may be achieved. Analogous benefits remain to be demonstrated for the hard ceramics such as Al_2O_3 or SiC. The low forming times or temperatures offers the opportunity to densify multiphase materials without the detrimental effects of significant coarsening (as could be useful for RSR materials), the reactivity of incompatible phases or crystallization of amorphous materials. Also contamination is minimized because there is no interaction with a hot furnace. However, some detriment may derive from the essential exclusion of impurity volatilization.

The properties of ceramics formed by high pressure, static techniques suggest problems which have not yet been adequately addressed for shock compaction. In several studies with static high pressure and lower temperature densification, rela-

tively "poor bonding" has been reported, as manifested by low strength or hardness. Undoubtedly some problems result from impurities or adsorbed gases at the powder surfaces, which may result in bloating and further property degradation after annealing. There may also be very high internal stresses, which can be detrimental. The high local shear strains which occur in shock compaction may alleviate some of these impurity problems, but it remains to be demonstrated. Significant attention must be given to outgassing powders prior to compaction; this may dictate a preference for coarser powder than would be preferred for low pressure sintering. The experimental exploration of dense, shock compacted regions should ideally be conducted in conjunction with numerical modelling of the shock consolidation process. The modelling of compaction requires an adequate pressure, volume relation as a function of the compact density, powder morphology, and powder properties. Some pertinent information already exists but additional information is required. A function describing the rate of densification (material viscosity) in terms of the shock pressure and duration, the induced temperature and the resultant shear strain is also required (see paper by G. Vineyard) in order to predict optimum consolidation conditions. Some general, simple viscosity descriptions may be suitable, and should be used (as already proposed) for preliminary comparison with experimental results. However, the material subtleties associated with the sintering mechanism, surface melting, etc., may be needed to achieve adequate

predictions of the optimum conditions for shock consolidation to full density without cracking. Further, more accurate descriptions of the temperature history will be required to understand microstructure and property development, than those required to describe shock wave development and gross compaction. Basic studies of consolidation and recovery mechanisms in ceramic powders, subject to shock, can then be initiated if the potential for superior materials can be convincingly demonstrated.

Self-Propagating High Temperature Synthesis

The magnitude and direction of the Russian program in SHS for producing specialty materials raises some interesting technical questions. In drawing comparisons to efforts in the West it should be noted that many closely related technical developments of in situ reactions are not recognized under the name SHS. Two basically different goals should be distinguished. First are the processes which aimed at production of near net shapes of compounds or cermets with controlled microstructure so as to be directly useful for their mechanical, electrical, or other properties with little or no further processing. In the second case an exotheric reaction is performed with the aim of producing a compound which is then further processed, usually by comminution and subsequent traditional powder techniques for reconsolidation. The efforts in the U.S. have been largely aimed at the first catagory. While the U.S.S.R. literature states an interest in making near net shapes the current results center on the second catagory.

In situ reactions may be classed as those where 1) at least one reactant is supplied by infiltration from the outside of a controlled porosity reactable body and 2) all reactants are initially contained within the body. In the first case several commercial products are available in the U.S. and play an important part in plans for high temperature structural materials in several DoD programs. Interest has centered on "reaction bonded" Si_3N_4 and SiC where the maturity of the process development is such that these materials are now serious contenders with the less shapeable, more expensive, hot pressed materials. A current DARPA program is underway to produce (near net shapes) of in situ reacted SiC with properties superior to those obtained in other ways. Steady improvement in properties has been possible through careful control of the reaction step, generally by slowing down the reaction to gain control over the heat liberation to minimize cracking, grain growth, porosity, and incomplete reaction. This direction seems to be exactly opposite to the Russian approach which strives for very rapid reaction, but with no evidence of microstructural control. It is noteworthy that the U.S.S.R. SHS effort has practically no attention focused on Si_3N_4 and SiC even though a very large number of other nitrides, carbides, silicides, etc., are mentioned.

The second catagory mentioned above is generally known as "reaction sintering" or "phase exchange" reaction. In both cases significant, but small scale development efforts on near net shapes of carbides, silicides, borides, and oxides have pro-

gressed over the past 25 years. In addition other "thermit" reactions have gained some use for welding and more specialized DoD use. In the case of reaction sintering a pressed porous body containing the solid reactables is reacted relatively slowly throughout the body usually with the production a liquid to aid the overall subsequent sintering of the new phase formed. Significant shrinkage (>40 vol%) from pore closure and reaction must occur in order to yield a solid cermet. If no auxillary liquid is formed full density is usually not obtainable. The U.S.S.R. process normally propagates the reaction as a plane front which appears to offer no special advantages and, on the other hand, creates special problems. A large reaction volume decrease must be accomodated over a very short distance (width of the reaction front) where, in addition, there is a very steep temperature gradient causing severe thermal strains in both the product and reactant regions.

In the U.S. a phase exchange reaction system for producing large near net shapes of various TiC based cermets has been demonstrated, but not commercialized. In this process 'cast-to-shape' porous carbon bodies are infiltered with various relatively low melting Ti alloys (Ni, Mo, Co, Cr) with minimal reaction. This pore free body may be further shaped by machining if desired. A controlled exothermic reaction is then initiated throughout the body converting the continuous carbon skeleton into a cemented carbide. The volume decrease is uniform and limited to that of the reaction since no pore need be closed.

Shaped bodies with controlled microstructures in Ni-Mo bonded TiC cermets over 2 inches in section have been produced. This process eliminates the need for presses, dies, powder making and handling and is capable of utilizing remelt of Ti mill scrap.

Is there a fundamental advantage to be gained by propagating an exothermic reaction in a plane front at a very rapid rate? At least for the case where a controlled microstructure-near-net shape is desired the answer appears to be negative. The very high temperature (1500-3000°C) of the narrow reaction front causes:

1) Gas liberation from vaporization of the reactants and products as well as from side reactions from impurities associated with the reactant powders (e.g., oxygen on carbon) which gives porosity and poor control over stoichiometry. Reactions that are in principle "gasless" actually are not.
2) Volume decrease due to the reactions (5-50 vol%) closure of the porosity of the original compact, and (30-50%) thermal strains that must be accommodated rapidly over very short distances (<1mm). Cracking, residual stress, and residual porosity are intensified.
3) Structural coarsening (especially in the presence of liquid) from the high uncontrolled temperature gives generally undesirable properties. Superior properties require grain size (~1-5 μm) which is generally finer than the original reactant powders. High temperature in

carbides leads to rapid grain coarsening (100-1000 μm).

4) Inherent size and shape sensitivity. The reactions are not really adiabatic and therefore the surface to volume controls heat transfer which effects the reaction rate. Regular reaction fronts can only be propagated in simple shapes, rods, tubes, plates, etc.

In the case where intermediate product is the goal rapid propagation may have some merit but must be compared to other material synthesis schemes. SHS is fundamentally a batch process. It requires producing fine element powders of controlled size and purity as well as tools and expense of preparing a controlled porosity body. The reaction atmosphere must be controlled, an ignition device must be provided and, in large scale, cooling is needed for the reaction vessel. In large scale a potential explosion hazzard exists in handling the fine reactant powders. While very high synthesis temperature can result in "better" purity, especially with respect to oxygen in carbides, it also yields a problem in stoichiometry control. The sample comparisons cited for purity improvement were in general made against inferior materials, e.g., $MoSi_2$ with >2% impurities. The SHS product is coherent enough to be difficult to reduce to powder, even though it is not of superior mechanical strength due to large grain size and porosity. Comminution contamination is therefore expected.

The energy saving claimed for SHS appears to be totally spurious. Using the combustion of high purity reactive metal

powders as a source of heat is certainly not energy prudent! For example to produce the Ti, conversion of the oxide to the chloride and reduction with another active metal (Mg or Na) is required. The Mg or Na requires substantial energy to produce and the whole process requires several high temperature furnace operations. This is to be compared with the direct reduction from the oxide with carbon or hydrocarbons or the continous reduction of $TiCl_4$ gas with hydrocarbons. In both cases large continous production of high purity, fine powder has been achieved and awaits a mass market. Processes of low temperature co-precipitation or continous gas phase reactions are available for direct powder production in many other materials. The claim that SHS requires less equipment is also questionable. Furnace pretreatments for the reactant powders, pressing equipment for the compacts, controlled atmosphere reaction vessels (with cooling), and comminution equipment are required to produce the powder.

The claim that many compounds can be made is certainly true, but thusfar no compound has been mentioned that has not been produced in other ways.

Finally it should be noted that a large part of the U.S.S.R. literature on SHS relates to modelling of the various versions of the process. This effort has been extensive and has progressed from very crude models to more complicated versions as the additional effects have been observed in the experimental program. Somewhat similar modelling exists in the U.S. litera-

ture but is generally found in the chemical engineering literature vs. the materials literature.

High Toughness, Hardness Materials

Materials with a combination of high toughness and hardness can be generated with two principal microstructural forms: a dispersed ceramic/ceramic system in which the dispersed phase undergoes a strain induced martensite transformation, and a metal/ceramic (cermet) combination in which the minor metallic phase is continuous. The former has been amply illustrated by incorporating fine ZrO_2 dispersoids in several chemically compatible matrices (i.e., Al_2O_2, ThO_2, mullite, spinel). Combinations of H ~16 GPa, K_{Ic} ~12MPa/m have already been demonstrated in Al_2O_3/ZrO_2. Shock wave consolidation offers the additional potential of incorporating ZrO_2 and other materials capable of a stress induced martensite transformation, (e.g., HfO_2 and, perhaps BN) into chemically unfavorable matrices, such as Si_3N_4 and SiC. Then the coupled advantages of a low average thermal expansion coefficient, high fracture toughness and high hardness may be realized. However, it should be appreciated that the residual tensile strain associated with thermal expansion mismatch between ZrO_2 and low expansion matrices may reduce the toughening increment that can be achieved by the crack tip transformation process.

Cermets of high toughness and high hardness have only been successfully achieved, with convential technology, by liquid phase sintering techniques. The best example is WC/Co,

which exhibits the properties, H ~2016 GPa, K_{IC} ~162MPa/m. The superior mechanical properties of this system can be attributed to three effects: a continuous metal infrastructure, (which requires the crack to deform metal ligaments to failure), good bonding between the ceramic and metal constituents and a high yield strength in the metal phase (associated with appreciable solubility of the ceramic phase in the metal). These effects are in part a direct consequence of the system properties needed for liquid phase sintering: essentially complete wetting of the constituents (i.e. a continuous metal film) and solubility of the ceramic in the metal (in order to achieve continuous mass transport during sintering). These liquid phase sintering pre-requisites have greatly restricted the range of metal/ceramic combinations that can be (conventionally) fabricated to full density. This range could be considerably expanded by shock compaction. However, it is emphasized that it is not sufficient to compact the metal/ceramic combinations. Good bonding is essential to high toughness; as exemplified by an estimate of toughness in the absence of bonding (D. C. Drucker), which predicts $K_{IC} \leq$ 1MPa/m - an order of magnitude smaller than that required of superior systems. Considerations pertinent to good bonding (e.g. some solid solubility, and a temperature large enough to induce limited interdiffusion) are thus of prime importance to studies concerned with the fabrication of mechanically superior cermets.

Based on the above criteria, WC-Co may exhibit the optimum mechanical properties expected from a cermet (unless C-BN or diamond were used). However, other hard ceramics (having high intrinsic E, H, and K_c) may permit the creation of cermets with lower chemical reactivity, etc. The most attractive oxide would appear to be Al_2O_3 (unless Al_2O_3 + ZrO_2 or t-ZrO_2 could be used to take advantage of transformation toughening). Good bonding could be anticipated with Al alloys and with NiTi, which is much stronger and quite corrosion resistant.

RESEARCH PRIORITIES

A brief summary of some research topics and priorities is presented in this section, including a list of material considered most suitable for imminent study.

Shock Activated Sintering

a. The existence of shock activated sintering should be subject to critical experimental evaluation to distinguish between comminution and other shock effects. This could be achieved by thorough characteriztion of a shock treated powder, and comparison of the sintering performance with that of a good sinterable powder of the same material, prepared by chemical means, with similar particle size distribution. This study should be conducted with powders of high purity and on a material with well-established sintering performance. Two good candidates are Al_2O_3 and SiC. These provide a basis for useful comparisons since the sintering of Al_2O_3 is better characterized

and understood than most ceramics, and SiC is unsinterable in pure form and several types of powders are available.

b. Should the existence of shock activated sintering be established, the microstructures of the final products and their mechanical characteristics should be subject to experimental determination. Some of the techniques are described in a following section.

c. The identification of superior microstructures created by shock activation could merit a comprehensive study of the specific mechanisms of activation, outlined in a previous section, and the limits of their applicability.

Shock Wave Consolidation

a. Since shock wave consolidation of many materials has already been established, exploration of the fabrication and properties of a range of materials (cermets, ceramic composites, etc.) seems warranted. Post-shock thermo-mechanical treatments should also be explored. For this purpose, small specimen tests on fully dense regions of (otherwise cracked) compacted materials would be adequate. For single phase ceramics, emphasis should be on identifying and understanding the origin of useful or unique properties. For cermets or composites a more exploratory effort would be appropriate.

b. The development of computer models of increasing complexity should proceed in conjunction with the experimental studies. Evidently, sophisticated materials models are only of merit if superior materials are identified from the experimental studies.

c. Should superior properties be achievable in small specimens, it would be appropriate to study and understand the densification and recovery processes and role of the initial compact conditions. Such information would facilitate subsequent application of shock compaction to other materials.

Characterization Studies

Microscopic characterization of powders and densified materials is essential. Transmission electron microscopy appears to be the most versatile method for characterizing both the powder and the consolidated bodies. High-voltage microscopy would be most appropriate for the powder; whereas the use of analytic microscopy would be most suitable for microstructure characterization (grain structure, phase composition and distribution, etc.) Adequate bulk chemical analysis, with attention to anion as well as cation impurities will also be important.

For shock activated powders it will also be necessary to use other techniques to adequately characterize particle sizes and distributions, degree of agglomeration, and surface area. For both powders and densified materials it would be of interest to use a variety of spectroscopic techniques to further characterize defects; however, such studies may be more important for understanding resultant properties (e.g., catalytic activity) than for understanding densification.

SHS

In view of the maturity (>10 years) of the materials preparation by SHS it is recommended that a literature search be

conducted in the areas of user applications to gain specific information about relative properties and performance of these materials compared to conventional materials. This search may be more difficult to conduct, but if truely superior cutting tools have been made by SHS the results should be found in the metal cutting literature.

The current LLNL program should at an early date confirm on small pore free regions (with techniques previously discussed) the mechanical properties obtainable in TiC, TiB_2, and AlN. Stoichiometry and oxide purity levels should also be established.

Long range efforts with in situ reactions should concentrate on near net shape controlled microstructure articles. Such efforts will likely employ slower, more controlled reaction conditions, and should be aimed at reducing the sizes of flaws which tend to be performance limiting in ceramics and cermets.

HIGH STRAIN RATE TECHNOLOGY

PROGRAM

July 9, 10, 1981

12:00 - 4:00 p.m. July 9

1. Introduction (Hucke, Evans, Coble)
2. Summary of NMAB report, V. Linse (Battelle)
3. Summary of Livermore Results, W. Gourdin (C. Cline, M. Wilkens, B. Holt)
4. Summary of Sandia Work, R. Graham
5. Summary of Battelle Work, V. Linse

8:00 - 12:00 July 10

Discussion of Fundamental Research Opportunities

1. Consolidation Models (high stress, high rate phenomena) -Johnson
2. Powders (shock activation, morphology, surface effects) -Cannon
3. Characterization (TEM, point defects) -Heuer
4. Toughness/Hardness -Evans

1:00 - 4:00 July 10

General Discussion -Hucke, Evans, Coble

HIGH STRAIN RATE POWDER TECHNOLOGY

OBJECTIVES

Reduce fabrication costs, produce new materials or materials with substantially improved performance by:

1. Use of rapid impulsive loading to consolidate powder materials into components with near net shape, and

2. Use of high pressure shock-wave loading to enhance the solid state reactivity of powder materials for subsequent processing.

GENERAL APPROACH

1. Predict microstructures (especially metal/ceramic combinations) which are likely to exhibit the maximum combination of toughness and hardness.

2. Develop a fundamental understanding of high-rate powder consolidation, as a basis for controlling microstructure development under shock conditions.

3. Develop a fundamental understanding of shock-induced defect structure and shock-induced comminution and the relationship to enhanced solid state reactivity.

TECHNIQUES

1. High strain rate compaction of powders to form unique consolidated products (e.g. unique cermets).

2. Shock activation of powders for subsequent enhanced sintering (e.g. covalent materials: SiC, Si_3N_4, BN, B_4C).

3. Formation of innovative microstructures by shock compression (e.g. in-situ formation of eutectics of ceramics and ceramic/metals).

GUEST ATTENDEES

Edwin K. Beauchamp	Sandia Laboratories
D. R. Clarke	Rockwell International Science Center
Carl Cline	Lawrence Livermore National Laboratory
William H. Gourdin	Lawrence Livermore National Laboratory
Robert A. Graham	Sandia National Laboratories
A. H. Heuer	Case Western Research University
D. Lynn Johnson	Northwestern University
M. L. Knotek	Sandia National Laboratories
Vonne D. Linse	Battelle Memorial Institute
Mark L. Wilkins	Lawrence Livermore National Laboratory
Guenter Winkler	Naval Weapons Center, Michelson Laboratory

APPENDIX I

SHOCK WAVE ANALYSIS

G. H. Vineyard

What else needs to be known about shock waves themselves in order to proceed with a strong R&D program in shock compaction? The answer, in a nutshell, is "a great deal".

The classical theory of shock waves assumes that a homogeneous fluid consisting of a single component (i.e., characterized by two thermodynamic variables, say, density and pressure) is compressed by a steady shock front to a well defined state of higher density and pressure. Then the Rankine-Hugoniot relation, which depends only on the additional assumptions of the conservation of matter, momentum, and energy, relates the variables of all possible shocked states to those of the initial state. The relation says nothing about the profile of the shock front, and is valid regardless of the lack of equilibrium in the front and its vicinity. The nature of the front can be calculated only by assuming an equation of motion - typically the Navier-Stokes equation, possibly including bulk as well as shear viscosities and thermal conduction - assuming an equation of state, and solving this equation, a process which generally must be done numerically.

A number of further refinements can be brought into the numerical work. For example, finite rigidity of the material can be introduced relatively easily, although the constitutive rela-

tions may be a subject of argument. Expanded materials (e.g., powders) can be handled by the same codes to the extent that the irreversible constitutive relations can be determined.

If more than one chemical species is present, i.e., if a chemical reaction can occur, the number of possible physical situations multiplies enormously. Some calculations have been made for detonation and deflagration waves in explosive materials, but to my knowledge the number of cases treated has been limited. For instances of interest in materials preparation, I believe virtually nothing has been done.

All of this work with the Navier-Stokes equation and generalizations thereon makes the further assumption that at each point in the shock front, local thermodynamic equilibrium (possibly under certain constraints) prevails. This assumption is weak; it surely becomes very bad at high shock intensities where the shock front becomes thin and deformation rates and property gradients become enormously high.

Microstructural changes of a variety of kinds are also induced by shocks. Dislocation, twins, point defects, clusters, etc., are created in profusion, and when this is taken into account the complete characterization of the material becomes even more complex, surely hopelessly so for any rigorous treatment.

The investigation of the use of shock to produce new and useful structures, starting with mixtures of powders or other fine grained materials can proceed in a purely empirical fashion, but the number of possible starting substances is enormous and

the range of shock pressures and other variables (initial temperature, for instance) makes a vast number even vaster. Therefore, the Edisonian approach, while capable of illustrating the range of possible effects and perhaps occasionally stumbling onto something useful, is not likely to come even close to exhausting the possibilities.

Consequently, the search needs to be guided by such information as can be extracted with reasonable effort from conceptual and calculational models. I believe that much more can be done along these lines and suggest that model calculations would be very useful as an adjunct to the experiments being supported.

Simple models can give estimates of simple parameters such as temperatures reached, shock front widths and rise times, shock duration, and unloading profiles. Even if the estimates are crude, they should be of value in rationalizing the observations. A discussion of many of these questions is given by G. H. Vineyard in DARPA MRC Report, July 1969, paper 34. For systems in which chemical reactions occur, model calculations could be made of the progress of the reaction through the shock front and afterward. Reaction rates as a function of pressure and temperature are needed as input, and these can be estimated to some degree of accuracy or measured independently. Rather elaborate codes for calculating shock profiles on the basis of various continuum models are in use at LLNL, LASL, Sandia and elsewhere.

Finally, I enter a plea for further efforts to understand what really takes place in strong shock fronts both in simple and complex systems. Most effort to date has concerned simple systems. It may be that the experimental and theoretical work now going on with complicated systems will help throw light on this aging mystery.

APPENDIX II

DYNAMIC CONSOLIDATION AND SYNTHESIS - COMMENT

J. J. Gilman

Temperature and time are largely interchangeable process variables in the manufacture of materials. This was convincingly demonstrated in Zener and Holloman for a prototype case (tempering of steel) some 35 years ago. The rate of a process is primarily determined by the forces driving it and the temperature. One driving force is pressure, but it has considerably less influence than other parameters such as shear stresses, chemical concentration gradients, electric fields, etc. Thus there is no a priori reason to expect that increasing pressures and decreasing times will, of themselves, produce exceptional materials, or facilitate consolidation in a remarkable way.

If it is true that high pressures and short processing times do not have intrinsic benefits for the manufacturing of materials, then proposals for the use of dynamic methods must be examined as they apply to specific cases to determine whether they are cost effective.

In special cases dynamic consolidation or synthesis processes may be cost effective, but in general they will not be because: firstly, they use energy inefficiently since they operate far from equilibrium; secondly, only a few shapes can be made because of the rarefaction waves that inevitably accompany compression waves; thirdly, they use labor inefficiently because

they are intrinsically batch processes and people cannot be present during an explosion or the firing of a gun for safety and health reasons; finally, they use capital inefficiently because relatively large facilities are required for work with explosives, and considerable material is destroyed during each consolidation or synthesis event.

Interest in dynamic consolidation and synthesis methods is not new. Both industrial firms, and governmental agencies including arsenals have given them substantial attention for at least 30 years. The empirical evidence is that they are not effective as a means for manufacturing materials. Therefore, the burden of proof is on present proponents to show that their lack of effectiveness can be changed in any truly significant way. Such proof should include a quantitative analysis of the costs that would be incurred during the manufacture of a specific prototype material or object. These costs should be analyzed relative to other methods for achieving the same goals. A rough analysis is presented here.

The energy that is actually needed to consolidate a material is certainly not more than the heat of melting. For iron (and its alloys) this is approximately 16 J/g; and for ceramics it might be as much as 20 J/g. On the other hand the energy of reaction in an explosive is about 4×10^3 J/g and experience indicates that 5-20 pounds of explosive (say 10) is needed to consolidate one pound of material. Thus about 2000 times as much energy is used in explosive compaction as is actually needed. This is inefficient, indeed!

The costs associated with using energy inefficiently in explosive compaction are both direct and indirect. Direct costs are associated with the cost of the explosive material itself. In fabricated form, this is at least 10 $/#. To this the cost of the material used for momentum trapping must be added. Also, direct labor costs are high because the large excess of energy that is necessary creates safety and health problems, and because the processing is done in small batches.

For a small facility (10 pounds of explosive or less) with a turnaround time of 12 minutes, the production rate would be 5# per hour or 40#/day (single shift). For safety reasons at least two skilled workers would be required, supported by two others. At 12 $/hr direct charge per worker and 50% overhead, the overall labor rate is 72 $/hr or about 14 $/# of product. The facility would need to be about 2000 ft^2 in size , and because of its technical content the equivalent rent of such a facility would be about 10 $/ft^2$ or 10 $/hr which yield s 2 $/# of product.

The above cost estimates indicate that the dominant cost factor is the direct cost of the explosive. Since this cost relates directly and fundamentally to the process it cannot be reduced substantially and places a severe limitation on the cost-effectiveness of the process. Also, it may be seen that using a large facility instead of a small facility will not change the costs substantially.

It might be argued that a means could be found to increase the efficiency with which the explosive material is used. But a very large change in efficiency would be needed. This is unlikely because the low efficiency arises from fundamental features of the process. One of these is that it operates very far from equilibrium so the thermal efficiency is very low. Another is that impedance matching is poor in transferring power from the source (the high explosive) to the product. Therefore, a large fraction of the power gets reflected instead of being transferred.

Since it is a costly process and does not appear to have intrinsic advantages, dynamic consolidation/synthesis has very limited utility. For a few very high-priced materials it may be cost-effective, but such a limited scope does not justify any substantial investment in R&D work.

UV AND VISIBLE EXCIMER AND RAMAN LASER COATINGS AND REFLECTORS FOR COMMUNICATIONS AND SPACE DEFENSE APPLICATIONS

N. Bloembergen, C. M. Stickley and H. V. Winsor

Approximately 25 outside users and developers of UV laser components and high energy optical coatings met with several members of the Materials Research Council in a workshop which concentrated on optical properties of surfaces and thin film coatings. The list of participants appears in Appendix A.

The previous review of this topic by the MRC was held eight years ago.[1] A considerable body of experience has been acquired in the intervening period. The pertinent developments in theory and experiment and the current state of the art were reviewed and discussed in a meeting, the program of which appears in Appendix B.

The basic operating conditions are:

Wavelength	351, 401, 495, and 505 nm
Pulse duration	1-4 μs
Pulse repetition rate	100 pps
Cavity of excimer laser	175°C, 90 psi

The coating requirements are:

Fluence	10 Joule/cm^2, minimum 30 J/cm^2, desired
Average incident power	1 kw/cm^2
Reflectivity	$R > 0.99$
Environment	Should withstand chemical and radiative conditions of excimer lasers: NF_3, F_2, NF_2, F, UV, and electric discharge radiation.

Metallic reflectors cannot be used in the UV, because the best metallic surface (unoxidized aluminum) still has an

intrinsic absorption loss of 8 percent for normal incidence. Reflector arrays with glancing angles are geometrically unacceptable. Totally reflecting dielectric prisms for the geometries of interest would present large optical thicknesses in the material, with concomitant unacceptable phase distortions due to differential thermal expansion even for very low intrinsic absorptivities, $\alpha = 10^{-4}$ cm^{-1}. The approach which has to be taken, therefore, is to construct a mirror using multiple dielectric layers deposited on either a metal substrate or substrates like fused SiO_2, ULE, etc.

There must at least be one optical transmission window. Again, geometrical considerations make it undesirable to place this window at Brewster's angle. The increase in cross-section and thickness would entail unacceptable thermal distortions in the optical wave front, and cavity design is more difficult. Thus there is also a need for anti-reflective coatings on the transparent window.

Typical dielectric coatings achieved so far have absorptivity in the range of 0.3-1.0 percent, and scattering in the range of 0.2-0.5 percent. The damage thresholds for repetitive and single pulses lie in the range of 2 J/cm^2 to 8 J/cm^2. Large spot sizes (1 cm) result in lower damage thresholds than with small sizes (<0.2 cm).

Most of the accurate UV damage threshold data on films are taken with laser pulses of relatively short duration, 0.1-10 ns. The energy fluence damage threshold for 1-μ second or

longer pulses will certainly not be lower, and there is good evidence that the damage threshold for such pulses exceeds 10 J/cm^2. For certain candidate films, there is a significant increase in the damage threshold as the wavelength becomes longer (i.e., to 1 μm). The absorptivity of the films is three or four orders of magnitude higher than for the single crystal bulk oxides and fluorides. It is clearly of extrinsic origin, as is the observed damage threshold.[2] The degree to which these are related is not clear.

While no specification for optical distortion was given, systems analyses indicate that tolerances of much less than λ/10 are desired. The current state of the art is about λ/10 at 633 nm, for films on a glass substrate (up to one meter in diameter). The reflectivity of such films at 351 nm is about 99.4 percent, with an absorption and scattering of 0.3 percent each. Metals can be polished about as flat as glass, but the scattering would be increased to 0.7 percent, making the total reflectivity 0.99. Clearly the critical parameter in maintaining passive optical quality is absorption in the coating. If this can be reduced to 10^{-3} or less, the goal of 1 kw/cm^2 incident beam power is attainable, while maintaining λ/40 optical quality. If practical optical fabrication remains at its present limit of about λ/10, then the threefold reduction in absorption may not be needed for achieving the 1 kw/cm^2 requirement.

Other important factors for achieving near-flat phase profiles are improved polishing, heat transfer, and fabrication

techniques of cooled mirrors. If the 0.5 percent scattering from molybdenum mirrors produces an intolerable increase in the scatter of the dielectric overcoated films, then the development of a scale-up facility for depositing CVD silicon carbide is called for. While this material has excellent characteristics for minimizing optical distortion (high ratio of thermal conductivity to thermal expansion coefficient) it also has superior polishability. Surface roughness of 8 angstroms has been achieved.[3] It should be noted that the industrial organization which has developed the polishing techniques for CVD SiC will not release them, nor the self-polished material itself. Thus an additional effort will be necessary to "re-develop" the polishing procedure.

The requirements on the damage threshold and absorption in the coating are only about one order of magnitude more stringent than what has already been achieved in some available film coatings, albeit not under the actual system operating conditions. It should be possible to improve the extrinsic properties of the films through a number of incremental gains so as to meet the requirements, if an optical component distortion of $\lambda/10$ is tolerable. Assuming this to be so, no intrinsic or theoretical limitations exist to prevent achieving the desired film and mirror properties.

POSSIBILITIES FOR COATING IMPROVEMENT

The cau- of film damage is probably absorption by small particulate inclusions. These occur in rather high density with

a wide distribution in size. In the case of AR coatings the damage occurs preferentially at the interface between the first layer and the window substrate. In reflective coatings the damage starts in the outer layers of the film. In either case the light field intensity is higher at these respective locations. The field may be enhanced by the electrostatic effect of cracks and pores.

The coatings usually have only 85 to 90 percent of the density of the bulk oxides and fluorides. Vapor deposited flims almost always exhibit a periodic columnar growth pattern. This is not surprising because perfect epitaxial growth is not possible in view of the mismatch in lattice constants between the successive layers themselves and the substrate. Growth starts preferentially at dislocations or other imperfections due to impurities. The spaces and pores between the columns readily absorb water from the ambient atmosphere or other impurities. At the wavelengths of interest water is not very absorptive and should not change the damage threshold. It would not be harmful, provided it remained pure and its amount remained constant. The water content of the film will, however, vary with the temperature of the film and the humidity of the atmosphere. This causes uncontrollable variations and inhomogeneities in the optical thickness of the film with concomitant phase front distortion. This question has yet to be addressed experimentally.

The nature of the absorbing inclusions is not known. Undoubtedly much could be learned by various analytical

techniques of surface technology, including

1. Secondary Ion Mass Spectroscopy (SIMS)
2. High Spatial Resolution Auger Analysis
3. Photoacoustic Spectroscopy (to measure absorption as a function of wavelength)
4. Scanning Calorimetry
5. Raman Microprobe
6. Ellipsometry

These rather elaborate, but powerful, techniques should be brought to bear on the problem only after the following more expedient measures have been exhausted.

Clearly the efforts to use very pure starting materials for the film evaporation should be continued. Perhaps zone refined single crystals should be evaporated. The likelihood for deposition of heavier particulates and inclusions could be diminished by a time-of-flight separation method, using a fixed slot and spinning disk aperture at a suitable distance to permit the passage of only atoms and molecules with relatively high thermal velocity. Since the presence of rotating objects in the evaporator chamber is objectionable (vibrations, lubricant vapors), a simpler and more effective way is to put the surface to be coated upside down one meter or more above the evaporator. The mean height which a particle of mass M will reach is given by $kT = Mgh$, where T is the temperature of the evaporator, $g = 981\ cm^2/sec$, and Boltzmann's constant $k = 1.38 \times 10^{-16}$. Taking $T = 10^3 °K$, and $h = 10^2$ cm one finds $M \approx 10^{-18}$ g. This implies that

particulates with more than a million atoms will be very unlikely to reach the surface. Although many of the data presented were taken with the height differential significantly less than one meter, a change in this distance to one meter will probably further reduce the large inclusion content in the films.

Very significant gains in film quality can probably be made by increasing the atomic agitation during the deposition. The conventional way is to raise the temperature of the substrate. Presumably an optimum temperature is found, because further heating would produce deleterious thermal stresses on cooling. The kinetic energy of the atoms during deposition can, however, be increased by ion bombardment (argon sputtering), by electron beam and/or laser beam heating. In the latter case, it should be possible by a suitable selection of (infrared) wavelengths to selectively heat the fluoride layers, the oxide layers or the substrate surface. It is expected that these techniques, either singly or in combination, will lead to films of considerable higher densities, with fewer pores, and fewer absorbing inclusions. The adherence to the substrate may also be improved in this manner, reducing the peeling problem. Variations in the optical density due to varying moisture content will also be reduced in the denser films, as will be the UV light scattering.

Laser annealing of the optical films after completion of the coating is another possibility. Such annealing is based directly on heating effects proportional to the absorptivity of

the layer at the selected wavelengths. It should be possible to preferentially heat and/or melt only the fluoride layers by irradiation of a laser pulse with suitable duration and wavelength. It is entirely possible that application of these methods will yield films with the required properties. The decrease in film absorptivity will, of course, reduce the heat load and cooling requirements of the substrate.

Another variant would be a neutral atom sputtering technique, although this may not have significant advantages over the above mentioned methods, which appear to be simpler to execute.

Other possible methods of deposition considered include:

1. Metal-organic chemical vapor deposition (MOCVD)
2. Sol-Gel[4] technique with subsequent leeching of a phase-separated material
3. Molecular Beam Epitaxy

These methods do not appear to be immediately suitable to the problem of reflective UV coating, consisting of oxide and fluoride layers, on a substrate of a molybdenum mirror, fused silica, or CVD SiC. The Sol-Gel technique[5] could perhaps be adapted to the problem of an AR coating on a window material. In any case, these approaches would require considerably more development work, which may not be necessary, if the suggested improvement in evaporative deposition have positive results. While it may be possible to reduce absorption of films, and thus solve the

heat load problem directly, the concept for the use of a heat pipe to cool mirror substrates ought to be explored. It could improve heat transfer characteristics dramatically.

Not nearly enough systematic work has been done on the influence of the radiative and chemical environment on the film properties. There is evidence, in several cases, that the repeated exposure to laser pulses below the damage threshold actually increases this threshold. This may be caused by thermal annealing of potential damage sites. There are other indications to vigorously pursue laser annealing at other wavelengths, mentioned earlier, in a systematic fashion. There is, fortunately, no evidence that exposure to visible and UV light, causes color centers with potentially troublesome absorption. A systematic investigation of the change in film properties due to large doses of UV radiation, e.g., from a high pressure mercury lamp, is however, desirable. If build-up of color centers should become troublesome, they could conceivably be annealed out by irradiation at longer wavelengths or by heating.

A systematic investigation of the influence of the chemical reactive atmosphere, characteristic of excimer lasers, should also be investigated separately from the UV irradiation problem.

RECOMMENDATIONS AND CONCLUSIONS

1. There are no known fundamental limitations which would prevent the attainment of films with required properties.

2. To reduce film absorption and inclusions, existing deposition techniques can be improved by a systematic application of ion beam, electron beam and/or laser beam excitation during the deposition process.
3. Laser annealing of films after deposition should also be exploited.
4. A systematic investigation of the influence of UV and discharge radiation on the film properties is desirable.
5. A systematic investigation of the influence of the chemical and physical environment on film properties is desirable. These investigations should also include other wavelengths, since the final system design is by no means frozen.
6. The investigations mentioned under points 2-5 could be carried out conveniently and adequately on a small scale with small samples, before scale-up to actual operating conditions.
7. Accurate damage thresholds should be determined for the pulse durations actually used (1-4 μs), for repetitive pulsing, and for larger spot sizes.
8. Polishing techniques and scale-up of CVD-deposited silicon carbide should be developed if the 0.5% scatter from moly-mirrors is judged to be intolerable.
9. Conduct an analysis of the heat pipe concept for cooling mirror substrates and develop it if significant gains appear possible.

REFERENCES

1. M. Sparks, H. Ehrenreich, W. H. Flygare, C. M. Stickley, MRC Summer Conference, Vol. 1, pp. 619-635, 1973.

2. T. W. Walker, A. H. Guenther and P. E. Nielsen, "Pulsed Laser Induced Damage to Thin Film Optical Coatings," I Experimental, II Theory. Accepted for publication in IEEE Journal of Quantum Electronics.

3. V. Rehnand, W. J. Choyke, "SiC Mirrors for Synchrotron Radiation", Nuclear Instruments and Methods 177, PP. 173-178, 1980.

4. S. P. Mukherjee, "Sol-Gel Processes in Glass Science and Technology", J. Non-Crystalline Solids 42, pp. 477-488, 1980.

5. S. P. Mukherjee and W. H. Lowdermilk, "Gradient Index Antireflection Films Deposited by the Sol-Gel Process," presented at the Conference on Lasers and Electro-Optics, Washington, D.C., June 1981.

APPENDIX A

ATTENDEES

Joe Apfel	Optical Coating Lab, Inc.
John Asmus	Maxwell Lab Inc.
William Barnes Jr.	Itek Corporation
Rettig Benedict	DARPA
H. E. Bennett	Naval Weapons Center
Jean Bennett	Naval Weapons Center
Ralph R. Berggren	AVCO Everett Res Lab
V. W. Biricik	Northrop NRTC
Ernest W. Bloore	US Army Arm Res & Dev Command
James H. Brannon	Maxwell Lab Inc.
George K. Celler	Bell Labs
P. Daniel Dapkus	Rockwell International
Dennis Fischer	Coherent Inc.
Samuel J. Holmes	Northrop
Austin Kalb	Litton G/CS
Tony Lenderlonek	OJAI Research Corporation
W. Howard Lowdermilk	Lawrence Livermore Nat Lab
H. Angus Macleod	Univ of Arizona
David Milam	Lawrence Livermore Nat Lab
Sgyama Mukherjee	Battelle Columbus Laboratory
Brian Newnam	Los Alamos National Laboratory
Victor Rehn	Naval Weapons Center
Keith Shillito	Air Force Weapons Lab
A. J. Sievers	Cornell University
Marshall Sparks	Scientific Research Center
William Spicer	Stanford Univ
James L. Stanford	Naval Weapons Center
James N. Tillotson	Rocketdyne
James A. Van Vechten	IBM, T. J. Watson Research
Frank Wodarczyk	Rockwell International
Harry V. Winsor	AFSOR/NE Bolling Field

APPENDIX B

AGENDA

THIN FILMS AND COMPONENT OPTICS FOR UV AND VISIBLE EXIMER AND FREE ELECTRON LASERS

Tuesday, 7 July 1981

Introduction

Dr. E. Joseph Friebele — DARPA/DSO
Objectives of Review and Presentation of DARPA Questions

LtC Rettig Benedict — DARPA/DEO
Laser Specifications, Goals, and Environmental Conditions

Existing Capabilities and Experiences

Dr. Marshall Sparks — Scientific Research Center
Analysis of Requirements

Dr. James L. Stanford — NWC
Technical Review of DARPA'S UVVLC Program

Dr. Jonah Jacob/Mr. John Boness — AVCO
Eximer Laser Components Experience

Dr. John Asmus — Maxwell Labs
Eximer Laser Components Experience

Dr. Vic Rehn — NWC
Synchrotron Light Source Components Review

Theoretical and Practical Limits

Dr. Marshall Sparks — SRC
Theoretical Factors in UV Optics

Capt Keith Shillito — AFWL
SOA and Trends of Mirror Heat Exchangers

Dr. Brian Newnam — LASNL
DOE Fusion Components Experience

Dr. Howard Lowdermilk — LLNL
DOE Fusion Components Experience

Dr. Harold Bennett — NWC
Pulse Distortion in High Power Optics

Dr. Jean Bennett — NWC
Roughness and Scattering in Optical Components

COMMENTS ON UV-VISIBLE LASER COMPONENTS WORKSHOP

H. V. Winsor

My first comment is that no clearcut approach has resulted from the workshop. This is because the problem is too complex for one solution to stand out.

The primary problems and difficulties raised during the workshop are grouped around the following central points:

a. repetitive laser pulse damage

b. environmental effects

c. mirror heat exchanger performance

d. thin film growth morphology and its control

e. surface and interface states

f. windows

These topics are discussed separately below.

Repetitive laser pulses may damage the component catastrophically, progressively, or prevent proper performance by distorting the laser wavefront. Effort should be expended to grossly identify the initiating center of catastrophic damage, but not to characterize the defect in detail unless that is the best route to eliminate the effect. Minimization of progressive failure or "fatigue" suggests reducing film porosity and absorption and improving film adhesion. The primary absorption problems (about which no good data currently exist) center on the effects of the environment in combination with the repetitive pulses. Simulated operational environment tests, and

measurements of the pulsed distortion of the mirror wavefront should be made as soon as practical. Propagation thresholds for damage must be measured as well as initiation thresholds, since isolated spots of damage may not destroy the usefulness of a mirror. Absorption must be measured versus service history polarization, wavelength, temperature and environment. Progressive increase in absorption must not occur. The repetitive thermal shock delivered by the laser pulse suggests watching the thermal expansion coefficients of the film materials, and processing to optimize the temperature rise of the film layers. No amount of optimization can remove the gradient in temperature with depth into the coating. It is perhaps critical to prevent repetitive opening and closing of cracks in thin film layers under the laser loading. This can accentuate corrosion or fatigue. Thus films in tension should be avoided. The annealing time for color centers should be short if the center absorbs at the laser wavelength.

The environmental conditions in which the mirror must operate range over these principal areas:

a. room temperature (gas or vacuum)
b. primary laser cavity (heated in cavity gas)
c. free electron laser cavity
d. space
e. exotic environment

Good data exists only for mirror and window coatings tested in air. This is likely to be the most benign environment. The varying humidity of the atmosphere will require eliminating

porosity from thin films so that the figure will remain good, or else require humidity control in the beam train region. The strong absorption that fingerprints and much dirt have in the UV suggests minimizing the porosity to reduce absorption and ease cleaning.

The eximer laser cavity environment should receive very high priority: If it is not tolerable, a complete re-working of current system concepts is indicated. Difficulties in this environment are likely to interact, so combined-effects testing should precede individual factor testing. Use of a fluoride outer film layer may be necessary to withstand attack by atomic fluorine, if the corrosion kinetics are unfavorable for a more "durable" film. Attack at the coating - substrate interface may be prevented, if necessary, by a thin overcoat of the fluoride of the substrate material. Photo-chemical corrosion at crack-tips may necessitate eliminating film porosity. Severe stress problems are likely in films with oxide or fluoride attack because of the increase in size of the ion compared with the atom. Surface photo-desorption by UV or x-rays and subsequent fluoridation of the surface should not result in rapid attack of the coating unless the fluoride is gaseous. It, therefore, appears wise to avoid materials with gaseous fluorides and materials which react strongly with fluorine. Color center and photo-chemical effects from the x-ray and UV-background must not weaken the film, contribute to creep in the film, or increase the absorption.

The free electron laser cavity environment appears to be similar to the synchrotron radiation environment. The very stringent vacuum requirements of the electron storage ring (if a ring is used) will require elimination of the "virtual leak" that a porous coating represents. Even monolayers of water may desorb under synchrotron radiation and laser flux combined. This may contribute to changing the optical figure of the coating even further than do humidity excursions in air. The strong background of synchrotron radiation may greatly speed diffusion of impurities, especially in a porous filmlayer. Surface charging by x-rays and electrons may result in preferential photodesorption or photo induced valance change and loss of surface layer stoichiometry. Film materials which resist photodesorption should be considered. Further studies should be performed to define the free electron laser environment more accurately. The higher laser loading anticipated for the free electron laser is likely to cause severe problems, even in a relatively mild environment.

The space environment is similar to the free electron laser environment in many ways. While it has been briefly investigated for IR coatings at 2.87 micrometers, it has not been characterized in the UV. Micrometeroid impacts will assure the presence of "damage initiation" sites, so the likely lower loadings are the principle assurance that the problem is soluable for a time. The lifetime of coatings in space should be studied and the engineering consequences drawn.

Exotic environments such as HgBr and other gases are to be avoided unless they are required. Mirror heat exchangers must dissipate the thermal load while remaining immune to cyclic fatigue and corrosion. Water does not appear to be as desirable a coolant at 170°C as it does at room temperature, due to the high pressure necessary to prevent boiling and the corrosion properties hot water. Heat pipe mirror heat exchanges would appear attractive because of the lower stresses, and increased ease of polishing while hot. Polishing hot appears to be a consideration with many implications, as is the need to frequently raise the mirror temperature to 170-200°C or to keep it at that temperature. An end run on the mirror heat exchanges problem using non-linear optical effects may be promising if it can be corrected for its own as well as other figure errors. Another difficulty with contemporary heat exchanges is inability to polish the mirror substrate to the desired 10Å rms roughness. Fifteen -30Å rms is equivalent to a total scattering of about .3-1% per mirror surface. SiC, Si, and SiO_2 are polishable to better than 5 Å rms. However, the coating may increase the effective optical roughness of the mirror above that of the substrate.

The morphology of optical thin film growth has the greatest impact of any factor discussed at the workshop - the index of refraction of the film layers is set by the absorption of water, and the other impurities that it attracts, into the cracks between the crystals that make up the thin film layers.

The morphology of film growth appears very similar to the growth of whiskers in oxide crystal melts under certain conditions. It appears that quartz, and other crystals, have different growth habits depending on the kind and amount of impurities that are added to the melt. If thin film growth is closely analogous to whisker growth, then the whisker growth would continue if the film were placed in the proper conditions. (Ref. Ceramic and Graphite Fibers and Whiskers, McCreight, Rauch, and Sutton, Academic Press (1965). It is suggestive that the impurity content required to modify thin film dislocation density (See for example, Chapter 4 of Impurity Doping Processes in Silicon, F.F.Y. Wang, Ed., North Holland (1981). (Chapter title: Growth of Doped Silicon Layers by Molecular Beam Epitaxy by J. C. Bean, Bell Telephone Laboratories, Murray Hill, N.J. 07974) is in the same range as the impurity concentration required to cause marked changes in the growth habits of crystals (See, e.g., Crystal Growth, H. E. Buckley, John Wiley & Sons, New York (1951), pp. 339-387). Many of these modified growth habits are needle-like, tending toward the whisker geometry. Further examples of the propagation of defects in single crystal films of silicon are given in Single-Crystal Films, M. H. Francombe and H. Sato, Eds, the Macmillan Company, (Pergannon Press Book) New York (1964) (see especially pp. 251-281). The principle impurities in cryopumped and ion pumped vacuum deposition systems are H, He, and the rare gases. These impurities should be checked for their effect on thin film growth by leaking them into the

chamber during film growth. Hydrogen especially has the potential of nucleating stacking faults in Si films.

If the growth morphology of thin film layers cannot be controlled through the variable parameters of the vacuum deposition methods used in industry, they might be controlled by introducing new process variables, such as electron, laser, or ion beam bombardment, either during or after growth. Laser annealing of the film material is a version of the above processes carried to the extreme of causing melting of the film. The scientific basis of laser annealing is not yet undisputed, but progress in laser annealing bears watching for its potential of improving thin film processing.

The primary result of the columnar growth of thin films is the dramatic increase in effective surface area caused by the connected porosity. Even if the additional surface (~900% of the film surface area!) were virgin, it represents a x10 increase in the surface state density. However, the surface is "optically contacted" to another surface, so the variable proximity of the other (nominally identical) surface can change the surface state energy distribution. Mobility is enhanced along the interface by the "respiration" of water and other vapors in and out of the pores, and by the working of one layer over the other by the laser induced thermal shock. Interface states that are important are the metal-air, metal-film; film-film, film-water, and film-air. Many of these interfaces have not been adequately characterized in the UV (or at any other wavelength).

The experience of the optical state community is likely to be important for components, which work in air, while the vacuum surface state community may have much to say for free electron laser and space environments. Exotic environments need investigation. eSince water is frequently absorbed onto the film, the broadening of surface states by proximity to water and the opposing surface should be carefully studied if the internal surface cannot be eliminated.

The continuing requirement for windows is perhaps just the tip of a large iceberg. Since centimeter thicknesses of optical material have an absorption equal to thin film coating layers, the optical distortion per pulse will be as large. However the window has a much longer thermal relaxation time constant (minutes as opposed to milliseconds) so the repeated distortions will add to create a much larger figure degradation. No technological solution to this problem exists until adaptive phase correction can be implemented. Birefringence in the window may not be controlled at all, even by adaptive optics. In addition, the problem of a window is seriously complicated by the temperature and pressure desired in the eximer laser cavity (175°C, 90 psiG). The pressure pulses in the cavity during lashing add to the high pressure to create very high stresses. A single window pane must be built to withstand these conditions and must also be of minimum thickness to minimize the figure distortions, so it will exhibit birefringence. Birefringence in the cavity of a laser will probably couple severely to the mode

structure and wavefront quality of the laser. Even a thermopane design will not be a simple solution to the problem. Doubling the number of surfaces will probably offset any savings due to reduced stress and temperature control. A Brewster's angle window is also fraught with difficulties. The area and resolved thickness are both about twice that of a normal window. Birefringence in a Brewster angle window will rotate some of the principle beam, causing reflections from the window to be parasitically diverted from the main laser beam. A further difficulty of all designs is the requirement of keeping the window's mechanical resonant frequency far away from any cavity source frequency. (Harmonics of the pulsing rate.) In view of the above discussion, the near term and long term priorities of the UV-visible laser components program could be set as follows:

NEAR TERM THRUSTS (approx. in priority order) (Applied Research)

<u>Better Films</u>

a. Investigate new deposition techniques for making a "perfect coating." MOCVD, MBE, ION DEPOSITION, LASER ANNEALING, and SOL-GEL processes may provide intrisic material quality in thin film form.

b. Study methods of passivating the internal surface of thin film layers if they cannot be eliminated. (Reactive atmospheres, exposure to selected condition, etc.

c. Study the absorption spectra of the film materials to determine the best wavelengths of operation, or the predominating impurities or defects.

d. Find ways to purify the thin film materials during film deposition using conventional methods. (Mass filtering, velocity filtering, photo-purification, photodesorption, etc.)

e. Try to have only compressive stress in the working films.

Damage Characterization

Test films for damage, distortion, and environmental resistance in eximer and free electron systems. Test in the combined environment only and try to avoid detailed characterization under partial conditions. Use actual conditions rather than simulated conditions. Expose enough area to assure finding any Echillies' heel.

Substrate Issues

a. Choose mirror material which can be polished and fabricated into the lowest absorption highest thermal figure of merit substrates. Scattering appears to be a less harmful condition than absorption.

b. Seek to match the thermal expansion coefficient and elastic modulus of the mirror or window with the thin films.

c. Consider carefully how to fabricate components which operate at elevated temperatures.

LONG TERM EFFORTS (No priority apparent) (Basic Research)

a. Try to understand the reasons for columnar growth in thin film materials.

b. Try to understand the ways in which columnar growth controls the optical and mechanical properties of thin film coatings.

c. Study optical surface states and try to understand how they are affected by common contaminants.

d. Study methods of film deposition to understand how defects are generated in the film.

Progress in the above areas may come from a number of research communities, including:

a. Electronic thin film preparation research

b. Electronic film characterization research

c. The rapid solidification powder program

d. Field ion microscope studies

e. Laser annealing for semiconductor, electronic or metallurgical processing

f. Surface state characteration in UV and Visible

g. Synchrotron light source research

h. Studies of crystal morphology changes with impurities

i. Surface chemistry and photo-chemistry

j. Surface physics and vacuum science

k. Plasma physics

l. Molten state physics

ACKNOWLEDGEMENT

This paper was written under the auspices of the DARPA Materials Research Council, Contract #MDA903-80-C-0505 with the University of Michigan.

FREE ELECTRON LASER OPTICS FOR SPACE DEFENSE APPLICATIONS

C. M. Stickley

In the meeting on UV-visible laser coatings and reflectors[1], the Materials Research Council was asked to address the optics situation with respect to free electron lasers (FEL's).

The basic operating conditions are:

Wavelength	350-450nm
Pulselength	10-100 psec
Rep Rate	10^7 pps
Cavity	Vacuum

The coating requirements are:

Fluence	0.1 J/cm^2(10^9 w/cm^2 peak)
Average incident power	10^6W/cm^2 set by electron beam area and interest in minimum resonator length
Reflectivity	R>0.99; AR
Environment	X-rays

The reader should review Ref. (1) (found elsewhere in these MRC proceedings) since all of the recommendations and conclusions found therein pertain to FEL optics with the exception of numbers one and seven. These differences will be discussed below.

Taking the latter first, the seventh recommendation pertains to pulsed damage thresholds measured at microsecond pulse lengths. The damage threshold is not an issue for FEL's

since pulse energies of 0.1 J/cm^2 or smaller, even with pulse durations of 10-100 psec, are insufficient to cause damage.

Going to the first conclusion in Ref. (1), for [illegible]'s this should be restated as:

1. While there are no known fundamental limitations which would prevent the attainment of films with the required properties, there are immense practical limitations to reducing the coating absorption by a factor of 1000 in order to meet the stated requirements. Consideration should be given to shifting the FEL wavelengths to 750-2000 nm.

The results of Spark's analysis of multi-layer dielectric mirror optical distortion, as presented at the meeting, can be scaled directly with coating absorption: as A is reduced from $5x10^{-3}$, the allowed average incident power without undue optical distortion rises proportionately. Thus, to handle the requirement of 1MW/cm^2 rather than 1KW/cm^2 would require a coating absorption reduction to $5x10^{-6}$. Clearly a break-through in coating technology will be required to achieve this, especially in the range of 350 to 450 nm.

Consideration should be given to moving the FEL wavelength of operation to the 750-2000 nm region for the following reasons:

1. Extrinsic absorption in coatings (and windows) through electronic transitions in impurities is reduced in the near infrared to 350-450 nm.[1]

2. High refractive index materials for coating stacks are available in the near infrared resulting in the need for many fewer layers to build up the reflectivity.

3. Allowable tolerances for optics fabrication (coating uniformity, flatness, etc.) would be eased by a factor of about 2.5, the ratio of the wavelengths.

4. Much of the very extensive R&D on polishing and coating technology in the 1060 nm laser fusion program would be applicable to the FEL optics problem.

5. Diamond is a realistic candidate for a FEL window material[2] due to its superior thermal conductivity. Synthetic, inclusion-free diamond is available in 5 mm diameter windows. Diamond will not be useful at 400 nm since absorbing color centers are created at this wavelength.[3] This limitation on the use of diamond does not exist between 750 and 2000 nm. Assuming a laser power of 100 Kw, an absorption of $10^{-4}cm^{-1}$, a 0.1 cm thick window would require the thermal contact to take away only 10 watts from the edge of the window.

6. Substrates for partially transmitting mirrors have the least absorption in the near IR range. This wavelength is too short for multi-phonon absorption and too long for electronic and multi-photon absorption. Weak absorption through overtones of molecular-ion-impurity vibrations is the dominant mechanism in this wavelength range.

7. Atmospheric transmission to space from a 3 km mountain peak is about 0.4 at 350 nm, 0.6 at 450 nm, and 0.9 at 1060 nm.

Three counter arguments for going to the near IR are the potential reduced coupling into laser hardening materials, the increased size of optics at a longer wavelength, wavelength, and a possible increased in jitter accompanying the increase in size of the optics.

With respect to the first of these, future laser protective materials will probably be designable as broad-band materials. Thus, the coupling differences might be minor. This whole subject deserves much more consideration than it has currently received.

With respect to the possible need for an increase in the size of the optics (and thus the cost) by the ratio of the wavelengths (say, 2.5) this will be so for diffraction-limited beams, but not so for jitter-limited beams. That is, for a wavelength of 400 nm, if the diffraction limited angle is 3×10^{-8} radian, corresponding to a 4 meter aperture, but jitter in the structure causes the beam to randomly move about (jitter) in a 10^{-7} radian angle, then an increase in the wavelength by a factor of 2.5 will not have to be accompanied by an increase in the size of the final optic since the beam-spreading angle is limited by jitter and not diffraction.

With respect to the third counter argument, there are indications that the jitter of large systems gets worse rapidly

with system size.[4] This would tend to favor UV wavelengths if the reflectors are the dominant massive element in the space system and if the jitter angle is less than the diffraction angle. Materials can be developed which have high damping, i.e., are effective in absorbing vibrations and thereby reducing jitter. These issues need further examination also.

ACKNOWLEDGEMENT

This paper was written under the auspices of the DARPA Materials Research Council, Contract #MDA903-80-C-0505 with the University of Michigan.

REFERENCES

1. N. Bloembergen, C. M. Stickley, and H. Winsor, "UV and Visible Excimer and Raman Coatings and Reflectors for Communications and Space Defense Applications", Proceedings of the DARPA Materials Research Council, Summer, 1981.

2. M. Sparks, "Theoretical Studies of High Power Infrared Window Materials," Second Technical Report to DARPA, Materials Sciences Office; Contract No. DAHC15-73-C-0127, 6 December 1973.

3. P. Liu, R. Yen, and N. Bloembergen, "Dielectric Breakdown Threshold, Two-Photon Absorption, and Other Optical Damage Mechanisms in Diamond", IEEE Journal of Quantum Electronics, QE-14, pp. 574-576; August 1978.

4. K. Soosar, Draper Laboratories, private communication.

MONOCLONAL ANTIBODIES AND THE DETECTION OF BIOCHEMICAL WARFARE AGENTS BY NUCLEATION PROCESSES

H. Reiss

ABSTRACT

We have investigated a method in which antibodies, specific to biochemical warfare agents as antigens, are used in conjunction with vapor phase nucleation to detect the biochemical agent.

The general scheme involves a hypothetical, volatile antibody which can be activated to bind to another antibody when it binds to the antigen so that a polymer forms which can act as a nucleating agent for a supersaturated "working" vapor such as water. The detection mechanism involves the observation of the liquid drops formed in this manner.

Leaving aside the question as to whether such antibodies can ever be formed, and whether or not they can be made specific outside of aqueous solution, we evaluate the theoretical limits of detection. We find that for reversible polymerization involving binding energies typical of antibody-antigen bonds (~5Kcal), such a method of detection would be so sensitive as to impinge on the single molecule level.

On the other hand, there are problems which transcend the production of suitable antibodies. These involve operation of an "upward" diffusion cloud chamber in an "open" mode so that the species to be detected can gain entry. The device in which

detection would be accomplished is the diffusion cloud chamber.

It is pointed out that very high levels of sensitivity in detection (and discrimination) have already been demonstrated in connection with the method of photoinduced nucleation in closed cloud chambers, and that the attempt to solve the (probably solvable) problem of operation in the "open" mode should begin with this process rather than the antibody-antigen reaction. In fact, it is strongly recommended that such a program be initiated. It is likely to be successful and very cost effective.

MONOCLONAL ANTIBODIES AND THE DETECTION OF BIOCHEMICAL WARFARE AGENTS BY NUCLEATION PROCESSES

Howard Reiss

INTRODUCTION AND MODEL

The ideas in this study are highly speculative and the analysis based on them is performed simply as a means of estimating the magnitudes which would be required of certain critical parameters (binding energies, free energies, etc.) should certain functional characteristics of antibodies or antibody-like molecules become feasible. The author is at best an educated layman in the field of molecular biology and it remains for more knowledgeable specialists to determine whether or not any of the required functional characteristics can ever be realized. With this massive disclaimer we proceed to the development of the above mentioned ideas.

We have in mind a metastable supersaturated vapor, e.g. water vapor, maintained indefinitely in that state. We would like to have water drops nucleated within this vapor only on the occasion that one or a small number of molecules of a biochemical agent enters the vapor. How this supersaturated state is to be maintained and how we are to admit the biochemical agent without triggering other processes leading to nucleation are questions whose discussion we postpone until the final sections of this study. Suffice it to say that they are difficult in themselves (but are not beyond the possibility of practical assault).

A more difficult question concerns how we manufacture the monoclonal antibody-like molecule. What we have in mind is an antibody from which all but the specific antigen attachment segment has been removed. This in itself may be possible, although the entire protein may be necessary before the specific segment may be activated. Furthermore we would like the molecule consisting of the specific segment to be small enough to be volatile so that it can eventually be a component of the supersaturated vapor. Unfortunately the "weak" forces holding the antibody to the antigen may (besides those due to hydrogen bonds) be either polar or hydrophobic[1] or both. These will not normally exist outside of aqueous solution, and so the method may be infeasible at the outset.

On the other hand there is the possibility (somewhat remote) that the process can be performed in supersaturated aqueous solution where we would be looking for precipitate[2] rather than drops. In this report, however we restrict analysis to the vapor case.

One final feature is required before we begin the analysis. We want the antibody-like molecule to have a functional group which may be activated to bind another antibody when the antigen is bound to its first binding group. Thus if we represent an antigen by a triangle

$\triangleright$ = antigen

and an antibody by the symbol,

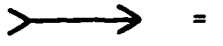 = antibody,

where the unopened "flaps" at the right end are to be noted, the binding of the antigen may be diagrammed as follows

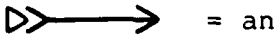 = antigen-antibody complex

where the opening of the "flaps" on the right is now to be noted. The implication is that the formation of the antigen-antibody complex activates the other end of the molecule so that it may now combine with another antibody as follows

This and the previous reactions are to be thought of as reversible. By a repetition of this process a polymeric species may be generated. This polymeric species may eventually act as a "foreign particle" assisting in the nucleation of the supersaturated vapor within which both the antigen and the antibodies are components.

The cooperative sort of interaction diagrammed above may not be entirely beyond the realm of possibility. The cooperative binding of oxygen by the four haems of the haemoglobin molecule is an example of this kind of behavior.[3]

THE EQUILIBRIUM POLYMERIZATION

We donote the partial pressure of the antigen (or contaminant) by P_c and that of the antigen by P_a. In addition the partial pressure of a "polymer" containing n antibody molecules will be denoted by P_n. We assume that all these gases behave ideally so that the respective chemical potentials are[4]

$$\mu_c = \mu^\circ_c + RT \ln P_c \quad (1)$$

$$\mu_a = \mu^\circ_a + RT \ln P_a \quad (2)$$

$$\mu_n = \mu^\circ_n + RT \ln P_n \quad (3)$$

where the μ_c°, μ_a° and μ_n° are the chemical potentials in the standard state, i.e. one atmosphere, and R is the gas constant, 82.054 cm^3 atm $mole^{-1}$ deg^{-1}. The absolute temperature is denoted by T. The law of mass action requires, at equilibrium, that for the reaction

$$M_c + M_a = M_1 \quad (4)$$

(where the M's are stoichiometric formulas)

$$\mu_1 = \mu_a + \mu_c \quad (5)$$

and, in general, for

$$M_{n-1} + M_a = M_n, \quad (6)$$

that

$$\mu_n = \mu_a + \mu_{n-1} \quad (7)$$

Substitution of Eqs. (1), (2), and (3) into Eqs. (5) and (7) gives

$$\frac{P_1}{P_a P_c} = K_1 = e^{-\Delta G^\circ_1/RT} \quad (8)$$

where

$$\Delta G_1^\circ = \mu_1^\circ - \mu_c^\circ - \mu_a^\circ \quad (9)$$

and

$$\frac{P_n}{P_a P_{n-1}} = K_n = e^{-\Delta G_n^\circ/RT} \quad (10)$$

where

$$\Delta G_n^\circ = \mu_n^\circ - \mu^\circ_{n-1} - \mu_a^\circ \tag{11}$$

where the ΔG°'s are the standard free energies of the reactions (all reactants and products at one atmosphere), and the K's are the equilibrium constants. We now make the simplification (since we are only interested in orders of magnitude) that all the ΔG°'s and hence all the K's are equal. Then the repetitive application of Eq. (10) beginning with Eq. (8) yields

$$P_n = P_c(P_a K)^n \tag{12}$$

It is convenient to use concentrations (moles cm^{-3}) instead of pressures. Then, for the respective concentrations the ideal gas law requires

$$C_c = P_c/RT \tag{13}$$

$$C_a = P_c/RT \tag{14}$$

$$C_n = P_n/RT \tag{15}$$

Substitution of these equations into Eqs. (8), (10), and (12), eliminating the pressures, gives

$$\frac{C_1}{C_a\, C_c} = RTK \tag{16}$$

$$\frac{C_n}{C_a\, C_{n-1}} = RTK \tag{17}$$

and

$$C_n = C_c(RTC_a K)^n \tag{18}$$

If the initial concentration of antigen in the vapor (before equilibration with antibody) is C_c°, then

$$C_c^\circ = C_c + C_1 + C_2 + \ldots = C_c + \sum_{n=1}^{\infty} C_n \tag{19}$$

Substituting eq (18) into this equation gives

$$C_c^\circ = C_c \left\{1 + \sum_{n=1}^{\infty} (RTC_aK)^n\right\} \tag{20}$$

and therefore

$$C_c = \frac{C_c^\circ}{1 + \sum_{n=1}^{\infty} (RTC_aK)^n} \tag{21}$$

If

$$RTC_aK > 1 \tag{22}$$

the denominator of Eq. (21) diverges, and the system is polymerized, essentially into the largest polymer. At the same time C_c will be zero, i.e. there is no free antigen. If

$$RTC_aK = p_aK < 1 \tag{23}$$

the denominator of Eq. (21) may be summed so that

$$C_c = \frac{P_c}{RT} = P_c^\circ/RT(1-P_aK) \tag{24}$$

or

$$P_c = P_c^\circ(1-P_aK) \tag{25}$$

We shall be primarily interested in cases which conform to Eq. (23).

We return, for the moment, to Eq. (16) and consider a value of K strong enough so that a fraction f of the antigen is bound in M_1 complexes at a fixed concentration C_a of antibody. (It is assumed that the antibody concentration so exceeds the antigen concentration, that C_a is unaffected by the complexation.) We also assume, just for the purpose of defining the strength of K that a constraint exists, preventing the formation of the higher order complexes M_2, M_3, etc. Then

$$C_1 = f\ C_1^{\circ} \tag{26}$$

and

$$C_c = (1-f)C_1^{\circ} \tag{27}$$

Substitution of these equations into eq (16) then gives

$$\frac{f}{1-f} = RTC_aK = P_aK \tag{28}$$

Thus p_a K may be defined in terms of f.

Clearly, if f = 0.5 so that half of the antigen is bound, $P_aK = 1$ so that total polymerization will occur. If, for example f = 0.2, then

$$P_aK = 0.25 \tag{29}$$

Furthermore, if P_a = 1 torr or 1.316×10^{-3} atm, then

$$K = \frac{0.25}{1.316\times10^{-3}} = 190 \tag{30}$$

but

$$\Delta G^{\circ} = -RT \ln K \tag{31}$$

and at T = 300°K, this implies that

$$\Delta G^{\circ} = 3.13 \text{ Kcal} \tag{32}$$

In Eq. (31) we use

$$R = 1.9872 \times 10^{-3} \text{ Kcal mole}^{-1} \text{ deg}^{-1} \qquad (33)$$

However in all other uses of R in this section, save for Eqs. (8), (10) and (31), $R = 82.054$ cm^3 atm mole^{-1} deg^{-1}.

The value of ΔG° expressed by Eq. (32) is in the range of the free energies characteristic of antibody-antigen binding. It is even somewhat low, the more typical value being somewhat in excess of 5 Kcal.[5] Nevertheless, we see that with small vapor pressures of antibody (~1 torr) reasonable binding fractions of the order of f = 0.1 to 1.0, correspond to realistic binding energies.

THE EQUILIBRIUM DISTRIBUTION OF EMBRYOS

In order to examine the role of the "polymers" of the previous section in the nucleation process we need to consider a specific system and also to choose a reasonable model for the interaction of the polymer with the condensing or nucleating vapor. Since we are only interested in order of magnitude results it is reasonable to keep things, in these respects, as simple as possible. Thus, we will assume that the concentrations of polymer species are so low that, in each developing embryo, there is at most a single polymer molecule. The working or condensing vapor we choose to be water. Furthermore, in the interest of simplicity we assume that the "surface" free energy of a single polymer molecule is identical to that of a water

droplet and that the entity formed when water molecules condense with a polymer molecule may be treated as liquid water condensed on the polymer particle rather than as a binary solution of water and polymer.

We even take further liberties. Thus, we treat a polymer molecule containing n antibodies as a spherical drop of water containing γn water molecules where γ will generally be a small number lying between 1 and 10. A polymer molecule upon which j water molecules have condensed is treated as a water drop containing $j+\gamma n$ water molecules.

If embryos containing more than one polymer molecule can form this will only increase the efficiency of the polymer molecules as nucleating agents, and therefore, the efficiency of detection. We will, however, only consider vapors containing few enough antigens so that the likelihood of this situation is remote. We also ignore embryos which may contain antigen or unbound antibody.

We begin by following the standard practice of nucleation theory, deriving the equilibrium distribution of embryos. The chemical potential per molecule of water monomers in the vapor is denoted by μ_w while in the bulk liquid (embryo) it will be denoted by ϕ_w. We have already the molar chemical potential of an n-polymer in Eq. (3), however, it is now convenient to write it for a molecule and to express it in terms of the mole fraction X_n of monomers in the vapor. Thus, we write it as:

$$\bar{\mu}_n = \bar{\mu}_n^\circ + kT\ln X_n \qquad (33)$$

where $\bar{\mu}_n^\circ$ is a function only of temperature and total pressure. The chemical potential of the polymer in the embryo will differ from that in the vapor in two respects. First, the free energy of mixing, characterized by the term $kT\ln X_n$ in Eq. (33), will be absent, although it will, in essence be accounted for by the pro per assignment of the free energy of mixing of the embryo itself, regarded as one of the vapor species. Second, the portion of $\bar{\mu}_n^\circ$ which is due to the surface free energy of the polymer is subsumed into the total surface free energy of the drop. Hence, this surface free energy should be subtracted $\bar{\mu}_n^\circ$ which remains in order to obtain ϕ_n, the chemical potential in the embryo. Thus:

$$\phi_n = \bar{\mu}_n^\circ - \text{surface free energy} \tag{34}$$

Since the surface of an n-mer is to be treated as though it were the surface of a water droplet containing γn water molecules, we have for the surface free energy;

$$\text{surface free energy} = 4\pi^2 r^2 \sigma \tag{35}$$

where r is the radius of the drop and σ the surface tension of water. Furthermore, if v is the volume per molecule in liquid water;

$$r = \left(\frac{3v\gamma n}{4\pi}\right)^{1/3} \tag{36}$$

and so equation (35) becomes;

$$\text{surface free energy} = 4\pi\sigma\left(\frac{3v}{4\pi}\right)^{2/3}(\gamma n)^{2/3} \tag{37}$$

and equation (34) becomes;

$$\phi_n = \bar{\mu}_n^\circ - 4\pi\sigma\left(\frac{3v}{4\pi}\right)^{2/3}(\gamma_n)^{2/3} \tag{38}$$

Now the free energy of an embryo containing an n-mer and j water molecules is;

$$\mu_{n+j}^\circ = \phi_n + j\phi_w + 4\pi\sigma\left(\frac{3v}{4\pi}\right)^{2/3}(j+\gamma n)^{2/3} \tag{39}$$

where the last term on the right is the surface free energy of the embryo as a whole. We obtain μ_{n+j}, the chemical potential of the embryo regarded as a species of the vapor phase by adding to μ_{n+j}° the appropriate entropy of mixing term, namely;

$$kT\ln X_{n+j} \tag{40}$$

where X_{n+j} is the mole fraction of embryos in the vapor. Thus,

$$\mu_{n+j} = \phi_n + j\phi_w + 4\pi\sigma\left(\frac{3v}{4\pi}\right)^{2/3}(j+\gamma n)^{2/3} + kT\ln X_{n+j} \tag{41}$$

Use of Eq. (38) turns this into;

$$\mu_{n+j} = \bar{\mu}_n^\circ + j\phi_w + 4\pi\sigma\left(\frac{3v}{4\pi}\right)^{2/3}(j+\gamma n)^{2/3} - (\gamma n)^{2/3} + kT\ln X_{n+j} \tag{42}$$

The law of mass action[6] for the equilibrium between water molecules in the vapor, n-mers, and embryos is;

$$\mu_{n+j} = j\mu_w + \bar{\mu}_n \tag{43}$$

Substitution of Eqs. (33) and (42) into this equation yields;

$$X_{n+j} = X_n\, e^{-W_{n+j}/kT} \tag{44}$$

where;

$$W_{n+j} = j(\phi_w - \mu_w) + 4\pi\sigma\left(\frac{3v}{4\pi}\right)^{2/3}\left[(j+\gamma n)^{2/3} - (\gamma n)^{2/3}\right] \qquad (45)$$

is the free energy or reversible work of formation of the embryo from n-mer and water molecules. Several convenient changes are possible in Eqs. (44) and (45). In the first place we multiply both side of Eq. (44) by the total number of molecules in a cubic centimeter of vapor to obtain;

$$N_{n+j} = Ne^{-W_{n+j}/kT} \qquad (46)$$

where Nn_{+j} and N_n are the numbers of embryos and n-mers per cubic centimeter, respectively. Second, we note that because the vapor is assumed ideal we may write μ_w in the form;

$$\mu_w = B_w(T) + kT\ln P_w \qquad (47)$$

where P_w is the partial pressure of water in the vapor. If the vapor is just saturated then $\mu_w(sat)$, the chemical potential at saturation, is, except for a very small term accounting for the variation of pressure on the liquid, equal to ϕ_w. Hence, we may write;

$$\mu_w(sat) = B_w(T) + kT\ln P_{ws} = \phi_w \qquad (48)$$

where P_{ws} is the saturation pressure, or equilibrium vapor pressure, of water at temperature T. Eliminating B_w between Eqs. (47) and (48) gives;

$$\phi_w - \mu_w = -kT\ln S \qquad (49)$$

where;

$$S = P_w/P_{ws} \tag{50}$$

and is the familiar "supersaturation".

Substitution of equation (49) into equation (45) gives;

$$W_{n+j} = -jkT\ln S + \alpha(j+\gamma n)^{2/3}-(\gamma n)^{2/3} \tag{51}$$

where we have introduced;

$$\alpha = 4\pi\sigma\left(\frac{3v}{4\pi}\right)^{2/3} \tag{52}$$

Combining Eqs. (46) and (51) we then have;

$$N_{n+j} = N_n \exp\{j\ln S - \frac{\alpha}{kT}\left[(j+\gamma n)^{2/3}-(\gamma n)^{2/3}\right]\} \tag{53}$$

We not substitute Eq. (28) into Eqs. (12) and (25), obtaining;

$$P_n = \frac{P_c^{\circ}(1-2f)}{f}\left(\frac{f}{1-f}\right)^n \tag{54}$$

In Eqs. (12) and (25) the pressures are measured in atmospheres so the pressures in Eqs. (54) are in atmospheres. However, the same proportionality factor converts both sides of Eq. (54) into any other units. Thus, Eq. (54) holds for any units. If, for example, we use dyne cm^{-2} and express k as erg $molecule^{-1}$ deg^{-1}, then Eq. (54) becomes;

$$N_n = \frac{P_c^{\circ}(1-2f)}{kTf}\left(\frac{f}{1-f}\right)^n \tag{55}$$

where, again, N_n is in molecules cm^{-3} and P_c° is expressed in dyne cm^{-2}. If P_c° is expressed in torr we get;

$$N_n = \frac{1315.79 P_c^\circ(\text{torr})(1-2f)}{kTf}\left(\frac{f}{1-f}\right)^n \qquad (56)$$

Substitution of this formula into Eq. (53) gives;

$$N_{n+j} = \frac{1315.79 P_c^\circ(\text{torr})(1-2f)}{kTf}\left(\frac{f}{1-f}\right)^n \exp\left\{j\ln S - \frac{\alpha}{kT}\left[(j+\gamma n)^{2/3} - (\gamma n)^{2/3}\right]\right\} \qquad (57)$$

in which k is expressed in erg $molecule^{-1}$ deg^{-1}.

This formula contains a hidden approximation which we must still discuss. This is the fact that Eq. (25) which we have used is based upon Eq. (19), which takes no account of the polymers which are in embryos. Normally, only a small fraction of polymers will be parts of embryos because the equilibrium number of embryos will be much smaller than the total number of polymers. For this reason we neglect this effect.

THE NUCLEATION RATE

The most modern procedure in nucleation theory recognizes that the process is a kinetic, and not an equilibrium one, and makes a real attempt to work with a non-equilibrium, steady state distribution of embryos. This does not normally introduce a substantial change into the predicted value of the critical supersaturation S_c, i.e., the value of S at which catastrophic collapse of the supersaturated state occurs, although it does introduce a sizeable change in the actual rate of nucleation it-

self. The more sophisticated theory is more complicated and, indeed, very much more complicated, for a multi-component system such as the one under investigation.[7]

Consequently, since we will only be interested in evaluating the critical supersaturation we will attempt the cruder derivation of the nucleation rate, using only the equilibrium distribution of embryos.

The general picture is as follows. For a supersaturated system, W_{n+j} appearing in Eq. (51), when plotted as a function of n and j, is a surface exhibiting a "ridge" over which the embryos, on the way to becoming drops, must grow. The ridge is characterized by the equation;

$$\left(\frac{\partial W_{n+j}}{\partial j}\right)_{j=j^*(n)} = 0 \qquad (58)$$

where $j^*(n)$ is the value of j at the ridge for each value of n. We are approximating the integers j and n as continuous variables. The growth or "flow" over the ridge is very slow (until the metastable state collapses) and so the embryos "behind" the ridge are in quasi-equilibrium and are characterized by the equilibrium distribution, Eq. (57).

Since each embryo can at the most contain only one polymer molecule the growth must occur by the addition of water molecules. The rate of nucleation is then determined by the rate at which water molecules hit and stick to embryos on the ridge. A ridge embryo which acquires a water molecule immedi-

ately grows "downhill" on the free energy surface and becomes a liquid drop. The ridge embryos are the nuclei and the rate of drop formation is the rate of nucleation.

Consider a particular "ridge" embryo of size $n+j^*(n)$, having an equilibrium concentration N_{n+j^*}. The surface area of such an embryo is;

$$4\pi\left(\frac{3v}{4\pi}\right)^{2/3}(j^*+\gamma n)^{2/3} \tag{59}$$

If we assume (as is usual in nucleation theory) that the velocity distribution of water molecules is Maxwellian, the rate at which water molecules strike one square centimeter of planar surface is;

$$\frac{1315.79P_w}{\sqrt{2\pi mkT}} \tag{60}$$

where k is expressed in erg molecule^{-1} deg^{-1} and P_w in torr. The quantity m is the mass of the water molecule expressed in grams. If we ignore the curvature of the embryo surface, the rate at which embryos of size $n+j^*$ are hit by water molecules is the product of the quantities in Eqs. (59) and (60). Furthermore, if it is assumed that every molecule that hits also sticks, the rate of nucleation per cubic centimeter will be given by the above product multiplied by N_{n+j^*}, and <u>summed</u> over n, in order to include the contributions of all the ridge embryos. Thus, the nucleation rate per cubic centimeter is;

$$J_c = \sum_{n=1}^{\infty} \frac{1315.79P_w}{\sqrt{2\pi mkT}} \left\{4\pi\left(\frac{3v}{4\pi}\right)^{2/3}(j^*(n)+\gamma n)^{2/3}\right\}N_{n+j^*(n)} \tag{61}$$

However, this is only the nucleation rate due to antigen. There is also a homogeneous nucleation rate characteristic of the pure water vapor which exists independently of whether antigen is present or not. This is obtained in a manner similar to that which led to Eq. (61). In this case, however, we have only one term to deal with rather than a sum since there is no n to consider. In fact if we take a typical term of Eq. (61) and replace the bracketed factor by:

$$4\pi\left(\frac{3v}{4n}\right)^{2/3}(j)^{2/3} \tag{62}$$

and $N_{n+j^*(n)}$ by;

$$N_{j^*} = \frac{1315.79P_w}{kT}\, e^{-Wj^*/kT} \tag{63}$$

where again P_w is expressed in torr, and where W_{j^*} is the reversible work of forming an embryo of j water molecules, we will have the correct expression for nucleation in pure water vapor, namely;

$$J_w = \frac{1315.79P_w}{\sqrt{2\pi mkT}} \left\{4\pi\left(\frac{3v}{4\pi}\right)^{2/3}(j^*)^{2/3}\right\} N_{j^*} \tag{64}$$

Now;

$$W_j = -kTj\ln S + \alpha j^{2/3} \tag{65}$$

where;

$$\alpha = 4\pi T\left(\frac{3v}{4\pi}\right)^{2/3} j \tag{66}$$

and j^* is determined as the root of;

$$\left(\frac{\partial W_j}{\partial j}\right)_{j=j^*} = 0 \tag{67}$$

The total rate of nucleation is then:

$$J = J_C + J_W \tag{68}$$

To put all this together, we require both $j^*(n)$ and j^*. Substituting Eq. (51) into Eq. (58), and Eq. (65) into Eq. (67), and solving for the respective roots gives

$$j^*(n) = \left(\frac{2\alpha}{3kT\ln S}\right)^3 - \gamma n \tag{69}$$

and;

$$j^* = \left(\frac{2\alpha}{3kT\ln S}\right)^3 \tag{70}$$

If we substitute these expressions back into Eqs. (51), and (65), respectively, we obtain;

$$W_{n+j^*(n)} = \gamma nkT\ln S - \alpha(\gamma n)^{2/3} + \frac{1}{3}\left(\frac{2\gamma}{3kT\ln S}\right)^2 \tag{71}$$

and;

$$W_{j^*} = \frac{1}{3}\left(\frac{2\alpha}{3kT\ln S}\right)^2 \tag{72}$$

Substitution of Eqs. (71) and (72) into Eqs. (57) and (63) and of the results into Eqs. (61) and (64), in which we also separately use Eqs. (71) and (72), and, finally, substitution of Eqs. (61) and (64) into Eqs. (68), gives;

$$\begin{aligned} J = {} & \frac{1315.79 P_W}{\sqrt{2\pi mkT}} \left\{\frac{\alpha}{\sigma}\left(\frac{2\alpha}{3kT\ln S}\right)^2\right\} \\ & \cdot \left\{\frac{1315.79\ P_W}{kT}\right\} e^{-\frac{1}{3kT}\left(\frac{2\alpha}{3kT\ln S}\right)^2} \\ & + \frac{1315.79\ P_C^{\circ}(1-2f)}{kTf}\ e^{-\frac{1}{3kT}\left(\frac{2\alpha}{3kT\ln S}\right)^2} \end{aligned} \tag{73}$$

$$\cdot \sum_{n=1}^{\infty} \left[\frac{f}{(1-f)S^{\gamma}}\right]^{n} e^{\frac{\alpha}{kT}(\gamma n)^{2/3}}$$

in which all the pressures are expressed in torr and k in erg molecule^{-1} deg^{-1}.

J varies so rapidly with S as the critical supersaturation, S^c, is approached that the point of collapse of metastability may be chosen without loss of accuracy to be simply at J equal to unity. Then one sets J = 1 in Eq. (73) and simply solves for the root S which satisifies the resulting equation. This value of S is the critical supersaturation, S_c. The critical supersaturation in the absence of antigen, i.e., for pure water vapor is obtained by setting J = 1 and $P_c^{o} = 0$, in Eq. (73), solving again for S_c as the root of the resulting equation.

Actually Eq. (73) can be simplified by treating n as a continuous variable and replacing the sum by an integral. Then it turns out that the integral can be evaluated by a peak integration. To simplify the notation we write:

$$\frac{f}{(1-f)S^{\gamma}} = \lambda \tag{74}$$

Then, the sum in Eq. (73) may be expressed as:

$$\sum_{n=1}^{\infty} \exp\left\{n\ln\lambda + \frac{\alpha}{kT}(\gamma n)^{2/3}\right\} \tag{75}$$

or, by the integral:

$$I = \int_{1}^{\infty} \exp\left\{n\ln\lambda + \frac{\alpha}{kT}(\gamma n)^{2/3}\right\} dn \tag{76}$$

The exponent in Eq. (76) has a maximum at:

$$n^* = \left(\frac{2\alpha}{3kT \ln\gamma \frac{I}{\lambda}}\right)^3 \gamma^2 \tag{77}$$

and the integrand, a sharp maximum. We expand the exponent about n^*, keeping only terms as far as the one in $(n-n^*)^2$. The limits of integration can now be chosen as $-\infty$ to ∞ for $n-n^*$ without appreciable error. The integrand becomes a Gaussian, and the result for I is:

$$I = \frac{2(2\gamma^{2/3}\pi/kT)^{1/2}}{3\ (\ln\lambda)^2} \exp\left\{\left(\frac{2}{3kT}\right)^3 \left(\frac{\alpha\gamma}{\ln\lambda}\right)^2\right\} \tag{78}$$

Replacing the sum in Eq. (73) by I, eliminating λ by Eq. (74), and writing P_w in the form:

$$P_w = SP_{ws} \tag{79}$$

where P_{ws} is the saturation pressure of water, we obtain:

$$\begin{aligned} J = {} & \frac{1315.79SP_{ws}}{\sqrt{2\pi mkT}} \left\{\frac{\alpha}{\sigma} \left(\frac{2\alpha}{3kT\ln S}\right)^2\right\} \\ & \cdot \left\{\frac{1315.79P_{ws}}{kT} e^{-\frac{\alpha}{3kT}\left(\frac{2\alpha}{3kT\ln S}\right)^2}\right. \\ & + \frac{1315.79P_c^{\circ}(1-2f)}{kT(1-f)} e^{-\frac{\alpha}{3kT}\left(\frac{2\alpha}{3kT\ln S}\right)^2} \\ & \left. \cdot 3\gamma\left(\frac{kT\pi}{\alpha}\right)^{1/2} \left(\frac{2\alpha}{3kT\ln\left[\frac{(1-f)S^{\gamma}}{f}\right]}\right)^2 \exp\left[\frac{\alpha}{3kT}\left(\frac{2\alpha\gamma}{3kT\ln\left[\frac{(1-f)S^{\gamma}}{f}\right]}\right)^2\right]\right\} \end{aligned} \tag{80}$$

Again, we obtain S_c from the root of this equation with J set equal to unity.

APPLICATION

In this section we apply Eq. (80) to some typical systems and discuss the results. We choose a system in which the partial pressure of antibody is low enough to be ignored in the nucleation process (but not in the polymer equilibrium) so that the theory of the preceding sections will be valid. This means that we do not (as we have not considered) consider the possibility of binary nuclei containing no polymers but only water and antibody. A suitably low partial pressure in this respect is:

$$P_a = 0.1 \text{ torr} = 1.316 \times 10^{-4} \text{ atm.} \qquad (81)$$

Since water vapor pressures in the system, as we shall see, will be generally of the order of 60 torr, P_a will be only 1.67×10^{-3} of this value. Equations (28) and (31) then require the following free energy of binding (Table 1) in order to establish various values of f at T = 300°K.

Table 1

Temperature = 300°K

f	ΔG° (Kcal)
0.1	4.017
0.3	4.822
0.4	5.085

at 300°K:

$$P_{ws} = 26.7 \text{ torr} \tag{82}$$

$$T = 72 \text{ dynes/cm} \tag{83}$$

$$v = 3\text{x}10^{-23}\text{cm}^3 \tag{84}$$

Furthermore, we choose:

$$\gamma = 3 \tag{85}$$

and we also have:

$$m = 3\text{x}10^{-23} \text{ g} \tag{86}$$

We have substituted these values into Eq. (80), set J=1, and solved for the root S_c corresponding to various choices of f and P_c^o. The results are listed in Table 2.

If P_c^o is set equal to zero in Eq. (80) then we have the case of homogeneous nucleation of pure water vapor. At 300°K, given the parameters of Eqs. (82) through Eq. (86), it turns out that:

$$S_c(\text{pure } H_2O) = 3.05 \tag{87}$$

None of the entries for S_c in Table 2 are as high as this so that, in principle, we should be able to detect the antigen at the specified levels of P_c^o by the drops which it causes to appear when $S=S_c$. To form some idea of concentrations of antigen involved, we should note that $P_c^o = 10^{-8}$ torr corresponds to $3.19\text{x}10^{-8}$ molecules of antigen per cubic centimeter while 10^{-16} torr represents 3.18 molecules per cubic centimeter. Thus, if the hypothetical system could be created, the detectability available in Table 2 extends down to the single molecule

Table 2

P_α (torr)	$\Delta G°$(kcal)	f	$P_c°$ (torr)	S^c
0.1	4.017	0.1	2.717×10^{-8}	2.9
0.1	4.017	0.1	2.844x10-^{9}	3.0
0.1	4.822	0.3	1.356×10^{-8}	2.4
0.1	4.822	0.3	9.757×10^{-11}	2.5
0.1	4.822	0.3	1.706×10^{-12}	2.6
0.1	4.822	0.3	3.516×10^{-15}	2,8
0.1	4.822	0.3	3.196×10^{-16}	2.9
0.1	5.085	0.4	3.910×10^{-10}	2.1
0.1	5.085	0.4	7.876×10^{-13}	2.2
0.1	5.085	0.4	6.806×10^{-15}	2.3
0.1	5.085	0.4	1.629×10^{-16}	2.4

level. The last entry in the table indicates that at $S_c = 2.4$ a P_c^o of 1.629×10^{-16} can be detected. This corresponds to about five molecules for cubic centimeter.

SOME CAVEATS

We conclude this analysis with a discussion of the problems which are bound to arise in an attempt to actually realize the scheme so far discussed. The problems are multiple and difficult. Some of them are not beyond solution; others may be.

The author is not an expert in molecular biology, but it appears to him that the most diffcult problem involves the production of an antibody fragment which will retain its specificity for the antigen, be easily vaporizable, and also be capable of activation so that the process of polymerization can occur. A fundamental difficulty in this respect is the fact that the mechanism of specificity almost certainly involves, among other things, hydrophobic bonding which will be largely absent in the vapor, but may be present in a developing embryo which has some of the characteristics of an elementary aqueous solution.

A somewhat qualitative by-product of this analysis based on the demonstrated sensitivity of the method in the vapor, is the likehood that the process could be carried out in supersaturated aqueous solution rather than in the vapor. However, the physical problems of instrumentation, maintenance of long term supersaturation, and avoidance of false alarms make this

possibility a question for an entirely separate anlaysis which we do not attempt here.

However, beyond the problem of securing the antibody there are others which, though probably solvable, are by no means simple. The apparatus within which the vapor process is envisioned to occur is an "upward" diffusion cloud chamber.[8] This instrument is indeed capable of maintaining steady states of supersaturation for indefinite periods of time. This is a demonstrated fact. Very high levels of detection sensitivity, in a microanalytical sense, have also been demonstrated for this apparatus.[9,10,11] So the capability to detect is also a fact. However, all of this detection has been limited to a closed system, and this restriction would have to be removed before the device could be used to monitor the environment.

To understand all of this, it is necessary to have a rough picture of the cloud chamber configuration. It usually consists of two circular metal plates separated vertically by a glass cylinder which may have optical windows and ports (for the addition and removal of gases and liquids) in it. The temperatures of the plates can be individually controlled. A shallow pool of working fluid (e.g., water) lies on the bottom plate. The space above the fluid contains an inert gas such as helium at a pressure of about one atmosphere. The lower plate is maintained at a higher temperature than the upper one. Hence, the system is heated from below, and the working liquid evaporates from the pool, diffuses through the helium, and condenses

on the cooler plate, above, where it drains to the glass cylinder and returns to the pool. It is this "upward" diffusion of working vapor which gives rise to the word "upward" in the description of the apparatus.

Heating from below introduces the possibility of deleterious convection, and special precautions are necessary to avoid this phenomenon. Convection problems have, however, been solved. The use of a light inert gas such as helium is part of the solution, taking advantage of the fact that the lower and warmer regions of the vapor will be mass loaded with the heavier molecules of the working fluid. Another part of the solution involves establishing conditions in the pool such that the first critical Raleigh number is not exceeded.

In any event, a scenario can be established in which a steady state of upward diffusion and reflux of the working fluid occurs such that steady gradients of temperature and partial pressure of working vapor occur. These gradients combine to produce a steady state of supersaturation for the working vapor which has its maximum at an elevation lying about three-quarters of the distance between the plates.

A key feature of the chamber is that it is "self-cleaning". Thus, if "particles" which can act as heterogeneous nuclei are present they are encapsulated by drops and fall-out of the vapor. Clearly this phenomenon is facilitated by the closedness of the chamber. To a certain extent, the control of convection is also made possible by the closedness of the system.

However, in order to perform chemical analysis it is necessary to open the system, so as to allow the species to be detected to enter. This leads to the possibility of introducing new and additional heterogeneous nuclei as well as to the initiation of convection. It is very probable that additional nuclei can be removed by modern methods of filtration, but the "upward" configuration is inherently so unstable that the avoidance of convection is another matter. On the other hand, some preliminary experiments have been performed with very slow flows (e.g., one cubic centimeter per minute in a two liter chamber) which indicates that the convection problem can also be solved.

If one wished to monitor multiple antigens, it would be necessary to include in the chamber vapors, an array of antibodies whose specificities cover the range of antigens involved. Aside from producing the antibodies, there is no additional problem associated with such multiple detection. However, one could not distinguish between the various antigens in this manner. Discrimination would require a separate chamber for each antigen. On the other hand, the cloud chamber would most likely be used as a stationary, rear zone, monitor and such duplication should also not pose a serious problem.

Up until now, detection in closed cloud chambers has been limited to methods involving photoinduced nucleation. In these methods the species to be detected is induced to undergo photo-chemical conversion through irradiation with light of definite wavelength. The photochemical product is a molecule

(e.g., a polymer, but also non-polymer species) of low volatility which can nucleate drops in the supersaturated working vapor. These drops are detected by light scattered from them. Specificity is achieved by selecting the wavelength of the light to match the photochemistry of the species to be detected. Thus, discrimination between multiple species is achievable in a single chamber.

Since photo induced nucleation is a demonstrated method of detection it would probably be useful to develop the "open" mode for the chamber by concentrating first on detection using this phenomenon. It may itself, rather than the antibody scheme, provide the ultimate method for delection of biochemical warfare agents. Later, if antibody-like molecules can be produced, the lessons learned about "open" operation can be transferred to that method.

As a matter of fact, since almost nothing is known about the "open" mode and since the capability of detection has already been demonstrated in the "closed" mode, it would be very useful to initiate a project, at this time, aimed at investigating the "open" mode. It would not be very expensive, and almost certainly cost effective.

ACKNOWLEDGEMENT

This paper was written under the auspices of the DARPA Materials Research Council, Contract #MDA903-80-C-0505 with the University of Michigan.

REFERENCES

1. M. V. Vol'kenshtein, "Molecules and Life", pp. 185-189 (Plenum Press, 1970)

2. Ibid, p. 361

3. G. H. Haggis, "Introduction to Molecular Biology", p. 289 (Longmar Group, 1974)

4. G. W. Castellan, "Physical Chemistry", 2nd edition, p. 231 (Addison-Wesley, 1971)

5. M. V. Vol'kenshtein, "Molecules and Life", p. 370 (Plenum Press, 1970)

6. G. W. Castellan, "Physical Chemistry", 2nd edition, pp. 236-238 (Addison-Wesley, 1971)

7. H. Reiss, J. Chem. Phys. 18 841 (1950)

8. J. L. Katz, J. Chem. Phys. 52 4733 (1970)

9. D. C. Marvin and H. Reiss, J. Chem. Phys. 69 1897 (1978)

10. J. L. Katz, F. C. Wen, T. McClaughlen, R. J. Reusch, and R. Partch, Science 196 1203 (1977)

11. A. W. Gertler, J. O. Berg, and M. A. El-Sayed, Chem. Phys. Letters 57 343 (1978); A. W. Gertler, B. Almeida, M. A. El-Sayed, and H. Reiss, Chem. Phys. 42 429 (1979).

AN EVALUATION OF SEMI-CONDUCTING BIO-SYSTEMS AS DETECTORS FOR CHEMICAL AGENTS

A. H. Francis

INTRODUCTION

The organo-phosphorus chemical warfare agents (nerve agents) are known to act strongly against the human cholinergic nervous system. The organo-phosphorus agents, as a class of chemicals, are strong phosphorylating agents which react with the hydrolytic enzymes (peptidases and esterases) containing the serine amino acid residue(I) in the catalytically active site

I.

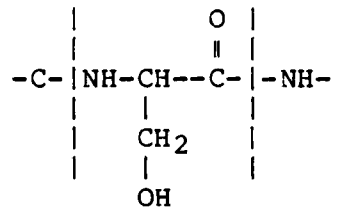

The normal enzymatic function, hydrolysis of the neuro-transmitter acetylcholine(II), is effectively blocked by the irreversible phosphorylation of the serine hydroxyl group(III).

II.

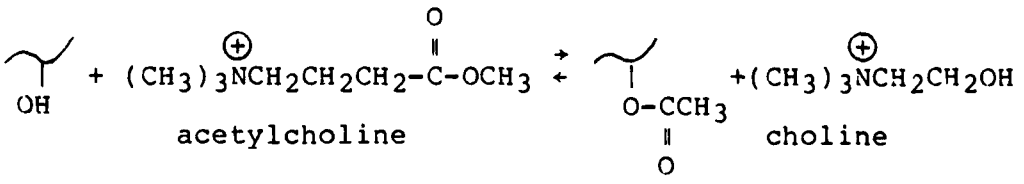

acetylcholine choline

III.

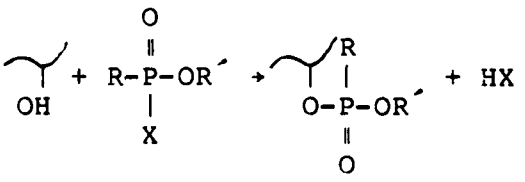

It is desired to obtain a detector for organo-phosphorus nerve agents which utilizes their characteristic anti-colergenic behavior. It has been suggested that such a detector might usefully employ protein substrates to obtain some degree of selectivity toward nerve agents. Further, it is suggested that the semi-conducting properties of biological materials such as proteins might be sensitive to surface or bulk chemi-sorption of organo-phosphorus compounds. Changes in the dielectric constant or the conductivity of the protein could then be used to indicate the presence of nerve agent. In the following sections, several aspects of this approach are developed in greater detail.

LITERATURE BACKGROUND

There is a considerable literature dealing with the semi-conductivity of biological materials, which is part of the larger subject of the semi-conductivity of organic materials. A great variety of organic materials behave as semiconductors in the restricted sense that the conductivity increases exponentially with increasing temperature according to Eq. 1.

$$\rho = \rho_o \, e^{-E/kt} \tag{1}$$

where E is the "band gap". It should be emphasized that this behavior does not in itself establish the existence of a semiconducting "band gap" in organic materials since a great many processes in materials exhibit exponential behavior (i.e., activated hopping conduction).

TABLE I

Effect of gas adsorption on conductivity of molecular solids (majority charge carrier = holes).

Gas	Type	Conductivity Change
NO_2	strong	reversible decrease
Cl_2	acceptor	
O_2		
I_2		
NO	weak	reversible decrease
SO_2	acceptor	
HCl		
HCN		
BF_3		
N_2		
CO_2	neutral	none
A	behavior	
C_2H_{12}		
$(CH_3)_3P$		
NH_3		
$(CH_3)_3N$		
C_2H_5OH	weak donor	reversible increase
$(CH_3)_2CO$		
H_2O		
$(C_2H_5)_2O$		

Organic Molecular Solids

The specific conductivity of most organic molecular solids (i.e., anthracene, naphthalene, etc.) is extremely small. Direct measurement methods yield ρ_o values of order 10^{-18} ohm^{-1}cm^{-1}. There is substantial evidence, however, that the conductivity is dominated by carrier injection from the electrical contacts employed. When 'contactless' measurements of conductivity have been made, values of ρ_o are typically $\sim 10^{-20}$ ohm^{-1}cm^{-1}.

The activation energies for organic semi-conductors vary over a wide range (1-3eV) and are strongly dependent upon chemical and mechanical composition. Additionally, it is important to note that the activation energy for surface conduction is typically considerably smaller for bulk conduction.

In view of the extremely low conductivity of most organic semiconductors, it has been widely held that semiconduction in these materials is extrinsic, since it is extremely difficult to achieve the levels of chemical purity necessary to eliminate extrinsic charge carriers at these low levels. Moreover, electrode injection, as noted above, may contribute extrinsic charge carriers. The results of several measurements on the sensitivity of organic semiconductivity to adsorbed gases support this point of view. When the majority carriers are electrons, electron donating gases increase conductivity and electron accepting gases decrease conductivity. When the majority carriers are holes, the behavior is reversed. The process

is represented schematically below.

Electron donating Electron accepting

For strong electron acceptors/donors, the semiconductivity is effected irreversibly, while for weaker acceptors/donors, the effect is reversible upon desorption of the gas. Finally, adsorption of some gases has no appreciable effect on the conductivity. Experimental results[2] for several gases are summarized in Table I.

Semi-conductivity in organic materials appears to be quite general and largely independent of the physical/mechanical properties of the sample. Thus, semiconducting behavior is exhibited by vitreous, amorphous, crystalline and many polymeric organic materials. The range of organic semiconducting behavior is illustrated by the experimental data[1] in Table II.

It is not clear from the available experimental evidence whether gas adsorption effects conductivity solely through carrier (electron or hole) injection. Gas adsorption may effect directly the mechanism of intrinsic charge carrier production.[3]

Generally, the effect of gas pressure on conductivity has been found to follow a Langmuir isotherm indicating that one type of chemisorption site usually dominates and that the effect is saturated with monolayer coverage. It is significant that

TABLE II

Semiconducting parameters for some selected Organic Materials

Material	E(eV)	$\rho_o(ohm^{-1}cm^{-1})$	$\mu(cm^2v^{-1}sec^{-1})$
polyglycine	1.5	2×10^6	
β-protein	1.4	$\sim10^{+18}$	10^4
hemoglobin	1.4	4×10^4	
anthracene	1.4	1×10^2	3
Nucleic Acid	1.2	3×10^3	
heme	0.8?	1.6×10^{-3}	
Phthalocycnine	0.7?	8×10^{0}	2

only small changes in conductivity upon surface adsorption result when the number of bulk charge carriers is large compared to the number of surface adsorbed species.

Correlations have been demonstrated between the number of π-electrons and the resistivity of an organic semiconductor. Generally, the activation energy decreases with an increase in the number of delocalized π electrons in the molecular unit. A simple model for organic semiconductivity has been developed[4] which invokes tunnelling by electrons and holes through the potential barriers between non-bonded molecular units and free conduction within the delocalized π-electronic structure of the molecular units themselves.

Bio-Materials

Semi-conductivity in proteins and amino-acids has been investigated by Eley and his coworkers[5] and in serum albumin by Douzou and Thuillier.[6] Dry amino-acids and proteins behave like semi-conductors with energy gaps in the range 1.2-1.5 eV and resistivities typically 10^{18} ohm-cm. Conductivity is associated with π-electrons moving in the C=O•••H-N bridges which are a common feature of most proteins. Thus, the conductivity of glycine is greater parallel to the hydrogen bonds than perpendicular (See IV).

Molecular orbital theory has been used to calculate the band structure of electrons moving in the hydrogen bonded system of a β-protein (IV).

IV.

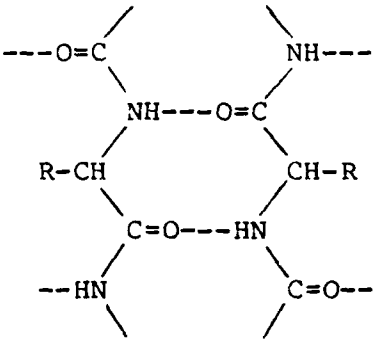

The energy levels fall into three narrow bands (~0.2 eV) the lower two are filled and the upper is empty.[7] If nitrogen is assumed to have an sp^2 hybridization a 1.50 eV bandgap is calculated in good agreement with experiment.

Adsorbed water strongly effects the semiconducting behavior of proteins, principally by decreasing the apparent bandgap. Thus, it has been suggested that the dominant charge carriers may be protons associated with water molecules structurally bound to the protein. The chemi-sorption of small amounts of electron acceptors on n-type semiconducting proteins is known to effect conduction dramatically by hole injection leading to p-type conduction.

Electron mobilities which have been reported for many proteins are unexpectedly large (10^4 cm^2/V sec). According to the band model applied to semi-conducting proteins, electrons and holes move with high mobility within the protein molecular unit and make tunnelling transitions through the potential barrier between non-bonded units. In this manner rather large charge displacements and high mobilities are achieved (See Table II).

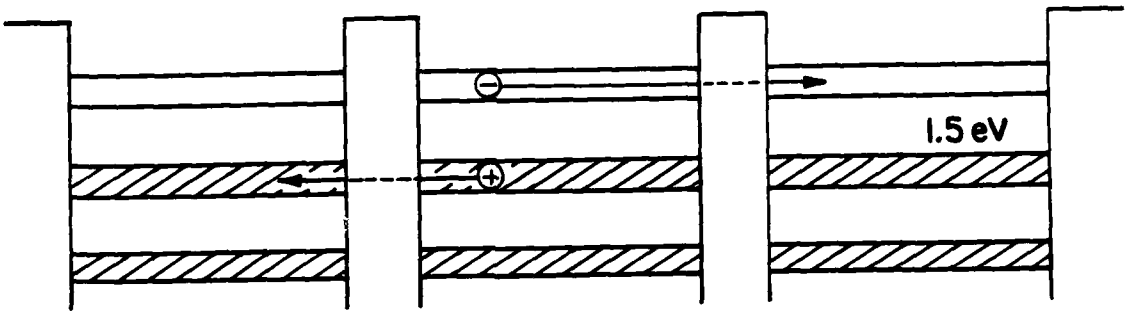

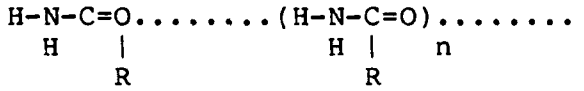

Polymers

Semi-conducting behavior has been observed in a great many polymeric materials. Strong surface adsorption properties are possessed by many polymers which are exploited in a variety of specific applications (extraction, ion-exchange, etc.). Moreover, in many polymers adsorption is accompanied by a change in electrical conductivity.

For example, the adsorption of H_2O or H_2S on p-type polyphthalocyanine results in electron donation from the adsorbate to the polymer which then becomes n-type. Chemisorption of molecular iodine on n-type polypyrrole converts it to p-type behavior while adsorption of H_2O enhances its n-type characteristics. As with adsorption on inorganic semiconductors, there is considerable synergism and addition at one site makes more difficult removal from or addition to another. For example, adsorption of hydrogen by polymers containing sp^2 non-bonding

electron pairs (polypyrroles, polypyridines, polyimidazoles) inhibits further electrophilic attack by delocalization of the positive charge.

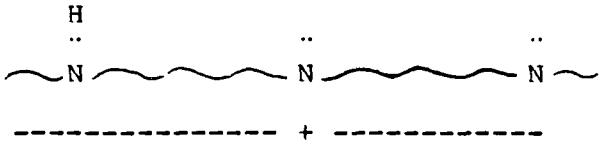

Similar effects may be observed for acidic groups. The general behavior is similar to the transfer of electrons from donor site to acceptor site through the conducting network of many carbons (chars, blacks, coals, etc.) Little use appears to have been made of these effects either scientifically or technologically.

Evaluation

There are a variety of scientific and technological problems associated with the development of an electronic chemical sensor (ECS). A useful ECS must ultimately control a specific electronic process by a specific chemical process, and, therefore, both chemical and electrical structures are involved.

Electronic Structure: Several electronic structures have been employed successfully in ECS devices and the entire field of chemical effects in electronic devices has recently been reviewed.[8] Chemical field effect transistors (CFET) and ion specific electrodes are two well-known examples. The principal advantage of ECS devices is their relatively low cost and simplicity of design. As an electronic structure, the CFET is a

high impedance, capacitative device and is susceptible to electronic interferences. This is not regarded as a major operational difficulty. The CFET functions by adsorption of the target chemical in the gate region of a conventional FET structure. Chemi-sorption must result in the flow of a small displacement current, in order to create a displacement field at the gate. To achieve this result, the chemical structure at the absorbing surface must be carefully designed. The selective detection of the ions of potassium and hydrogen in solution using a CFET has been demonstrated. Selectivity with respect to hydrogen is achieved by coating the gate region of the device with palladium which is selectively permeable to H_2. Neutral carrier molecules (crown ethers) have been utilized in a CFET sensitive to potassium ion. Selectivity toward large molecules will undoubtedly require more complicated chemical structures. Work to date using CFET detectors has concentrated on the measurement of concentrations in aqueous solution. Adsorption from solution is a far more selective process than adsorption from a gas as a result of solvent-solute interactions. Thus, the demonstration of specificity in the gas phase CFET is likely to be more difficult.

Chemical Structure

The major difficulties in the development of ECS devices appears to be in the development of a chemical structure which will:

1. Selectively immobilize the target molecule.

2. Provide the necessary "interface" to the electronic structure through membrane polarization, charge carrier injection or structural modification of the conductivity. The principal advantage attached to the use of semiconducting organic materials is the integration of the chemical and electronic structures. The electrical properties of organic semiconductors outlined in the previous section would permit construction of a variety of high impedance ECS devices.

Aside from the question of long term chemical stability of the devices and the need for specialized associated electronics to properly interface the high impedance sources, the principal limitation on the use of organic semi-conductors would appear to be in attaining the desired selectivity toward nerve agents. A rather wide variety of chemicals will produce a change in conductivity (see Table I) and it is likely that only a crude delineation between them could be obtained by this means. Hydorcarbons, for example, would be unlikely to provide interferences. The common atmospheric pollutants (NO, NO_2, SO_2, O_2, O_3, etc.) are generally electrophilic and could be distinguished from the nucleophilic nerve agents. Ammonia, amines and alcohols, however, present potential interferences (see Table I). Generally, there is no great selectivity in absorption of gases on a solid surface, particularly when the gases are near saturation concentrations. There would appear to be no real advantage to the use of biological rather than synthetic polymer

semi-conductors, the major requirement being only that the surface have a high density of basic groups. There is no reason to believe that the serine reside exhibits selectivity toward phosphorylation by nerve agents.

In order to improve selectivity and prevent surface contamination of the semi-conducting element the device would probably require pre-filtering by a selectively permeable membrane.

The pesticide/herbicide literature is quite extensive and contains detailed experimental and theoretical consideration of adsorption, diffusion and permeation by classes of chemicals closely related to the organo-phosphorus nerve agents (malathion, parathion, acephate, schradan, etc.). A recent extensive treatment of the dynamics of pesticides in relation to biological response has been given by G. S. Hartley and I. J. Graham-Bryce[9].

Generally, membrane diffusion is highly temperature-sensitive, concentration dependent and subject to co-penetrant interferences. When the molecular weight of the polymer monomeric unit is large compared to that of the penetrant, considerable variation in diffusion constants can be achieved among different penetrants. The data assembled in Table III is representative of the dependence of the diffusion constant on the molecular weight and geometry of the penetrant. It has been shown:

TABLE III

Penetrant	Mol. wt.	D($cm^2/sec \times 10^9$)
propane	44	4.81
n-butane	58	3.24
n-pentane	72	2.64
iso-pentane	72	1.32
iso-butane	58	1.45
neo-pentane	72	0.62

that the mobility of organo-phosphorus compounds in certain polymeric materials decreases among isomeric butyl compounds as normal>secondary>iso>tert, 60:40:20:1. If it is assumed that the penetrant diffuses downward from a boundary plane through a material thickness d and that the concentration at the surface (C°) is constant in time, then the mass of penetrant per unit area (M) reaching the detector at steady state depends linearly on the diffusion constant (D).

$$M = C^\circ Dt/d \tag{2}$$

Therefore, a selectivity of 60:1 in favor of normal butyl organo phosphorus compounds over the tertiary butyl derivatives could be achieved in the absence of co-penetrant effects.

The critical dependence of D upon polymer type is illustrated by the diffusion of water in polyethylene (3000×10^{-9} cm^2/sec), collagen (0.5×10^{-9} cm^2/sec) and PTFE (0.06×10^{-9} cm^2/sec). The concentration of penetrant at the detector from a limited surface source obeys equation (3).

$$C = \frac{M^\circ}{\sqrt{Dt}} e^{-d^2/4Dt} \tag{3}$$

where M° is the original mass of penetrant per unit surface area (dose). The concentration at the detector reaches its maximum value in a characteristic time τ given by

$$\tau = d^2/2D \tag{4}$$

which is the limiting response time for the ECS device. Using

the data for water diffusion given above and d = 2.5×10^{-3} (1 mil), the response times for polyethylene (1.08 sec) collagen (1.8 hour) and PTFE (14 hour) are sufficiently dissimilar to permit selective identification.

ACKNOWLEDGEMENT

This paper was written under the auspices of the DARPA Materials Research Council, Contract #MDA903-80-C-0505 with the University of Michigan.

REFERENCES

1. C. G. B. Garrett (1959) in "Semiconductors" (N. B. Hannary, ed.) p. 634, Reinhold, New York.
2. A. G. Chynoweth, J. Chem. Phys. 22, 1029 (1954).
   A. Bree, L. E. Lyons, J. Chem. Phys. 25, 384 (1956).
   D. M. J. Compton, T. C. Waddington, J. Chem. Phys. 25, 1075, (1956).
   W. G. Schnieder, T. C. Waddington, J. Chem. Phys. 25, 358, (1956).
   A. T. Vartanyan, Dokl. Akad. Nauk SSSR 71, 641 (1950).
   T. C. Waddington, W. G. Schneider, Can. J. Chem. 36, 789 (1958).
3. R. G. Kepler, Phys. Rev. 119, 1226 (1960).
4. D. D. Eley, G. D. Parfitt, Trans. Faraday Soc. 51, 1529 (1955).
   D. D. Eley, D. Spivey, Trans. Faraday Soc. 56, 1432 (1960).
5. M. H. Cardew, D. D. Eley, Disc. Farad. Soc. 51m 1529(1959).
   D. I. Spivey, Trans. Farad. Soc. 56, 1432 (1960).
   D. D. Eley, G. D. Parfitt, M. J. Perry, D. H. Taysum, Trans. Farad. Soc. 49, 79 (1953).
   D. D. Eley, G. D. Parfitt, Trans. Farad. Soc. 51, 1529 (1955).
   D. E. Eley, Research 12, 293 (1959)
6. P. Douzou, J-M. Thullier, J. Chem. Phys. 57, 96 (1960).

7. M. G. Evans, J. Gergely, Biochim. et Biophys. Acta 3, 188 (1949).

8. NATO Advanced Studies Summer School, Proceedings, "Sensors and Actuators", Elsevier-Sequoia, 1981 Ed. J. Zemel, P. Bergveld.

9. G. S. Hartleg, I. J. Graham-Bryce, "Physical Principle of Pesticide Behavior", Academic Press, London, 1980.

ASSESSMENT OF DOD NEEDS FOR A SYNCHROTRON RADIATION SOURCE

H. Ehrenreich, T. C. McGill, and G. H. Vineyard

INTRODUCTION

A request to MRC for a review of the usefulness of synchrotron radiation as an analytical tool to solve problems of importance to DoD was addressed by a meeting organized by W. E. Spicer (Stanford) and held on 9-10 July 1981. An agenda for the meeting and a list of MRC members in attendance is appended to this report.

The questions to be considered by MRC were outlined by S. Roosild: (1) What can synchrotron radiation do for the advancement of materials science? (2) What are DoD's needs for synchrotron facilities with respect to source characteristics and in terms of geographic considerations? These questions were answered at least in part during the course of the meeting. The first was given in terms of a number of specific examples taken from work performed at SSRL, Stanford. The "most desirable" source characteristics depend of course on the experiment under consideration. The machine operated by the Stanford Synchrotron Laboratory is versatile, having a spectral range (~3-10^4 eV) which extends from the UV through the X-ray UV (XUV) to the X-ray range. A large amount of significant data has been obtained dealing with a variety of physical systems and phenomena.

As the only machine on the US West Coast, its geographical location is of considerable importance to the very

active user community in that part of the country. In view of the many groups dealing with semiconductor problems, a relative emphasis on the latter in the presentations was not surprising.

Because SPEAR is not fully dedicated to the production of synchrotron radiation and because of the number of scientists wishing to use SSRL for projects of direct interest to DoD is larger than that which can be accomodated, the MRC was asked to comment about the advisability of setting up a DoD funded UV and XUV line. Among, the factors to be considered are:

1. The magnitude of the DoD need.
   - to what degree are proposed experiments crucial
   - are the geographical considerations compelling
2. The merits of SSRL relative to other facilities that are presently or will become available at Brookhaven, Cornell, Wisconsin, and NBS with respect to
   - spectral range and intensity
   - user mode
   - accessability
3. The use of the necessary funds ($2M in capital expenses and $1/4M per year operating expenses) for a central DoD facility at SSRL or individually funded projects at SSRL and other available facilities.

Based on the presented material at the workshop it is possible to comment concerning the first point. The second is more difficult since the relative merits of various facilities were not assessed during the meeting, even though members of some of the

other organizations were present (G. Lapeyere, Stoughton, and G. Vineyard, MRC and Brookhaven). This question might be addressed by a sufficiently broadly based panel of synchrotron radiation experts who can supply additional input to that contained in the present report. Concerning the third question, it can be argued that the user community on the West Coast is sufficiently diverse and able that this facility will be useful, and probably essential in a number of ways.

TECHNICAL AND SCIENTIFIC ISSUES

Some of the uses of SSRL of present and potential interest to DoD were well described during the course of the meeting. The primary use of the intense continuous source of UV and XUV radiation from the SSRL source has involved the study of surface and interface phenomena, particularly in semiconductors. The program has had major impact in the DoD program to evaluate the application of various 3-5 semiconductors (e.g., GaAs and InP) in the fabrication of high speed electronic and opto-electronic devices.

W. E. Spicer reviewed his group's contribution to the development of a microscopic model for Fermi level pinning by surface or interface states, which is one crucial determinant of semiconductor device performance and reliability. The Fermi level pinning position in GaAs is responsible for the as yet limited success in fabricating Schottky barrier field effect transistors in GaAs. By contrast, in InP the pinning position

is such that the likelihood of fabricating metal-insulator semiconductor field effect transistors is very promising. The SSRL experiments performed in this connection have been most useful in elucidating the features of the interface structure responsible for the Fermi level pinning.

R. S. Bauer (Xerox) described his work on the oxidation of Si and the formation of heterostructures between two semiconductors (e.g., Ge/GaAs). Synchrotron radiation (SR) was used to excite core electrons into the vacuum where they were detected and energy analyzed. Because of the short electron mean free paths for ejection, this spectroscopy is very surface sensitive. Thus the presence of a signal from a given core level provides a unique signature for the presence of an atomic species at or near the surface.

The shift in the position of the core levels gives information about the character of the chemical binding in which the atom is participating. By use of this spectroscopy, Bauer and coworkers have been able to obtain information about the initial stages of oxidation of Si and the growth and interface properties of Ge-GaAs semiconductor-semiconductor interface.

M. Knotek of Sandia Laboratories described his work on photon stimulated desorption spectroscopy. In this technique SR is used to produce a core level excitation which results in the desorption of a specific ion species that is subsequently detected. This spectroscopy permits the identification of atomic species residue on the surface. Knotek has applied it to a

number of materials which are of importance in catalysis, corrosion, laser windows, and electronics.

V. Rehn of the Naval Weapons Center described the use of SR to carry out diagnostics relevant to laser optics. Radiation at about 300 eV has been used to make measurements of the scattering from surface roughness of metallic mirrors. This experiment has allowed the verification of theoretical methods for treating the scattering from metallic mirrors. It has also provided information of the surface roughness of these materials. Rehn also described the use of SR to measure the optical properties of materials that are candidates for use as optical components in UV laser systems. Finally, he reported use of SR and photon stimulated description to characterize the impurities present on the surface of superconducting metals, which are of interest in the Josephson junction technology.

D. Shirley (Berkeley and LBL) discussed the use of XUV synchrotron radiation to measure the normal photoelectron diffraction which provides structural information on surface adsorbed species. To date the technique has been applied to atoms and small molecules on the surfaces of transition metals (CO on tungsten). However, the technique could be applied very fruitfully to a more extensive set of substrates and overlayers of interest in semiconductor, corrosion, and catalytic science.

Operational and Scheduling Difficulties at SSRL

The present facility at SSRL is funded by the National Science Foundation. The facilities for UV and XUV are in great

demand. The present procedure requires the submission of a proposal for each project. The proposal is refereed on the basis of scientific merit only (as opposed, for example, to technological utility). Time is awarded on the basis of proposal review. Because of the shortage of facilities many very good to good proposals have to be rejected. Proposals totalling 2 to 3 times the available time have received acceptable reviews. Furthermore, proposals addressing studies with important technological implications for DoD which are less concerned with forefront science typically receive less priority under presently existing NSF guidelines and hence are frequently declined.

The regional users of SSRL, to a considerable degree, consist of groups which are actively participating in DoD programs particularly in the field of electronic and optical materials. These programs are being hampered by the lack of available time on the currently available SSRL facilities. Some experiments, (for example, those on heterostructure growth) may be "on line" for three weeks and then be "off" for almost a year before additional beam time becomes available.

Proposal for A DoD Sponsored Beam Line at SSRL

In order to overcome the difficulties described in the preceeding section the group at SSRL wishes to propose a DoD sponsored UV and XUV beam line with adequate instrumentation and support staff at SSRL. The facility would require approximately $2M in capital expenditure and $1/4M per year operation and maintenance cost (assuming a support staff of three). According

to R. Bachrach (Xerox), the design of the facility would take in-to account recent developments in wigglers and undulator so as to produce a state-of-the-art UV and XUV facility.

Fifty percent of the time available would be used at DoD's discretion while the other 50% would be bid for according to standard SSRL procedures. The Naval Weapons Center (G. Winkler) indicated a willingness to act as the focus for the DoD's interaction with the facility at SSRL.

Spicer indicated that he believed that the establishment of such a facility by DoD would increase the current level of use of SR for DoD related activities from its present level of 10-20% to a level which is more nearly commensurate with DoD requirements for the optimal development of appropriate technologies of the types described in this report.

CONCLUSIONS AND RECOMMENDATIONS

1. Synchrotron radiation is a versatile experimental tool for a number of experiments [UV Photoemission (UPS), angular resolved photoemission (ARUPS), extended fine structure X-ray absorption spectroscopy (EXAFS) X-ray photoemission spectroscopy (XPS)] which yield a great deal of fundamental insight concerning a number of technologically important matters. Among these are:

   a. Interfaces and surfaces involving semiconductors and/or metals,
   b. Chemical environments of a given atomic species (important in chemical and biological systems),

c. Fermi level pinning,

d. Lithography,

e. Testing of UV and X-ray optical components,

f. Catalysis,

g. Corrosion,

h. Small particle phenomena (including catalysts and prototypes involving elements of submicron circuit elements,

i. Surface structures.

Basic insight offered by these experiments has been useful in spawning new inventions of technological importance.

2. On the other hand, SR is one (albeit a very successful one) of a number of techniques for obtaining microscopic information. The information obtained from SR experiments along with those produced by other experiments (e.g., LEED, TEM, and optical experiments) are all necessary to provide a complete description of the microscopic phenomena. Further, it should be noted that our level of understanding of the microscopic phenomenon is not such that these fundamental experiments replace the empirical investigations that have previously characterized many of these fields.

3. On the basis of research quality and geographical considerations, a DoD supported beam line at SSRL has definite merit, particularly as it pertains to semiconductor device research, which is heavily concentrated on the West Coast. Furthermore, academic institutions use SR to train students in the sort of science that is directly relevant to DoD needs.

4. Since DoD must be concerned with an optimal use of its financial resources, it should consider the following questions as it considers the Stanford proposal:

a. Are the required funds optimally used in supporting a dedicated beam line rather than being disbursed to individual investigators at SSRL and elsewhere? (Consider however, the scheduling problems at SSRL!)

b. Industrial users have invested in dedicated beam lines at the facilities near completion at Brookhaven. Among these are Bell Labs, IBM, Xerox, and Exxon, as well as a number of government labs. Can DoD, which is trying to leapfrog current industrial capabilities in many areas such as VLSI, afford to have the facilities at its disposal be of marginal adequacy?

c. If DoD regards SR as an important tool for investigation furthering its capabilities then it should be prepared to make the sort of commitments implied by the following questions:

(i) Is DoD willing to commit funding for a number of years, five as a minimum? A new beam line will require such a time to give a proper return on the instrument.

(ii) Are there groups at other centers who could make competitive proposals? In particular the synchrotron group at Stoughton, Wisconsin, might be a competitive site. We do not wish to diminish the obvious attractive features of the SSRL proposal. At the same time the SSRL capabilities are not unique and it would be prudent of the DoD to make some kind of investigation as to what efforts could be mounted by other groups and at other centers.

(iii) What support of synchrotron UV and XUV work are the various services planning? How much overlap would there be with this proposal?

5. The views expressed in this report concerning the Stanford proposal of a DoD funded beam line are obviously positive. Because of its obvious importance, this proposal merits the most careful consideration.

AGENDA

SYNCHROTRON RADIATION (SSRL) UV AND XUV:
OPTIMIZATION OF DOD UTILIZATION

Thursday, 9 July 1981

Chairman: Dr. Gunter Winkler, NWC

Dr. S. Roosild, DARPA, MSO
Introduction

Professor W. Spicer, Stanford University
Purpose of Meeting

Professor I. Kindau, Stanford University and SSRL
An Example of the Present and Potential XUV and Other Synchrotron Facilities Using SSRL as an Example

Dr. M. Knotek, Sandia Laboratory
Photon Stimulated Desorption Spectroscopy

Dr. V. Rehn, NWC
Laser Optics Diagnostics and Other Studies

Formal and Informal Discussion

Friday, 10 July 1981

Professor Dave Shirley, Director LBL
National Overview of Synchrotron Radiation Sources and Facilities

Professor W. Spicer, Stanford
Possible Configuration and Philosophy of DoD Line

Dr. R. Bauer, Xerox (Head SSRL Users' Organization)
a) Comments of the SSRL Users' Community
b) Studies of Heterojunction and Other Device Configurations on an Atomic Level

Professor W. Spicer, Stanford
The Unified Model for Schottky Barrier and MOS Interface
State Formation in 3-5 Semiconductors: A Case Study

Dr. R. Bachrach, Xerox
Potential DoD Beam Lines

Professor W. Spicer, Stanford
Summary

Formal and Informal Discussion

SYNCHROTRON RADIATION (SSRL) UV AND XUV;
OPTIMIZATION OF DOD UTILIZATION

MEETING ATTENDEES

Dr. Robert Bachrach
Xerox

Dr. Robert S. Bauer
Xerox

Dr. Richard G. Brandt
Office of Naval Research

Dr. S. Hagstrom
Xerox

Professor R. M. Hexter
University of Minnesota

Dr. M. Knotek
Sandia Laboratory

Professor G. J. Lapeyre
Montana State University

Professor I. Lindau
Stanford University

Dr. V. Rehn
NWC

Professor Dave Shirley
LBL

Professor W. Spicer
Stanford University

Dr. H. H. Wieder
NOSC

Dr. Gunter Winkler
NWC

Professor Henry Ehrenreich
MRC, Harvard University

Professor Anthony Francis
MRC, University of Michigan

Professor Thomas C. McGill
MRC, California Inst. of Tech.

Professor M. J. Sinnott
MRC, University of Michigan

Dr. George H. Vineyard
MRC, Brookhaven National Lab.

Professor Mark S. Wrighton
MRC, Mass. Inst. of Tech.

Major H. V. Winsor
AFOSR/NE

Dr. S. A. Roosild
DARPA-MSO

CHEMICALLY SENSITIVE FIELD EFFECT DEVICES FOR DETECTOR APPLICATIONS

M. S. Wrighton

INTRODUCTION

It is well known that field effect devices such as MOSFET's are sensitive to chemical impurities. A number of researchers have suggested that the chemical effects on field effect devices could be exploited in detector applications, and articles describing the use of field effect devices in chemical sensing have been appearing in the open literature[1] since about 1970 with the report of a pH sensitive semiconductor system[2]. So far the systems demonstrated include $H_{(g)}$ atom, $H_2(g)$, $H^+_{(aq)}$ and $K^+_{(aq)}$ detectors that employ different chemically sensitive elements. As will be developed below, it should be possible to significantly improve the state-of-the-science in this area by a basic research effort.

Advantages of Field Effect Sensors

In any chemical sensing system there is emphasis on speed, sensitivity, selectivity, and stability/reliability. There are some possible advantages in using field effect devices in chemical sensing. A key advantage is the "gain" associated with the field effect device upon receiving a chemical "signal". Basically, we can regard the gate region as the chemically sensitive region of a field effect device, Fig. 1. In manufacturing of MOSFET's the usual aim is to fabricate a gate region that

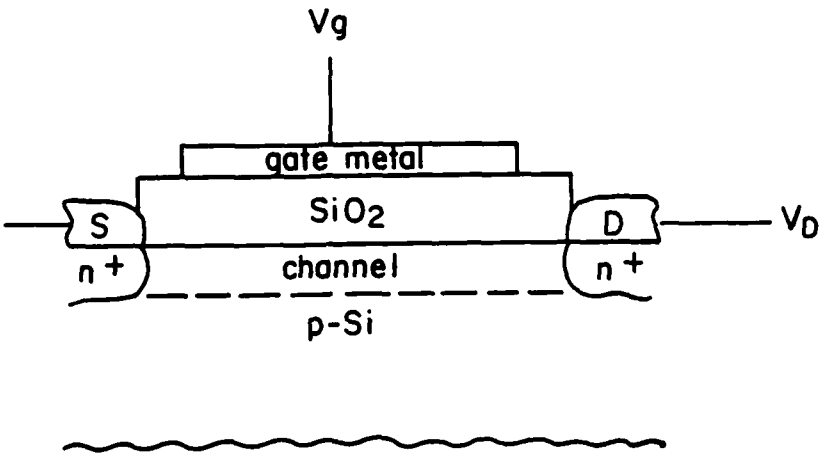

Figure 1. Typical MOSFET structure. Variation in gate metal, channel surface, SiO_2, etc., can alter conductivity in the channel. Chemical sensors employ gate elements that alter channel conductivity in the presence of chemicals.

is chemical insensitive and reproducible. For chemical sensing, the aim would be to fabricate a gate that responds to changes in the contacting environment such that the gate voltage, V_g, needed to open the channel is altered in a rapid, reproducible, and reversible manner. A chemical can be evidenced by a change in the drain current, I_D, in a manner that depends on the nature of the chemical and its concentration at a fixed value of drain voltage, V_D, and at a fixed V_g. Generally, any chemical effect that changes the characteristics of the device could be exploited. Field effect device characteristics are treated in detail in Sze[3] and will be the same for chemically sensitive devices except that the properties of the gate become a deliberate variable.

A second possible advantage for field effect chemical sensors is the fact that the sensing element itself can be regarded as just another element in an electronic device. This would allow the development of sensors having very small physical dimensions as well as the possibility of using a two-dimensional array of different chemical sensing elements to record a time dependent signature of a chemical environment with two-dimensional geometrical characteristics. Importantly, being a part of the electronic device allows the amplified signal from the sensor to be processed easily.

State-of-the-Science

Despite the efforts from over a decade of research, relatively little in the way of chemical sensors based on field

effect devices has been done. Work on H atom detection[4], pH in solution[2,5], H_2 in the gas phase[6] and K^+ in H_2O[7] has been reported. The H_2 detection is perhaps the best understood work. The H_2 detector exploits Pd as the gate metal of a MOSFET[6a] or the metal of a semiconductor/metal Schottky barrier.[6b] The reaction of H_2 with Pd produces a change in the work function of Pd leading to an equal change in the barrier height of an n-CdS/Pd interface or to a change in the characteristics of the MOSFET. Problems include: (i) response time limited by the hydriding rate, (ii) reaction of PdH_x with O_2 to yield H_2O giving rise to drift and irreversibility, and (iii) irreversibility of the hydriding reaction itself. Despite the difficulties the Pd/H_2 system illustrates the principle of how changes in the work function induced by the presence of a specific chemical can change the surface field sufficiently to change device characteristics in a deliberate fashion.

Studies of pH sensitive field effect devices have included the simple use of the gate SiO_2 as the H^+ sensitive element[5]. In such a device the gate metal can be simply replaced by the solution. Typically, the solution is electrically connected to the p-Si substrate through the use of a reference electrode immersed in the solution contacting the gate SiO_2, Fig. 2. The pH sensitive devices suffer from problems attributable to irreversible SiO_2 changes and changes in the Si/SiO_2 interface. Notice, Fig. 2, that when a solution contacts the MOSFET there is a need to protect the contacts with some protec-

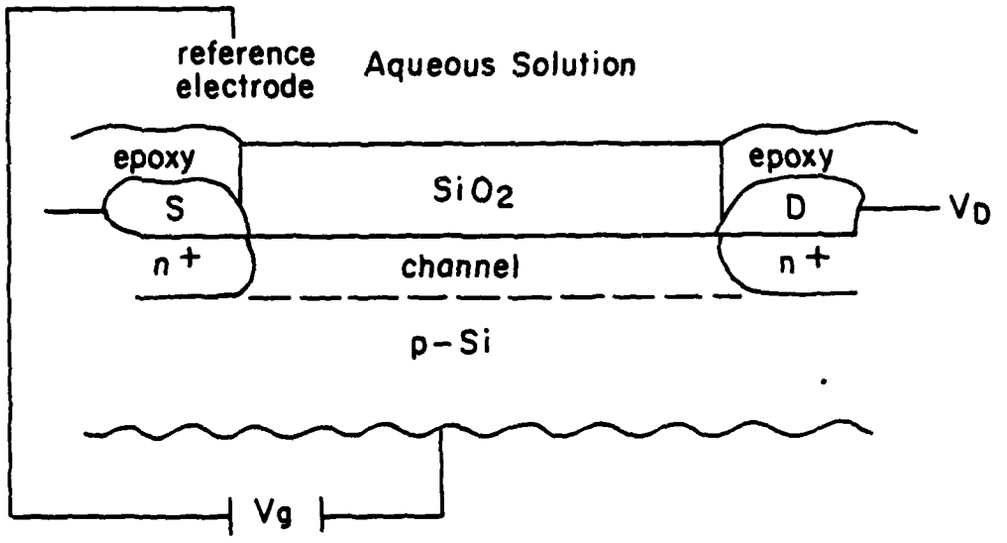

Figure 2. pH Sensitive MOSFET. "Reversible" hydration of SiO_2 at different pH's gives change in channel conductivity at fixed V_g.

tive coating such as an epoxy. The pH field effect sensor works well enough to illustrate a point: variation in the gate insulator properties can be exploited in chemical analysis.

A more sophisticated example of a change in the gate insulator properties comes from work with valinomycin incorporated into a polymer as a specific K^+ ion transport agent[7]. A device configured as in Fig. 3 has been reported to be useful for the analysis of K^+ in aqueous solution. The principle here is that deliberate modification of the properties of the gate region is possible through clever interface synthesis employing molecular level understanding of the interations of the chemical to be detected.

To briefly summarize the state-of-the-science, there have been several important proof-of-concept demonstrations of deliberate modification of the gate properties of field effect devices. The reports come from different research groups lending credence to the firmness of the claims so far. In general, the work has been rather timid with respect to the chemical manipulations of the interface and with respect to the range of device materials employed. Use of materials other than Si/SiO_2 has not been investigated and such might be a small, but practical, driving force for the development of a manufacturing capability for other IGFET devices.

Research Opportunities and Ideas

A number of specific areas of research could impact the viability of field effect devices as chemical sensors. Several

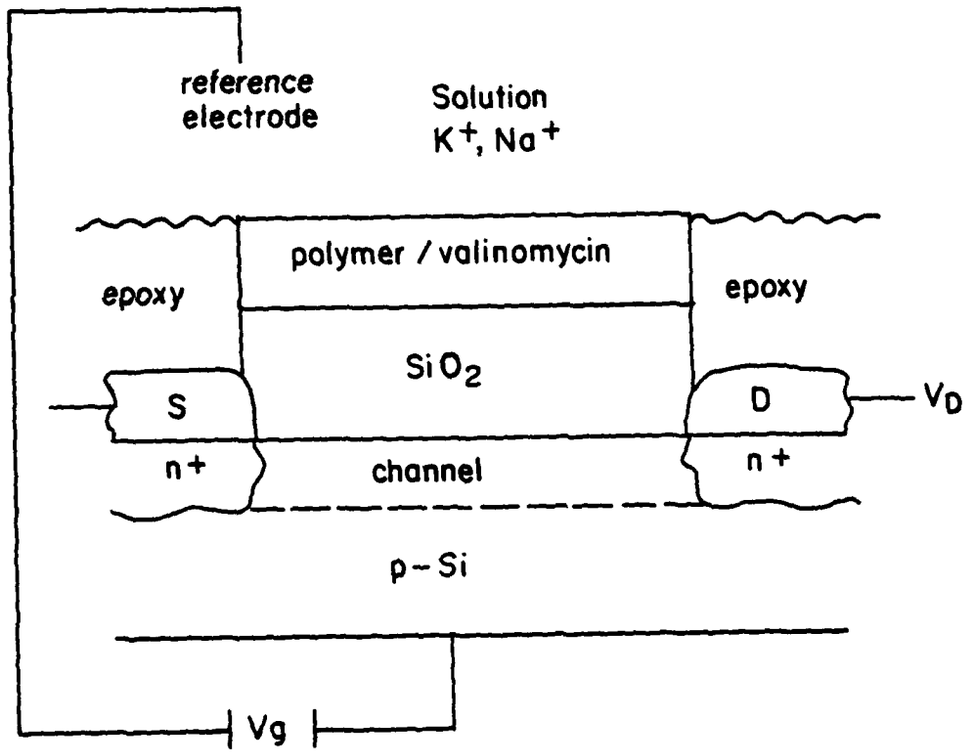

Figure 3. K^+-selective MOSFET sensor. Valinomycin, specific for K^+, in polymer over SiO_2 changes gate properties in response to solution $[K^+]$ variation.

areas where fruitful effort could be applied are summarized below.

Specific Surface Chemistry of the Channel Region. Response of the Si/SiO_2 interface to changes in solution pH suggest that it may be possible to find specific chemistry of the channel surface that will result in large changes in the surface field. Indeed, the open literature reveals several cases that would be good, immediate targets for study. For example, it is reported that GaAs, InP, and a number of other semiconductors exhibit large changes in surface properties upon variation of the pH of a contacting medium as illustrated in Fig. 4.[8] Thus, the pH detector represented in Fig. 4b should be viable, provided that the Fermi level pinning of GaAs can be removed by the eletrolyte solution. A similar device based on p-InP is more likely since the pinning is known to be associated with a very large barrier height.[8]

Another example of specific semiconductor surface chemistry is the effect from I^- on WS_2 and related semiconductors, Fig. 5a, leading to the viability of an I^- detector, Fig. 5b. Yet another example is the effect of S^{2-} on CdS and related semiconductors, Fig. 6a and a possible S^{2-} detector, Fig. 6b.[10]

These three examples (pH, I^- adsorption, S^{2-} adsorption) illustrate the possibility of detector systems that employ a channel simply exposed to the solution. A major question is whether the surface of the semiconductor would have the chemical integrity required for durability. A second issue of course is

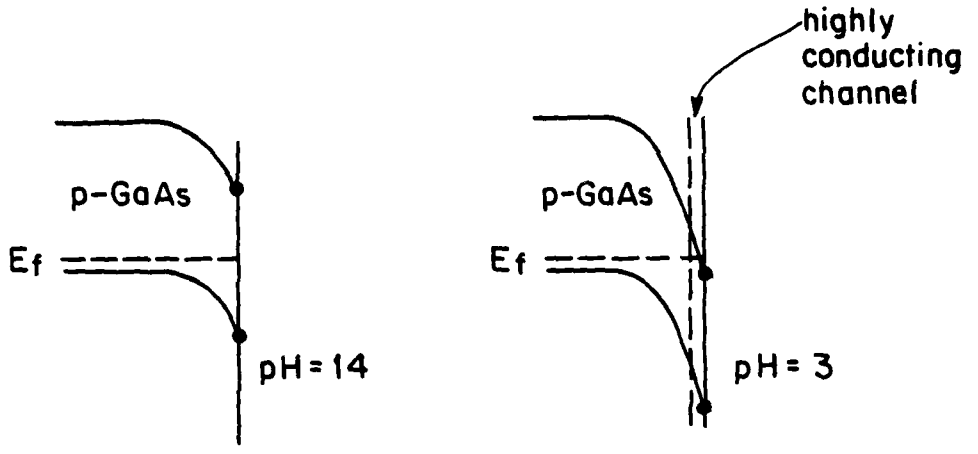

Figure 4a. Effect of pH variation on band bending of p-GaAs at a fixed potential of the GaAs.

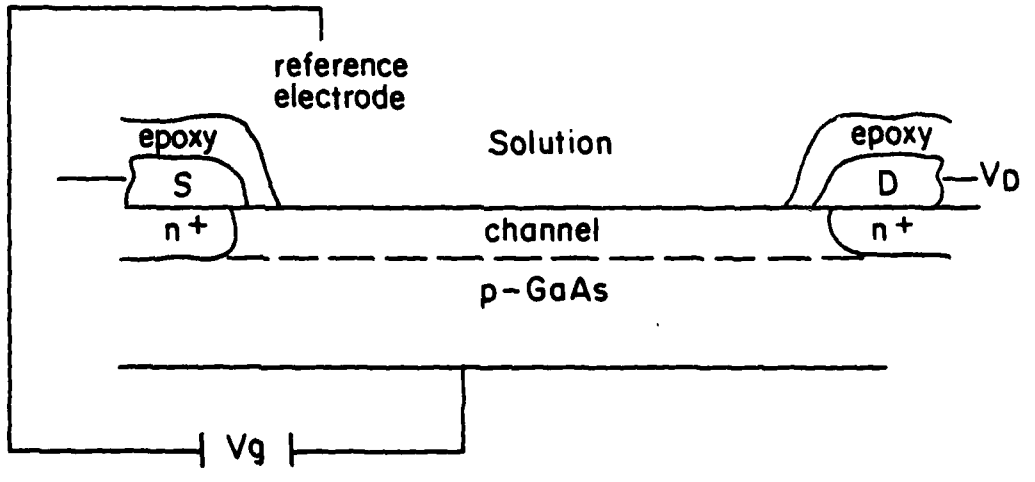

Figure 4b. Field effect pH sensor based on chemistry of the surface of the channel resulting in the pH effect represented by Figure 4a.

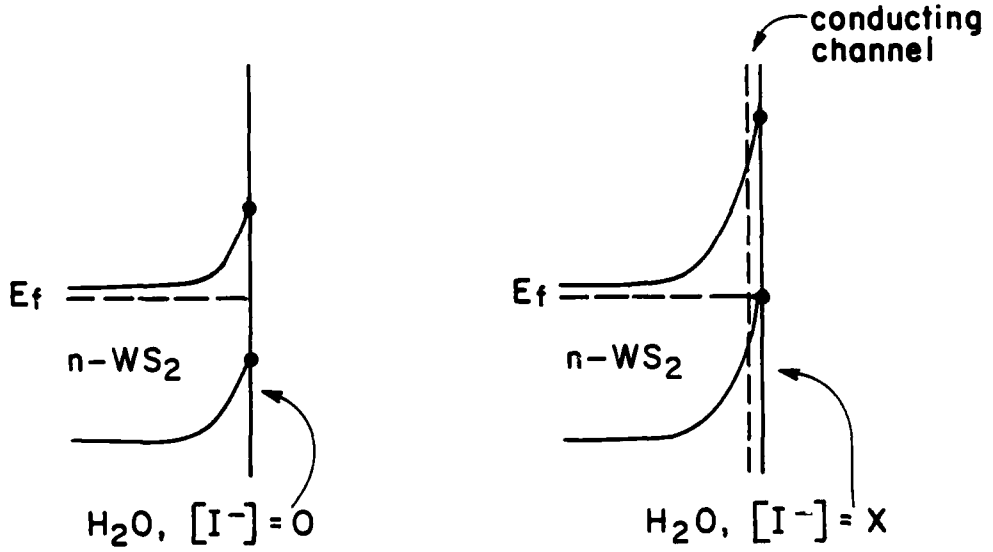

Figure 5a. Effect of specific I^- adsorption on n-WS_2.

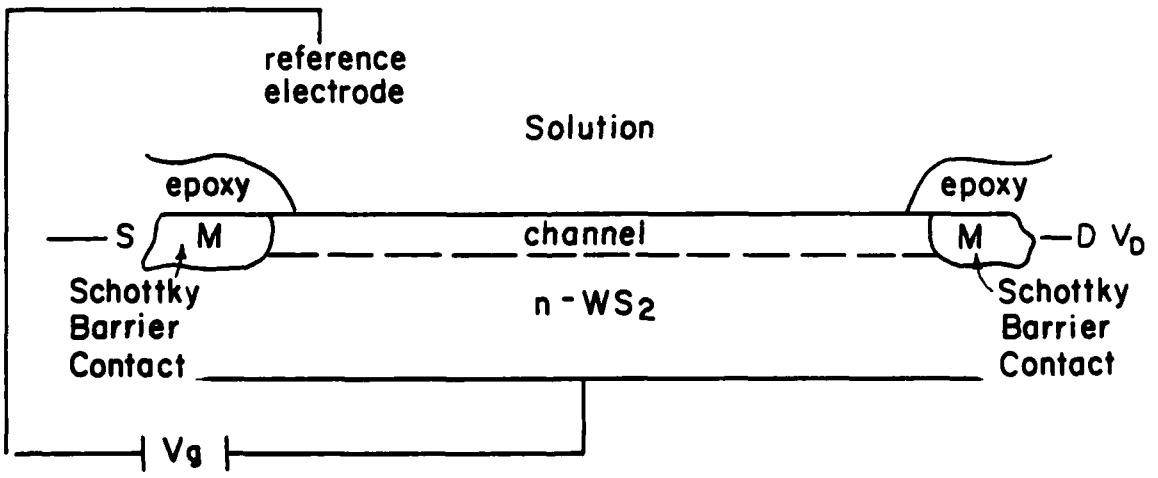

Figure 5b. Possible I^- detector based on chemistry represented by Figure 5a.

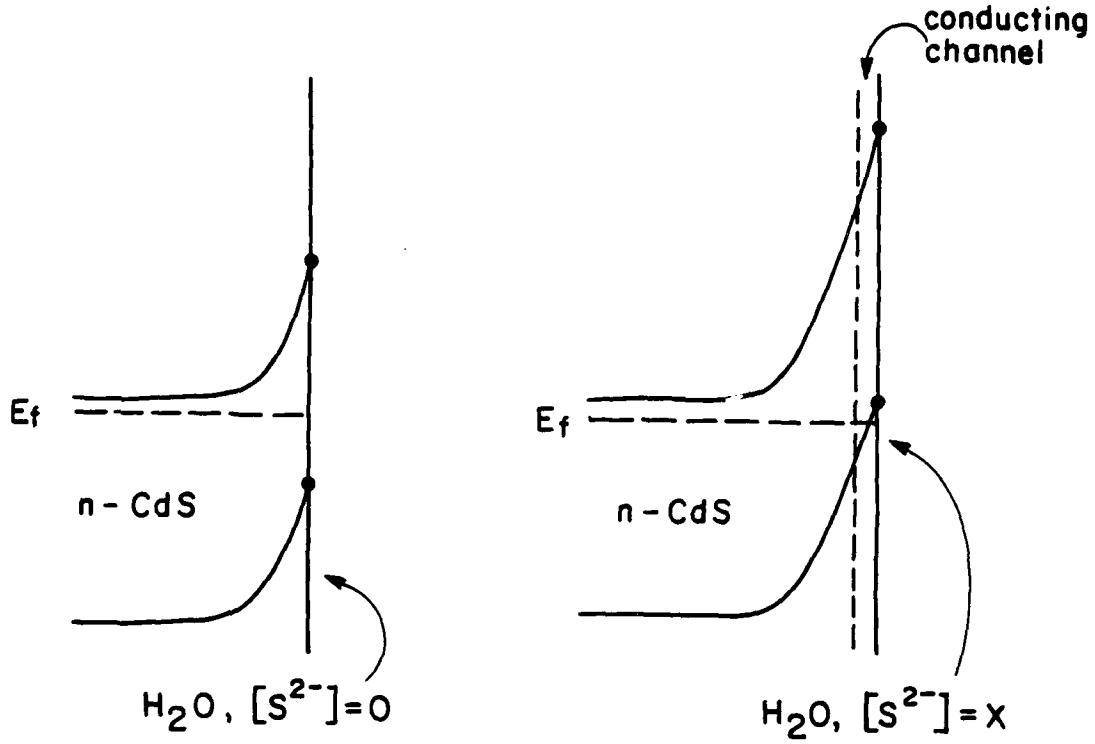

Figure 6a. Effect of specific S^{2-} adsorption on n-CdS.

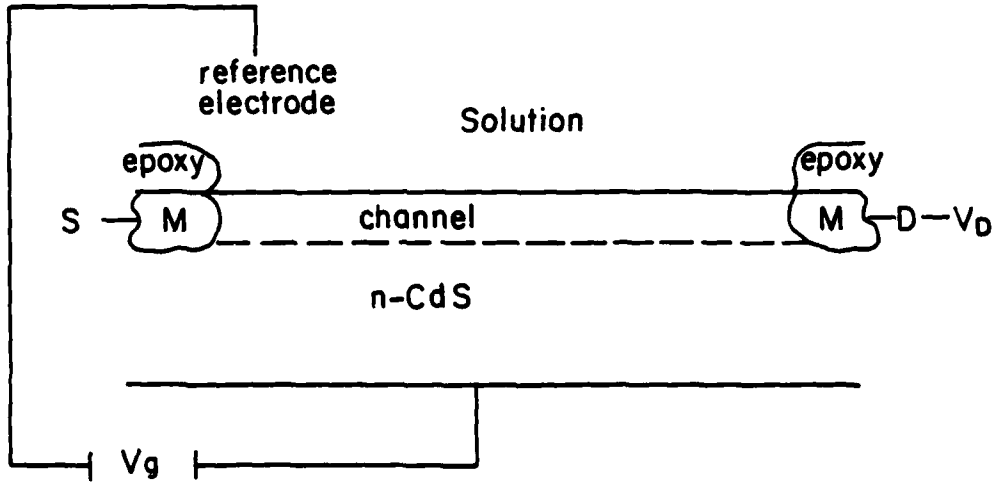

Figure 6b. Possible S^{2-} detector based on chemistry represented by Figure 6a.

whether specific semiconductor surface chemistry exists for analytical problems of consequence. The third issue is whether exotic materials such as WS_2 can be used in practical integrated circuits.

Polymer Overcoats for the Gate Region. The valinomycin example[7] illustrates the principle of a selective polymer overcoat to manipulate gate properties only in the presence of a certain chemical. In this area, the selectivity of the typical MOSFET toward different chemicals could be manipulated by variations in the polymer. It is likely that an understanding of SiO_2/polymer interfaces is essential and the use of covalently anchored polymers is probably desirable in order to minimize pinholes in the polymer and to achieve a durable, persistently attached polymer. Redox polymers and simple ion exchange polymers could be useful. Selectivity in detection would appear to only be limited by synthetic capability. A large amount of work[11] in the area of electrochemistry (chemically modified electrodes) and chromatography provides the evidence that tailoring the gate of a MOSFET should be possible.

Specificity Through the Use of Enzymes. Enzymes interact with specific substances and can, in principle, be coupled with the IGFET to produce sensitive and specific sensors. For example, nitrogenase operates to effect the reduction of N_2 to NH_3; formate dehydrogenase works on the CO_2/HCO_2^- couple. Thus, specific N_2, NH_3, CO_2, HCO_2^- detectors can be envisioned provided the enzyme action can somehow be sensed by the field

effect device. Generally, redox active enzymes do not equilibrate with surfaces.[12] In solution, so-called "mediators" are used to effect equilibration of enzymes with conducting surfaces.[13] Development of synthetic pathways to surface mediator/enzyme/SiO_2 gate assemblies should lead to very specific, sensitive devices.

Gate Metals That Are Chemically Sensitive. The detection of H_2 using Pd as the gate metal suggests that a chemically sensitive contact can be exploited. Conducting organic and inorganic polymers such as polyacetylene, polypyrrole, $(SN)_x$, phthalocyanines, etc., do respond to chemical environment. As with polymer overcoats generally, progress here is limited by synthetic capability.

CONCLUSIONS AND RECOMMENDATIONS

Understanding and manipulating chemical gate devices will come from an interdisciplinary research effort in the following areas:

- chemically sensitive insulator materials
- semiconductor/chemical interfaces
- polymer/enzyme interfaces
- chemically sensitive gate metals
- protection overcoats
- structural analysis of synthetic interfaces
- two-dimensional array sensor systems

Research ability in these areas exists in academic institutions, government laboratories, and private industry and research

institutes. The required understanding overlaps that needed in the fields of electrochemistry, biochemistry, surface science, catalysis and electronic device engineering. DARPA should capitalize on the emerging developments in fundamental aspects of surface chemistry and foster specific work on surface chemistry of Si, SiO_x, GaAs, InP and other practical and promising electronic device materials. Detection of chemical and biological warfare agents using IGFET devices will likely require attention from DoD, since NSF and NIH will not likely be funding work of direct relevance to these analytical problems.

ACKNOWLEDGEMENT

This paper was prepared under the auspices of the DARPA Materials Council, Contract #MDA903-80-C-0505 with the University of Michigan.

REFERENCES

1. NATO Advanced Studies Summer School, Proceedings, "Sensors and Actuators", J. Zemel and P. Bergveld, Eds., Elsevier-Sequoia (1981); R. G. Kelly, Electrochim. Acta 22, 1 (1977).

2. P. Bergveld, IEEE Trans. Biomed. Eng., Vol. BME-17, p. 70 (1970).

3. S. M. Sze, "Physics of Semiconductor Devices," Wiley, New York, 1969.

4. J. N. Zemel, IEEE Trans., NS-18, 78(1971); J. J. Young, J. N. Zemel, Appl. Phys. Lett. 27, 455(1975).

5. T. Matsuo, K. D. Wise, IEEE Trans., BME-21, 485(1975); C. C. Wen, J. N. Zemel, Thin Solid Films 69, 275(1980).

6. (a) Lundstrom, S. Shivaraman, C. Svensson, L. Lundkvist, Appl. Phys. Lett. 26, 55(1975);

   (b) M. C. Steele, B. A. MacIver, Appl. Phys. Lett. 28, 687(1976).

7. S. D. Moss, J. Janata, C. C. Johnson, Analyt. Chem. 47, 2238(1975); C. C. Wen, I. Lauks, J. M. Zemel, Thin Solid Films 70,333(1980).

8. cf. R. N. Dominey, N. S. Lewis, M. S. Wrighton, J. Amer. Chem. Soc. 103, 1261(1981) and references therein.

9. J. Gobrecht, H. Tributsch, H. Gerischer, J. Electrochem. Soc. 125, 2085(1978); D. Canfield, B. A. Parkinson, J. Amer. Chem. Soc. 103, 1279(1981); G. S. Calabrese, M. S. Wrighton, J. Amer. Chem. Soc. 103, 6273(1981) (in press).

10. A. B. Ellis, S. W. Kaiser, J. M. Bolts, M. S. Wrighton, J. Amer. Chem. Soc. 99, 2839(1977).

11. R. W. Murray, Accs. Chem. Res. 13, (1980) and references therein.

12. E. Margoliash, A. Schajter, in "Advances in Protein Chemistry," Vol. 21, C. G. Anfinsen, M. L. Anson, J. T. Edsall, F. M. Richards, eds., Academic Press, (1966) Chapter 2.

13. R. Szentrimay, P. Yeh, T. Kuwana, ACS Symposium Series 38, 143(1977).

USE OF MONOMOLECULAR LAYER TECHNIQUES IN MICROLITHOGRAPHY

M. S. Wrighton

INTRODUCTION

Organized, monolayer assemblies of long-chain fatty acid molecules have been studied quantitatively for over 50 years.[1,2] A typical representation of a monolayer assembly of molecules is shown in Fig. 1, and a typical fatty acid, stearic acid, $C_{17}H_{35}COOH$, is shown in Fig. 2. Monolayers of such molecules can be formed by dissolving the acid in a volatile solvent that is imiscible with the H_2O and adding the fatty acid/solvent drop-wise to the surface of quiet H_2O. The hydrophilic "head" groups associate with the H_2O while the hydropholic "tail" are repelled from H_2O. The spontaneously formed assembly represented by Fig. 1 can be stable indefinitely.

One of the important quantitative measurements that can be made is the pressure-area curve, Fig. 3, that allows the determination of the area per molecule of a monolayer. Early on the area per molecule of fatty acids was found to be ~21Å^2/molecule, independent of the length of the hydrophilic tail. This result lends credence to the representation in Fig. 1 for the close-packed monolayer (position [3] in the pressure-area curve of Fig. 3) where the size of the head group controls the area/molecule in the monolayer.

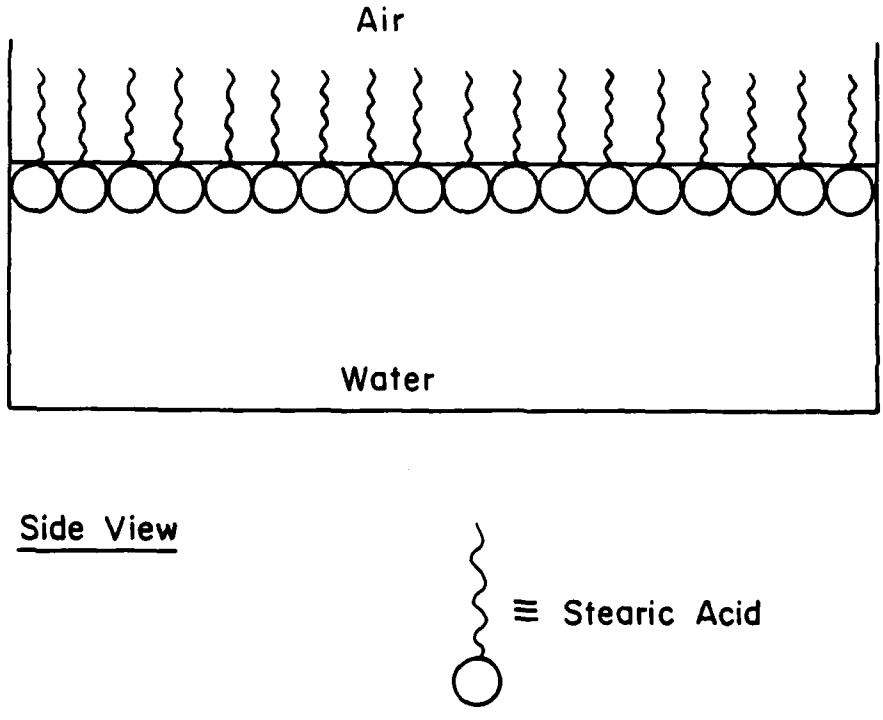

Figure 1. Representation of a monolayer of stearic acid on H_2O.

Typical Monolayer-Forming Molecule

Octadecanoic Acid (Stearic Acid)
($C_{17}H_{35}COOH$)

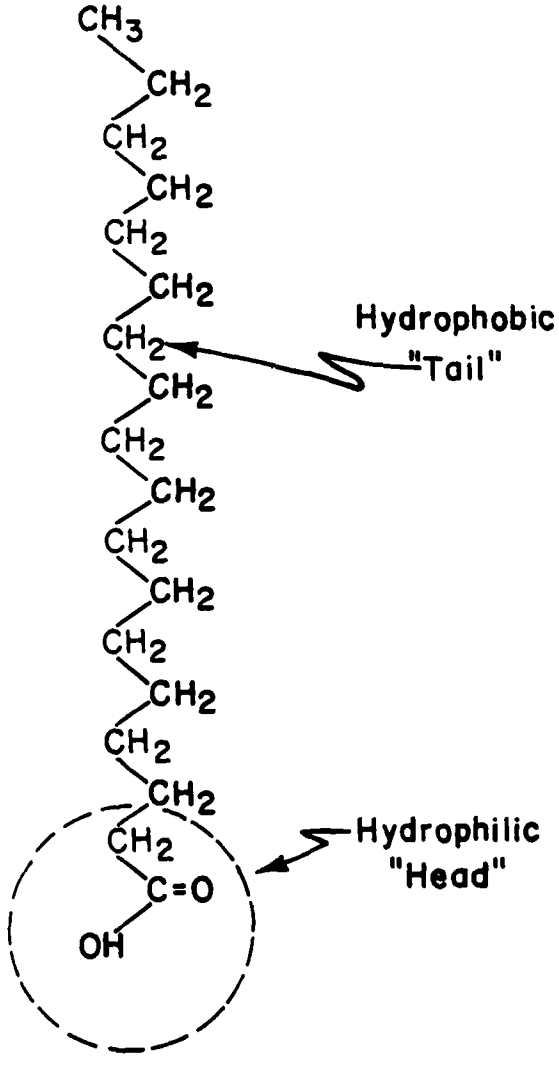

Figure 2. Typical Monolayer-Forming Molecule.

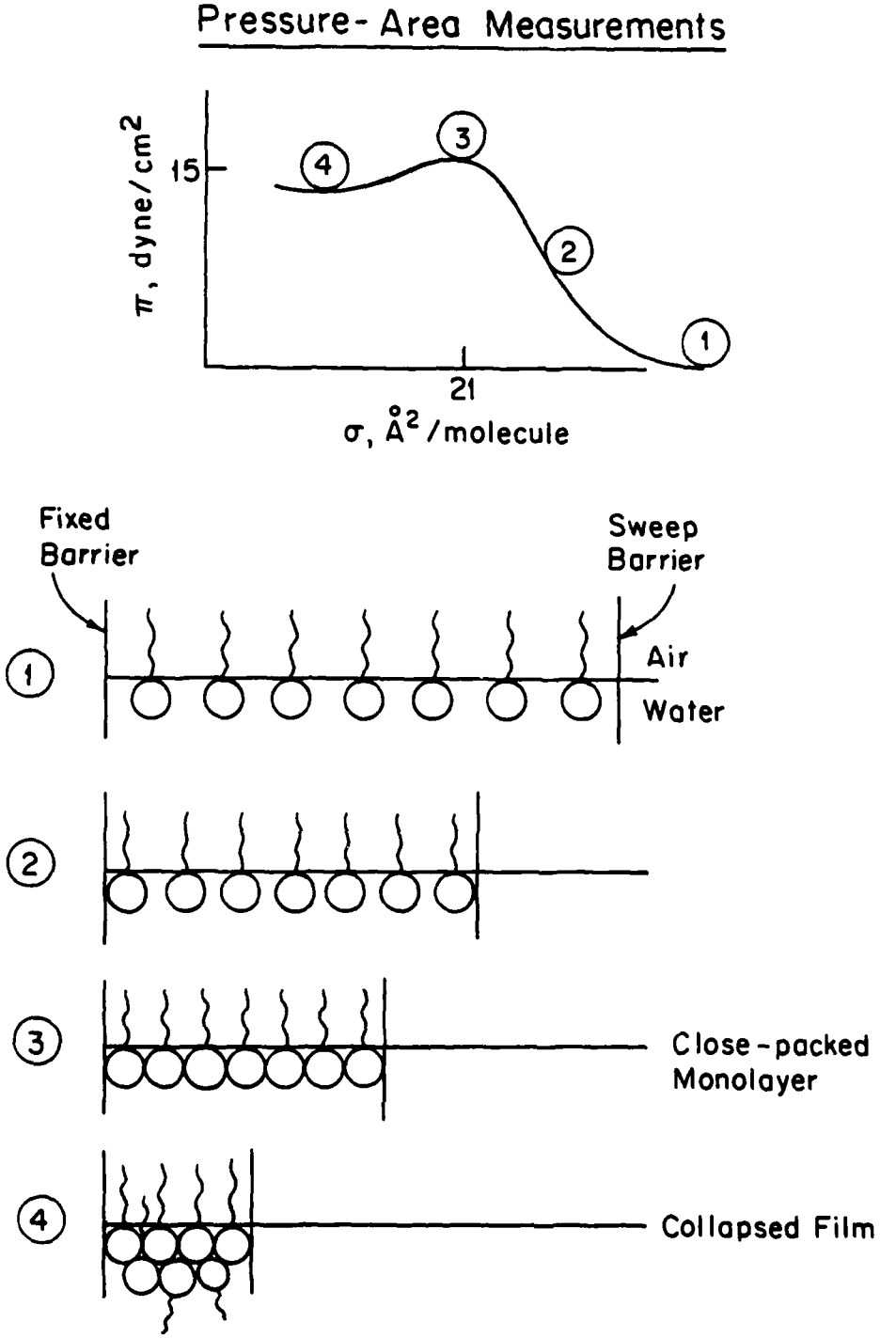

Figure 3. Representation of a pressure area curve using a film balance.[2]

The formation of the oriented monolayers on a liquid surface is possible because the monolayer forming molecules are insoluble in the medium. Such monolayers have the following general characteristics: (i) the monolayers are thin - perhaps as thin as 10-20Å, (ii) the monolayers can be thermodynamically stable but are mechanically fragile, (iii) the structure may be dynamic (in principle, gas, liquid, and solids are possible in two-dimensions), (iv) the molecules are oriented.

Monolayers do have fundamental and possibly practical uses. Monolayers on liquids can reduce the rate of evaporation of the underlying liquid. Hence, there are possible applications in reducing the rate of H_2O evaporation from reservoirs in dry areas. Monolayers may be useful in corrosion inhibition and adhesion. A monolayer (or less) coating of $-Si(CH_3)_3$ groups on electronic materials according to Eq. (1) promotes adhesion of the photoresist material.

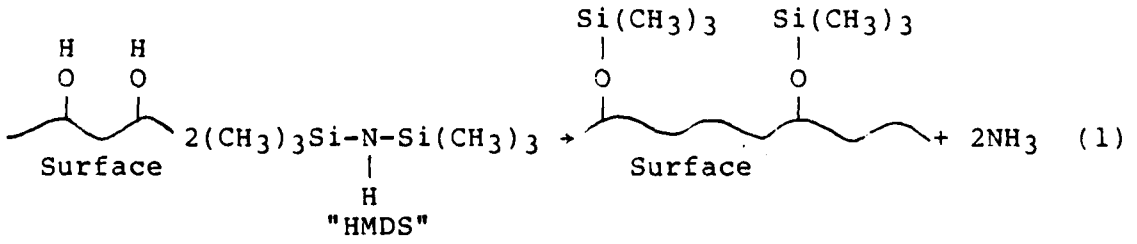

(1)

Of interest to DARPA are fundamental studies of relevance to the possible use in e⁻beam lithography and in understanding the properties of electronic devices. The use of

Langmuir-Blodgett[1,2] techniques can be employed to prepare organized multi-layer assemblies on solid substrates. Such transfer techniques are essential to the use of monolayers in electronic devices. Multi-layer synthesis is described below.

SYNTHESIS OF MULTILAYER ASSEMBLIES

Monolayers can be transferred to solid surfaces as sketched in Fig. 4. The properly pretreated surface will yield an oriented monolayer of the same area/molecule as on the liquid when the substrate is withdrawn from the liquid as shown in Fig. 4. Multilayers can be built up as represented in Fig. 5 by re-inserting the covered substrate. On the insertion the bilayer that forms mimics a biological bilayer membrane accounting for the interest in monolayer techniques from biophysicists. Upon withdrawal of the bilayer a third layer is deposited with the head groups interacting with each other. Of the order of 100 layers can be deposited on surfaces and the resulting assemblies, though fragile, can be used in subsequent experimentation.

Multilayers are oriented assemblies of molecules that can have different chemical functionalities in the various layers. For example, assemblies like that represented by Fig. 6 have been used to study the efficiency of energy transfer vs. distance between donor and acceptor. The technique simply involves examining the efficiency of fluorescence quenching of the donor by the acceptor as a function of the number of spacer

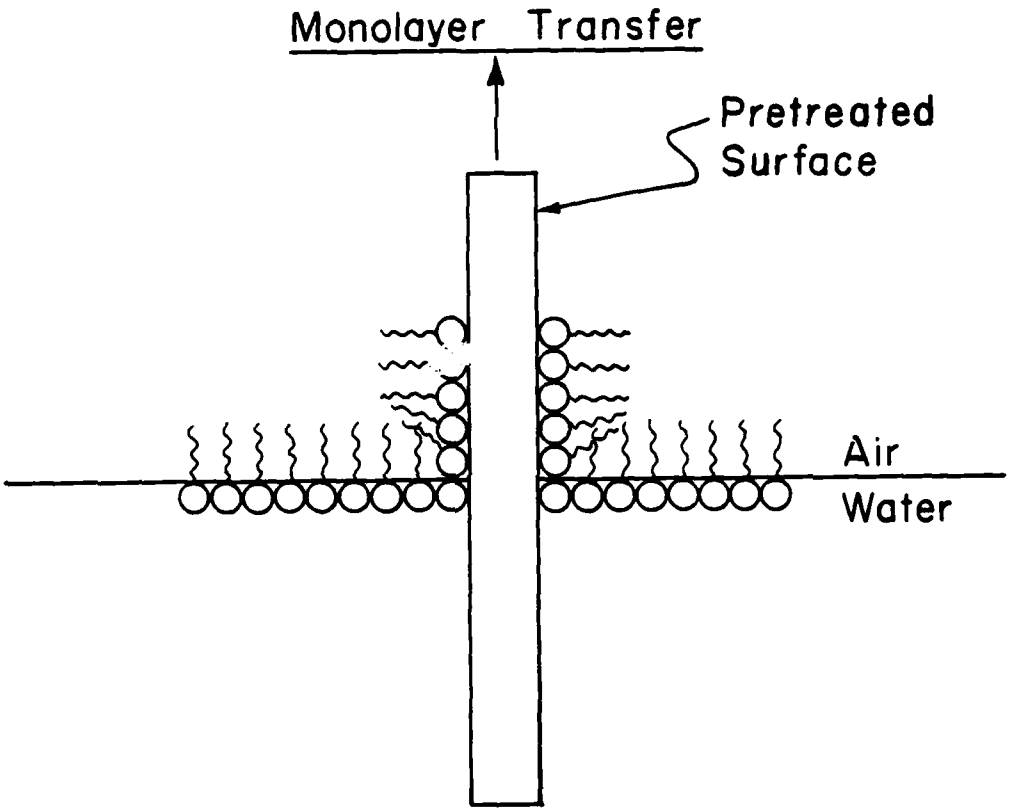

Figure 4. Transfer of a monolayer to a solid substrate.

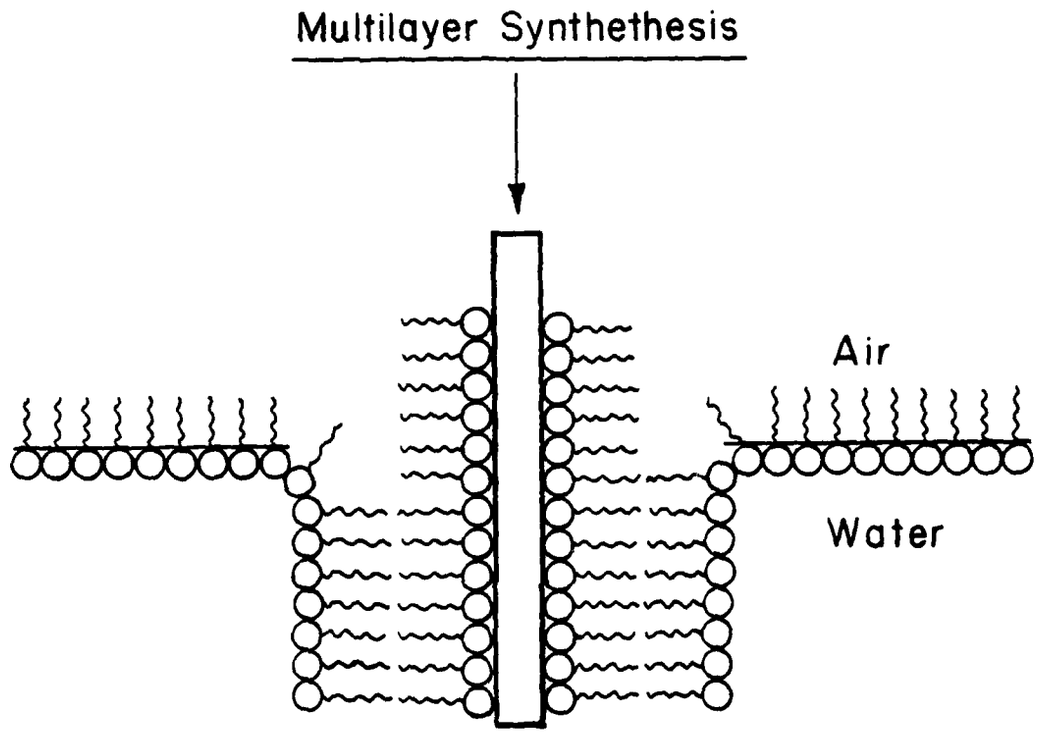

Figure 5. Formation of a bilayer on a solid substrate.

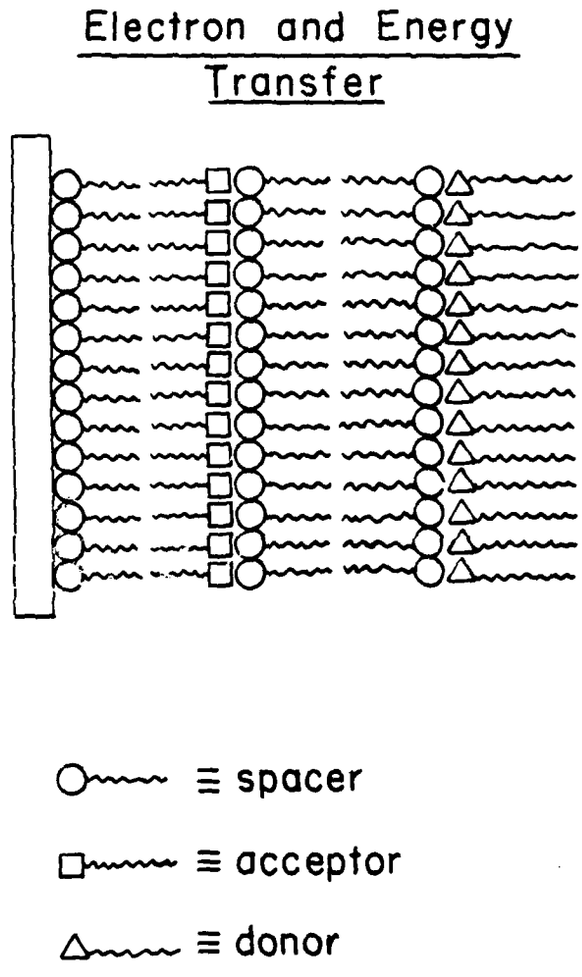

Figure 6. Representation of an assembly for study of energy transfer efficiency vs. distance between a donor and acceptor.

molecules between acceptor and donor. With patience and synthetic expertise it is probable that any chemical functional group can be oriented in monolayer/multilayer assemblies.

e⁻Beam Lithography. Assembly of polymer monomers into monolayer/multilayer arrays makes possible ultra-thin e⁻beam resist materials. It may be possible to exploit such arrays to achieve the high resolution resist material needed in submicron device fabrication. Figure 7 represents the idea and Fig. 8 shows a long chain fatty acid that terminates in a double band that can be e⁻beam polymerized. It is well known that reactions of monolayers can be effected with light or e⁻beams.[2-3] Figure 9 illustrates a literature claim[4] concerning resolution obtained using a multilayer of 15 monolayers.

CONCLUSIONS AND RECOMMENDATIONS

Monolayer techniques may be useful in obtaining the high resolution necessary for submicron device fabrication, but at present there are many fundamental questions that remain unanswered. A basic issue of course is whether there are other approaches to thin film (~100Å) resists that are pinhole free. The advantage of monolayers is that the molecules are oriented and this fact should be useful in controlling polymerization and in achieving pinhole-free polymer. Monolayers certainly offer an unusually good opportunity to prepare surfaces that can be used for purposes of basic study and characterization. Research in this area could lead to new types of ordered, layered structures including semiconducting and metallic conducting organic

Microlithography

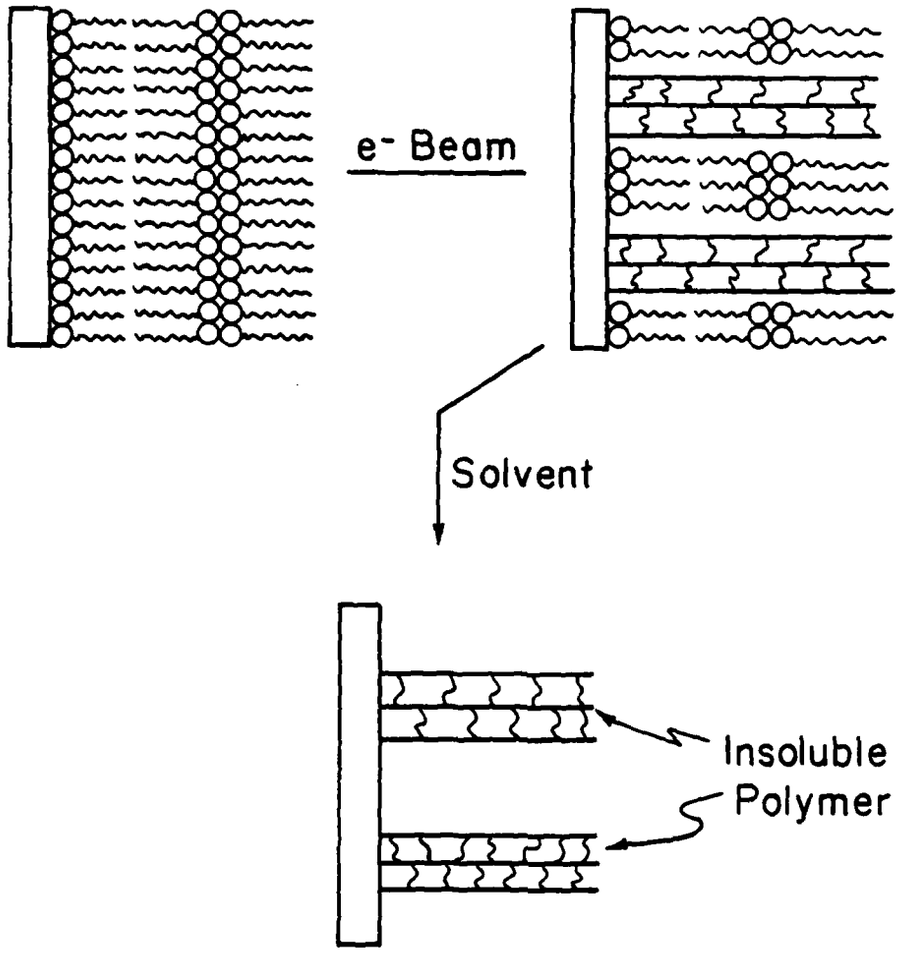

Figure 7. e⁻Beam Resist.

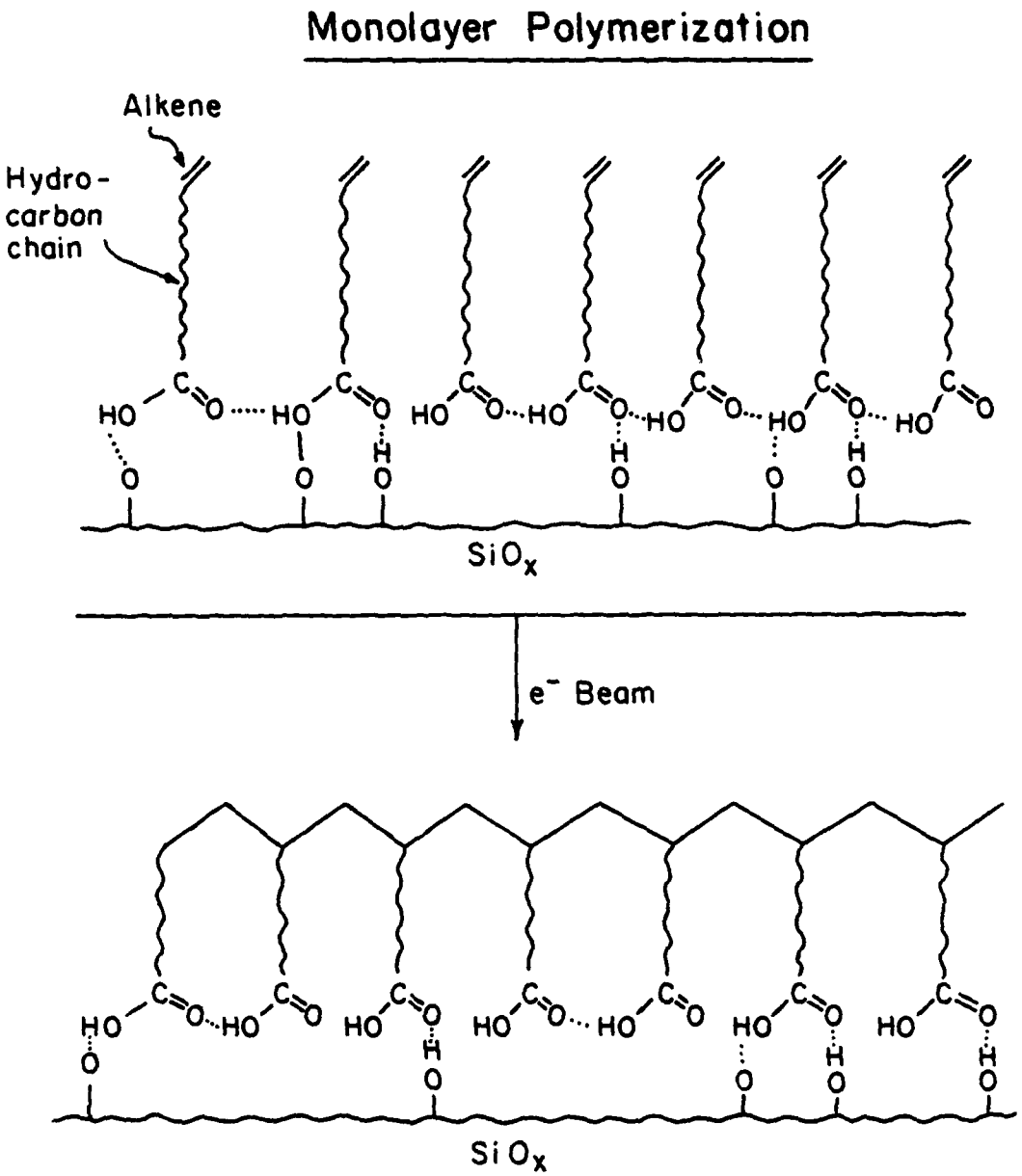

Figure 8. e⁻Beam induced formation of a monolayer polymer.

Resolution Demonstrated

Solid State Technology, 22 (5), 120 (1979)

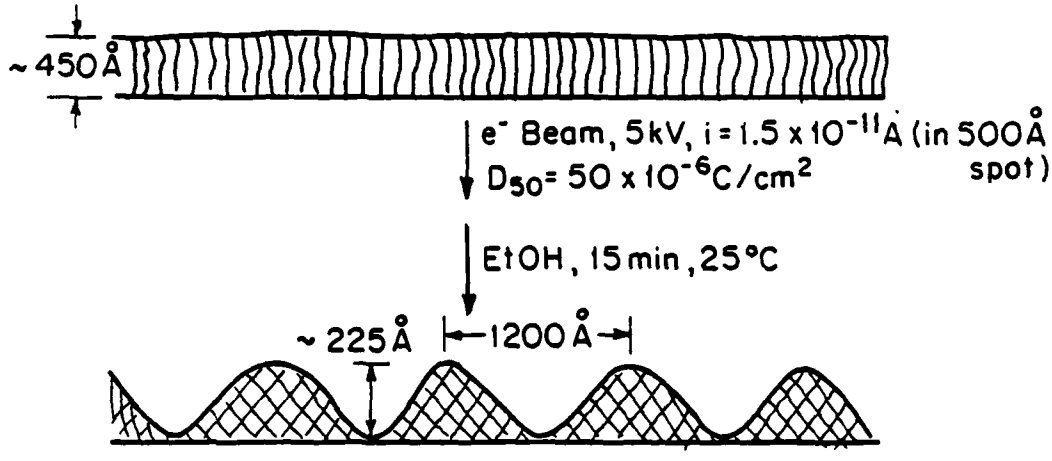

Resist: 15 layers of ω-tricosenoic acid
$(CH_2 = CH-(CH_2)_{20}-COOH)$

Substrate: Al on glass or Si

Figure 9.

polymers. DARPA should launch an effort to determine the minimum thickness or resist that can be used; i.e., can one monolayer of a polymer such as polyethylene actually protect a surface in a subsequent processing step? Additionally, the question of the extent of polymerization within and outside an e^- beam spot is answerable. Classical Langmuir-Blodgett monolayer techniques are probably too time consuming and irreproducible to be useful. However, other deposition techniques such as that for HMDS (Eq. (1)) may be useful. Toward this end, reactions such as those represented by Eqs. (2) and (3) seem worthwhile. Chemistry of this kind will very likely underpin certain aspects of the fabrication of submicron devices.

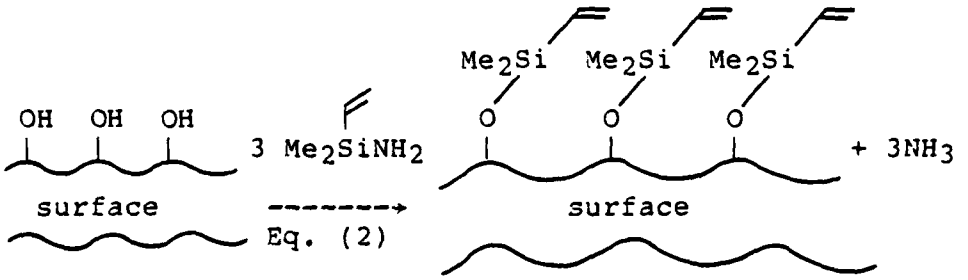

(2)

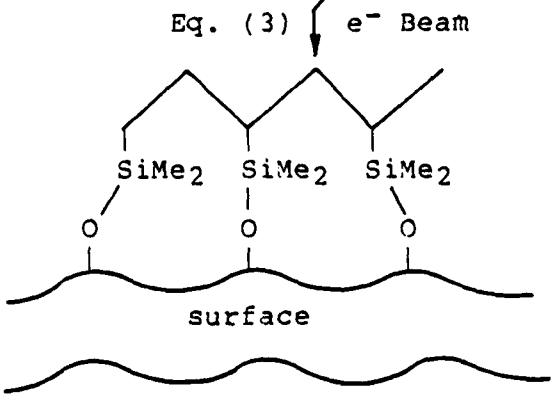

(3)

ACKNOWLEDGEMENT

This paper was prepared under the auspices of the DARPA Materials Research Council, Contract #MDA903-80-C-0505 with the University of Michigan.

REFERENCES

1. G. L. Gaines, Jr., "Insoluble Monolayers at Liquid-Gas Interfaces," Wiley, New York, 1966.

2. A. W. Adamsen, "Physical Chemistry of Surfaces," 2nd Ed., Wiley, New York, 1976.

3. M. Puterman, T. Fort, Jr., J. B. Lando, J. Coll. Sci. 47, 705 (1974); A. Barraud, C. Rosilio, A. Randel-Teixier, J. Coll. Sci. 62, 509(1977) and references cited in both.

4. A. Barraud, C. Rosilio, A. Raudel-Teixier, Solid State Technology 22(8), 120(1979); Thin Solid Films 68, 7, 91, 99 (1980).

NUCLEATION AND GROWTH OF SEMICONDUCTORS ON DISSIMILAR SUBSTRATES

T. C. McGill and J. O. McCaldin

INTRODUCTION

Some of the most exciting developments in recent years in semiconductor materials has been in the field of preparation of single crystal semiconductors on typically dissimilar substrates. These include the growth of single crystal Si on glassy substrates and the preparation from vapor and liquid phases of semiconductor layers (e.g., growth of HgCdTe on CdTe). These techniques of material preparation promise to provide technology for the fabrication of a whole new set of device structures which could be of great importance to the DoD.

R. A. Reynolds (DARPA), H. Ehrenreich (MRC), T. C. McGill (MRC), and J. O. McCaldin (CalTech) organized a meeting to investigate some of the recent developments in this field that are of potential relevance to the DoD. The program concentrated on the growth of HgCdTe layers on CdTe substrates, and the preparation of single crystal Si layers on insulating substrates. The techniques for preparing HgCdTe are of potential importance in the fabrication of economical, high performance infrared detector arrays. The successful fabrication of single crystal Si on dissimilar substrates could be the technological base for three dimensional device structures, as well as providing a planar technology with good device isolation, low power

consumption, and a relatively high radiation resistance. Further, the participants at the meeting were directed to address the generic questions of what parameters determine the success or failure of attempts to grow single crystal layers on dissimilar substrates.

The meeting agenda and list of participants are attached in the Appendix. The one day meeting consisted of four presentations on the question of growth of Si on dissimilar substrates. J. Bloem (Philips, Eindhoven) presented his work on the nucleation and growth of polycrystalline Si from the vapor on amorphous SiO_2 and SiN substrates. H. J. Leamy (Bell Laboratories) discussed in situ crystal growth of single crystal Si on amorphous SiO_2 substrates. J. C. Bean (Bell Laboratories) presented the results of recent studies on growth of Si and various layers involving Si by molecular beam epitaxy. K. Carey (Hewlett-Packard) discussed the growth of Si on sapphire.

The work on HgCdTe was presented in four talks. J. O. McCaldin (CalTech) presented a brief historical review of the attempts to grow large single crystals of II-VI semiconductors on dissimilar substrates. J. B. Mullin (Royal Signal and Radar Establishment) presented his recent work on the growth of CdTe and HgCdTe layers on CdTe substrates using chemical vapor deposition from organometallic vapors (OMCVD) of the Cd and Te in the presence of a Hg source. J. Lagowski (MIT) discussed the work at MIT aimed at growing single crystal layers of HgCdTe using a isothermal growth process. J. P. Faurie (LETI/LFR,

Grenoble, France) described his successes in growing CdTe, HgTe and HgCdTe layers on CdTe substrates using molecular beam epitaxy (MBE). After the formal presentations an informal discussion was held to identify some of the most important issues.

MEETING HIGHLIGHTS

Mercury Cadmium Telluride

Mercury cadmium telluride is the key material in the military programs to produce infrared detector arrays. The economical fabrication of these arrays along with the fabrication of progressively more complicated associated electronics act as a driving force for fabricating reproducible, uniform layers of HgCdTe with electrical and optical properties suitable for infrared optoelectronic device application. At the present a totally acceptable method for fabricating these layers has not been demonstrated. Hence, there is interest in exploring new fabrication techniques for thin films of this material. the major problem is dealing with the very high vapor pressure of Hg at relatively low temperatures.

At the meeting two very new and potentially technically important techniques for growing HgCdTe layers were presented. J. B. Mullin described his very recent work on the growth of CdTe, and HgCdTe organometallic chemical vapor deposition (OMCVD) in the presence of a elemental Hg source in a stream of hydrogen. This technique has a number of potential advantages. Reasonable growth rates can be attained at relatively low sub-

strate temperatures. Thin layers of HgCdTe can be prepared with different electrical properties on HgCdTE or CdTe layers. Previously HgTe has been grown on CdTe substrates by OMCVD by Kuech and McCaldin[1]. However, preliminary attempts to extend this process to HgCdTe resulted in premature reaction between the organometallics and the deposition of a polycrystalline powder on the substrate. Mullin[2] has carried out a systematic study of the reaction of organometallics as a function of various growth parameters such as temperature and pressure. He has used liquid Hg source. From these studies he has arrived at a process to grow HgCdTe[3] at approximately 10 μm/hour at T_S~400°C. Layers with $0 \leq X \leq 0.30$ have been produced. While these layers at present have rather poor electrical properties, no attempt has been made to remove contaminants from the sources. Hence, at this early stage, it is difficult to access the electrical properties of the layers which may be ultimately obtained by this technique.

J. P. Faurie described his recent successes at obtaining growth of HgCdTe using molecular beam epitaxy (MBE).[4] This is the first report of successful growth of HgCdTe by the MBE process. This technique has the possibility of producing abrupt heterojunctions made up of high purity single crystalline layers as well as the advantages quoted above for MOCVD. He has obtained growth rates of 0.4-4 μm/hour at substrate temperatures between 100-120°C. Surface studies of the HgCdTe layers in the ultra high vacuum system showed that the HgCdTe surface was

relatively stable against loss of Hg. He stressed the importance of substrate preparation. The electrical properties of these layers are exceedingly poor at present.

Recent results on preparation of HgCdTe layers using the evaporation, condensation, and diffusion process (isothermal growth process)[5] were presented by J. Lagowski. Heat pipes were used to obtain very uniform temperature profiles. By using a Te rich source, layers with mirror like surface morphology, radial compositional uniformity and high electron mobility were obtained. Growth temperatures of between 530°C to 575°C were employed to produce growth rates as high as 5 μm/hour. These techniques produce interesting layers of HgCdTe. However, it may be difficult to produce thin layers with good compositional uniformity or multilayered structures using this technique.

Silicon

Silicon is the workhorse of the modern electronics industry. Fabrication of single crystal islands of silicon at any point desired on a semi-insulating substrate promises to add a whole new dimension to modern Si electronics. H. J. Leamy described a number of ways of fabricating single crystal Si on amorphous substrate by first depositing an amorphous or polycrystalline layer of Si on the substrate and then crystallizing the layer by annealing the layer with heat produced by a laser, electron beam, or thermal source. Isolated single crystal islands have been produced by annealing confined areas of noncrystalline Si on SiO_2 substrates. Oriented single crystals of

Si have been produced by annealing noncrystalline layers that are in contact with a single crystal layer at some point. Many of the steps in the process are presently understood only empirically.

J. C. Bean described his work on Si molecular beam epitaxy. He has gone through an extenisve development program to produce techniques for handling the rather high temperatures required for Si MBE and the very reactive nature of Si. Bean has developed methods of doping the layers since many of the classical dopants cannot be incorporated easily in the growing layers. The growth of high quality layers of Si on Si has been demonstrated. He has obtained single crystal growth of Si on sapphire and grown some transition metal silicides on Si. These techniques provide versatility in preparing Si device structures and may offer a unique preparation technique for certain applications.

K. Carey described his recent work on the growth of Si on sapphire. Using TEM he has found that substantial changes occur in the nucleation process and the interface defects for variations in substrate temperature from 900°C to 1000°C. The processes of nucleation and defect formation are such that the optimum temperature for growth is about 960°C. These studies indicate that substantial changes in growth characteristics can occur over a rather narrow temperature range.

J. Bloem presented the results of his classic study of the processes of nucleation and growth of Si during chemical

vapor deposition on SiO_2 and SiN substrates. He has studied the kinetics of the nucleation and growth process in order to delineate the processes governing the establishment of nucleation sites followed by the growth of crystallites. This study shows that the number of independent nucleation sites is very large. This observation should be contrasted with the situation described by other speakers where as small as possible number of nucleation sites are desired.

GENERAL DISCUSSION

One of the principle subjects for discussion was what are the properties of substrate and layers which yield high quality single crystals. John Hirth (MRC) speculated that high quality crystalline layers would be obtained when either there is a very nearly perfect lattice match between substrate and layer, or when the substrate and layer have no relationship (e.g., a disordered substrate). In the first case, we obtain true epitaxy. In the second, the random nature of the substrate prevents it from providing a barrier to the orienting forces acting in the layer. Approximate lattice match between substrate and layer (e.g., Si on sapphire) while appearing to approach the perfection of exact lattic match may in fact contain built-in sources of interface defects which can substantially limit their usefulness in the fabrication and operation of devices.

H. Leamy and K. Carey stressed the importance of stress fields in these films and the lack of our understanding of their influence on growth.

R. Reynolds indicated that we lack a fundamental understanding of the properties of materials which facilitate the coalescence of nuclei into a single crystal. Both the control of nucleation and the properties of grain boundaries were thought to be important in these processes.

J. Bean, J. Mullin, and J. Faurie stressed the importance of substrate preparation in obtaining good results in the growth of crystalline layers. Cleanliness, chemical purity and crystalline quality were listed as very important substrate properties in determining the success of growing single crystals.

H. Leamy stressed the need to attain a more basic understanding of nucleation, growth, and annealing processes.

CONCLUDING COMMENTS

The recent advances in the preparation of HgCdTE by vapor phase and molecular beam epitaxy could be important milestones in the development of infrared detector technologies. While the techniques are currently in a very early stage of development and the layers produced so far are not of sufficient quality to be used in devices, these preparation techniques satisfy some of the key requirements for advanced infrared sensor technologies and, hence, should be pursued virorously.

The techniques for growing Si on amorphous substrates are developing along lines that are likely to result in new device structures (e.g., three-dimensional device structures) and new methods of fabricating structures already available (e.g., planar Si devices on insulating substrates). Given DoD's needs for the most advanced electronics, these technologies could be of significance to the DoD prior to their introduction in commercial technologies. Hence, the DARPA programs in this area are particularly appropriate.

The understanding of the basic processes that control the preparation of single crystals on dissimilar substrates is almost totally lacking. Much of the work is largely empirical. This approach can yield useful results but it can lead to failures without adequate information to provide guidance to determine whether the approach is appropriate or some other is more likely to succeed. Given the current approach to research in this country, it is hard to see how this kind of basic understanding will be attained.

In summary, the recent developments in preparing semiconductors on dissimilar substrates show promise of making substantial contributions to the technology of making electronic devices. This area is one that is appropriate for DARPA funding.

REFERENCES

1. Kuech, T. F. and McCaldin, J. O., "Low Temperature CVD Growth of Epitaxial HgTe on CdTE," J. Electrochem. Soc. 128, 1141-44 (1981).

2. Mullin, J. B., Irvine, S. J. C. and Asher, D. J., "Organometallic Growth of II-VI Compounds," J. Crystal Growth 55, XXX (1981).

3. Irvine, S. J. C. and Mullin, J. B.,"The Growth by MOVPE and Characterization of $Cd_xHg_{(1-x)}Te$," J. Crystal Growth 55, XXX (1981).

4. Faurie, J., J. Crystal Growth (to be published.).

5. Becla, P., Lagowski, J., Gatos, H. C. and Ruda, H., "A Modified Approach to Isothermal Growth of Ultrahigh Quality HgCdTe for Infrared Applications," J. Electrochem. 128, 1171-1173 (1981).

APPENDIX

MATERIALS RESEARCH COUNCIL
July 23, 1981

NUCLEATION AND GROWTH OF SEMICONDUCTORS

INTRODUCTION:

R. A. Reynolds (DARPA) "Introductory Remarks"

SILICON: H. Ehrenreich, Chairman

J. Bloem (Philips, Eindhoven) "CVD Growth of Si"

H. J. Leamy (Bell Laboratories) "Beam Processing for Thin Film Crystal Growth of Si"

J. C. Bean (Bell Laboratories) "Growth of Si by Molecular Beam Epitaxy"

HgCdTe: T. C. McGill, Chairman

J. O. McCaldin (CalTech) "Historical Survey of the Growth of II-VI Thin Films"

J. B. Mullin (RSRE) "Growth of HgCdTe"

J. Lagowski (MIT) "New Approaches to Isothermal Growth of HgCdTe"

SHORT PRESENTATIONS

K. Carey (HP) "Recent Results on Si/Al_2O_3"

J. P. Faurie (Laboratoire d' Electronique, Grenoble) "Growth of HgCdTe by Molecular Beam Epitaxy"

Round Table Discussions

NUCLEATION AND GROWTH OF SEMICONDUCTORS

ATTENDEES

Name	Affiliation
H. Ehrenrich	Harvard
S. Roosild	DARPA
T. McGill	Cal Tech.
D. Reynolds	DARPA
J. Hirth	Ohio State
H. Reiss	UCLA
J. C. Bean	BTL
J. Lagowski	M.I.T.
H. Leamy	Bell Labs.
F. Spaepen	Harvard
J. B. Mullin	RSRE (UK)
J. P. Faurie	LETI/LIR (France)
K. W. Carey	Hewlett-Packard
W. E. Spicer	Stanford Univ.
M. S. Wrighton	M.I.T.
E. E. Hucke	Univ. of Michigan
J. Bloem	Philips Res, Eindhoven, Holland
R. M. Cannon	Mass Inst. of Tech.
H. H. Wieder	NOSC San Diego
M. J. Sinnott	Univ. of Michigan
J. L. Margrave	Rice Univ/MRC
Jim McCaldin	Cal Tech.
Ted Wong	New England Research Ctr.

DIFFUSIONAL INSTABILITY OF p/n HETEROJUNCTIONS

J. J. Gilman

The junction between two dissimilar semiconductors is subject to degradation by intermixing of the atoms in a zone of microscopic thickness (approx. 10^{-5} cm.). The driving force for this mixing is large at p/n junctions because the local electric field acts on the partially ionized atoms. This augments the driving force due to the chemical potential difference that would be present if the junction occurred between two intrinsic semiconductors (no p/n junction).

The local electric field is approximately equal to the average energy gap, $\langle E_g \rangle$ divided by the thickness of the junction where the thickness is defined as the tangent-intercept-thickness, d. Since d is approximately one-tenth micron and E_g 1-2 eV, the local field is about 10^5 V/cm.

For a particle of unit charge the mobility, μ of a particle is related to its diffusion coefficient, D by the Einstein relation:

$$\mu = \frac{D}{kT} \ (cm^2/V\text{-}sec) \qquad (1)$$

where k = Boltzmann's constant, and T = temperature. Thus the diffusional velocity is:

$$v = \left(\frac{\langle E_g \rangle}{d}\right) \mu = \left(\frac{\langle E_g \rangle}{d}\right) \frac{D}{kT} \qquad (2)$$

and the diffusional relaxation time is:

$$\tau = \frac{d}{v} = \frac{d^2 kT}{\langle E_g \rangle D} \qquad (3)$$

or, since $D = D_o \exp(-Q/kT)$ where Q is the activation energy for diffusion, the relaxation time may be written:

$$\tau \approx \left(\frac{d^2 kT}{\langle E_g \rangle D_o}\right) e^{Q/kT} \qquad (4)$$

From this expression, it may be concluded that the dominant parameters in determining stability are Q and T; small changes in either of them become strongly amplified.

As an example, consider a solar-cell junction for which $\langle E_g \rangle$ would be about 1.5 eV, D_o might be 10^{-3} cm^2/sec, the temperature in sunlight might be 400°K, $d = 10^{-5}$ cm, and $k = 8.6 \times 10^{-5}$ eV/°K. Then:

$$Q > \frac{1}{29.1} \ln(1.4 \times 10^{17}) = 1.4 \text{ eV. } (32 \text{ kcal/mol}) \qquad (5)$$

This is not a large activation energy for solids with this energy gap value, particularly if they are in the amorphous state.

In conclusion, it has been shown by means of a simple model that diffusional instability may well exist in p/n heterojunctions and should be investigated in designing them, and in measuring the behavior of prototypes.

ACKNOWLEDGEMENT

This paper was written under the auspices of the DARPA Materials Research Council, Contract #MDA903-80-C-0505 with the University of Michigan.

MARTENSITE NUCLEATION IN CERAMICS IN RESIDUAL STRAIN FIELDS

A. G. Evans

INTRODUCTION

The toughness of ceramic materials can be considerably enhanced by inducing a zone of martensitically transformed material around a crack. The magnitude of the toughening is strongly dependent upon the critical stress needed to activate the transformation; specifically, the relative increase in toughness is given by;

$$\Delta K_{Ic}/K_{Ic} \sim V_f e^T_{ij} E/(p^c_{ij}\ p^c_{ij})^{1/2} \qquad (1)$$

where e^T_{ij} is the unconstrained strain of the fully transformed particles, p^c_{ij} is the critical transformation stress, E is Young's modulus and V_f is the volume concentration of particles. A low, but reproducible critical transformation stress is thus needed in order to achieve optimum toughness. The critical stress is associated with the nucleation of the martensite transformation. The intent of the present paper is to examine the nucleation problem in the presence of residual strain associated with thermal expansion mismatch or anisotropy.

The residual strain from thermal expansion anisotropy could be a particularly potent source of martensite nucleation in the presence of facetted particles, because of the existence of strain singularities at the facet corners. Therefore, the formation and growth of a martensite nucleus from a facet corner is analyzed.

RESIDUAL STRAINS IN FACETTED PARTICLES

The residual strains that develop adjacent to facet corners in particles subject to thermal contraction anisotropy are dominated by the singular terms. These terms are associated with the second step in the Eshelby procedure; notably, the application of tractions along the particle interface. The singular residual strains can thus be deduced from the elastic strains associated with a distribution of uniform line forces located within an infinite solid. The pertinent shear strains are given by:

$$\frac{2\pi e_{xz}}{\Delta\alpha\Delta T} = \cos\beta \int_0^{\ell} \frac{(\lambda\cos\beta - x)}{[\lambda^2+2\lambda(z\sin\beta - x\cos\beta)+x^2+z^2]} \left[(1-\nu) + \frac{2(1+\nu)(z+\lambda\sin\beta)^2}{[\lambda^2+2\lambda(z\sin\beta - x\cos\beta)+x^2+z^2]}\right] d\lambda \tag{2}$$

where β is the included angle (Fig. 1), ℓ is the facet length. μ is the shear modulus, $\Delta\alpha$ is the thermal expansion differential, ΔT is the cooling range and (x,z) are the coordinates with respect to the facet corner. For tractions distributed as shown in Fig. 1, the singular residual shear strain can be obtained from Eq. (2) as $(\chi << \ell)$;

$$e_{xz} = \frac{(1+\lambda)}{2\pi} \Delta\alpha\Delta T(\sin 2\beta)^2 \ln(\ell/x) \tag{3}$$

The residual shear strain thus scales with the facet size and the maximum occurs at included angles of $\pi/4$ or $3\pi/4$. Thermal contraction anisotropy also introduces a singularity in the

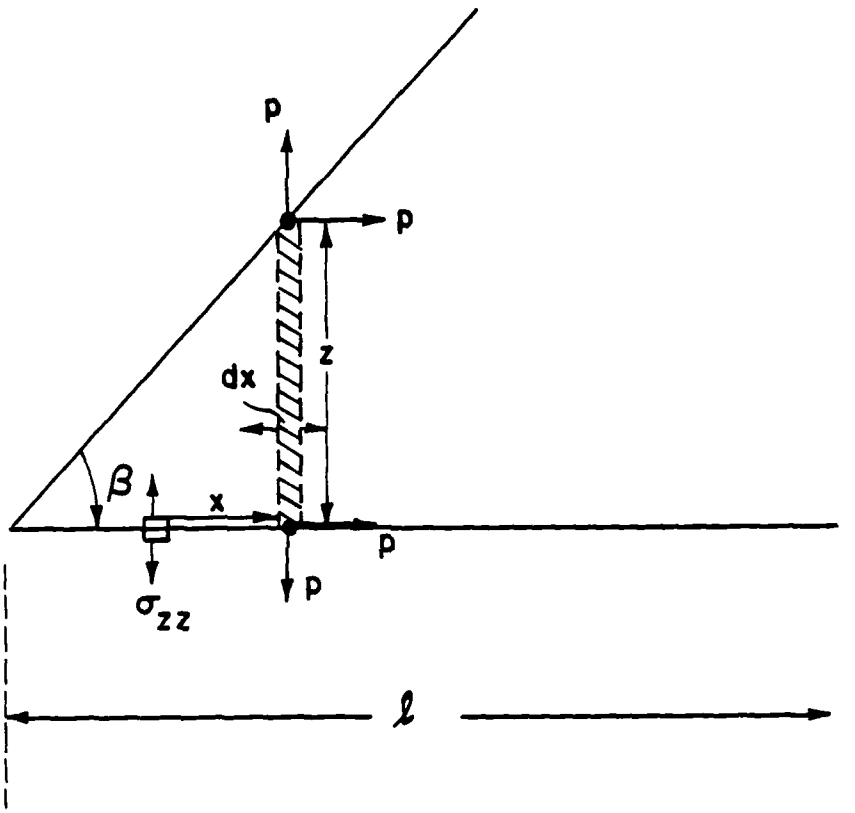

Figure 1. The corner configuration used to evaluate the residual strain concentration.

dilational strain. The corresponding equations are:

$$\frac{2\pi e}{\Delta\alpha\Delta T} = (1-\nu^2)(1+\nu)(1-2\nu)\cos\beta \int_0^{\ell} \frac{(z+\lambda \sin\beta)\, d\lambda}{[\lambda^2+2\lambda(z\sin\beta-x\cos\beta)+x^2+z^2]} \quad (4)$$

which yields the singular strain ($\chi<<\ell$);

$$e = \frac{(1-\nu^2)(1-2\nu)(1+\nu)}{2\pi} \Delta\alpha\Delta T \sin 2\beta \ln(\ell/x) \quad (5)$$

The strain can thus be compressive or tensile, depending upon the included angle and the sign of the contraction anisotropy. Again, the stress scales with the facet length and the imposed thermal strain.

Residual strains also develop as a consequence of a mismatch in thermal contraction between particle and matrix. The singular terms can again be deduced using equations (2) and (4). The residual shear strain derived as above is given by ($x<<\ell$);

$$e_{xz} = \frac{(1-\nu)}{\pi} \Delta\alpha_m\Delta T \sin^2\beta \ln(\ell/x); \quad (6)$$

where $\Delta\alpha_m$ is the mismatch in the thermal contraction coefficient. The maximum shear strain in this instance obtains for an included angle of $\pi/2$. Analysis of the dilational strain does not provide a singularity.

MARTENSITE NUCLEATION IN RESIDUAL STRAIN FIELDS

A martensite transformation will proceed whenever the potential of the system decreases with increase in the proportion of the transformed phase. The terms that contribute to the

potential depend upon the specific character of the nucleus. For a coherent nucleus, the chemical free energy and the strain energy are the essential terms; while, incoherency introduces an additional interface energy. The strain energy change at the nucleus is modified in the presence of residual stress. The magnitude of this modification is determined before exploring the net change in potential.

Strain Energy Modification

In the presence of residual strain, e^R_{ij}, within a volume V, there exists an initial strain energy;

$$\phi^i_{e\ell} = \Lambda\ \mu(e^R_{ij})^2 V \tag{7}$$

where Λ depends upon the shape of the region subject to strain. After transformation, with an associated unconstrained strain, e^T_{ij}, the strain energy becomes;

$$\phi^t_{e\ell} = \Lambda\mu(e^T_{ij} - e^R_{ij})^2 V \tag{8}$$

The change in strain energy is thus:

$$\Delta\phi_{e\ell} = \Lambda\mu e^T_{ij}(1 - 2e^R_{ij}/e^T_{ij})V \tag{9}$$

The modified strain energy change associated with the existence of the residual strain is thus dependent upon the parameter,

$$\zeta = (1-2e^R_{ij}/e^T_{ij}) \tag{10}$$

From Eqs. (3), (5) and (6), for $\nu = 1/4$, the strain energy modifications are;

$$\zeta^{\text{dilation}} = [1-(5/8\pi)\sin\beta(\Delta\alpha\Delta T/e^{T})\ \ln(\ell/x)]$$

$$\zeta^{\text{shear}} = [1-(5/4\pi)(\sin 2\beta)^{2}(\Delta\alpha\Delta T/e^{T}_{13})\ln(\ell/x) \qquad (11)$$

$$\zeta^{\text{mismatch}}_{\text{shear}} = [1-(3/2\pi)\sin^{2}\beta(\Delta\alpha_{m}\Delta T/e^{T}_{13})\{n(\ell/x)$$

The significance of the residual strain to the nucleation process thus depends primarily upon the concentrated strain ratio, $\Delta\alpha\Delta T\ \ln(\ell/x)/e^{T}_{ij}$, and upon the adjacence of the facet angle to $\pi/4$, $\pi/2$ or $3\pi/4$. It is expedient, therefore to examine the magnitude (relative to unity) of the strain ratio in ZrO_2, in order to identify conditions for which the residual strain may exert an important influence upon nucleation. The thermal contraction anisotropy strain in tetragonal ZrO_2 at room temperature, $\Delta\alpha\Delta T$, is $\sim 4\times10^{-3}$. A typical facet size for retained tetragonal ZrO_2 is 0.2 μm, and the smallest conceivable nucleus is 0.5 nm. The maximum concentrated thermal anisotropy strain, $\Delta\alpha\Delta T\ \ln(\ell/x)$, for a nucleus located in the facet corner is thus $\sim 2.5\times10^{-2}$. Hence, this source of residual strain can only reduce the <u>dilational</u> contribution to the strain energy by, at most, 10%.

The deviatoric transformation strain depends upon the character of the nucleus. For a coherent nucleus, $e^{T}_{13} \sim 8\times 10^{-2}$, and the residual strain reduces the transformation strain energy change by up to 15%. For an incoherent nucleus the choice of habit plane determines the transformation strain. For ZrO_2,

the habit plane with the minimum shear strain has $e^T = 6x10^{-2}$. The influence of the residual strain is thus comparable to that for the coherent nucleus. It may be concluded, therefore, that the residual strain associated with the thermal contraction anisotropy in ZrO_2 can have a significant, but not dominant, influence upon the strain energy change associated with the martensite nucleus.

Thermal contraction mismatch effects can be more important. For example, in Al_2O_3/ZrO_2, the thermal mismatch strain $\Delta\alpha_m\Delta T$ is $\sim 9x10^{-3}$. The residual shear strains that derive from both the expansion mismatch and the expansion anisotropy can thus reduce the shear contribution to the strain energy by up to 70%, at small martensite nuclei. This strain energy alleviation could exert a major influence upon the nucleation of the transformation within facetted ZrO_2 particles embedded in an Al_2O_3 matrix.

The Nucleation Barrier

The magnitude of the nucleation barrier depends upon the specific morphology of the nucleus. The strain energy of the nucleus could, of course, be mimimized by selecting a plate morphology. However, in typical martensites, the formation of an extended nucleus would be accompanied by dislocation generation at the habit plane. The associated interface energy would be a deterrent to nucleation (of unknown magnitude) and an additional dislocation nucleation requirment would be imposed on the martensite nucleus. Hence, a coherent, approximately

spherical, nucleus appears more likely. The shear stresses established by the nucleus might then induce interface dislocations and permit the extension of the nucleus into a martensite plate. The energy changes associated with this hypothetical transformation sequence are examined in this section. The strain energy of a coherent spherical nucleus subject to a uniform dilation e^T and a shear e^T_{13} is given by;

$$\Delta\phi_{el} = \left(\frac{8\pi}{9}\right)\left\{\frac{\mu r^3}{(1-\nu)}\left[\frac{(1+\nu)}{3}(e^T)^2 + \frac{(7-5\upsilon)}{5}(e^T_{13})^2\right]\right\} \qquad (12)$$

where r is the radius of the nucleus. This strain energy increase is accompanied by a decrease in chemical free energy ΔF_{chem} of ~200MPa per unit volume (at room temperature). The total energy change, in the absence of an applied stress is then (for $\nu = 1/4$),

$$\Delta\phi = (4/3)\pi r^3 \left\{\frac{10}{27}\mu(e^T)^2\left[1-\left(\frac{5}{8\pi}\right)\sin 2\beta\left(\frac{\Delta\alpha\Delta T}{e^T}\right)\ln(\ell/r)\right]\right. \qquad (13)$$

$$\left. + \frac{46}{45}\mu(e^T_{13})^2\left[1-\frac{\ln(\ell/r)\Delta T}{2\pi e^T_{13}}\left((5/2)\Delta\alpha(\sin 2\beta)^2+3\Delta\alpha_m\sin^2\beta\right)\right]-\Delta F_{chem}\right\}$$

The solution is exemplified for the Al_2O_3/ZrO_2 system and a facet angle of $\pi/2$, whereupon;

$$\frac{\Delta\phi}{\mu(e^T)^2} \approx (4/3)\pi\left\{1/3 + (e^T_{13}/e^T)^2\left[1-\ln(\ell/r)\left(\frac{\Delta T\Delta\alpha_m}{2e^T_{13}}\right)\right] - \frac{\Delta F_{chem}}{\mu(e^T)^2}\right\} \qquad (14)$$

which for the strain and chemical energy characteristics noted above becomes,

$$\Delta\phi/\mu(e^T)^2\ell^3 \approx (r/\ell)^3[1-0.1\ \ln(\ell/r)] \qquad (15)$$

Small nuclei can thus form with a net energy decrease. Specifically, stable nuclei with dimension r $\sim 2\times10^{-4}$ ℓ can exist at the facet corner. However, for a minimum nucleus of ~5Å, a facet dimension of ~2μm would be needed to ensure the existence of a martensite nucleus. This is larger than the dimension of the facets in particles at the critical size. It seems unlikely, therefore, that the residual strains are of sufficient magnitude to nucleate the transformation. An additional source of initial strain should thus be sought.

ACKNOWLEDGEMENT

This paper was written under the auspices of the DARPA Materials Research Council, Contract #MDA903-80-C-0505 with the University of Michigan.

ZIRCONIA TRANSFORMATION TOUGHENING

B. Budiansky, A. G. Evans and J. W. Hutchinson

Phase transformation toughening of ceramics containing zirconia (ZrO_2) particles has been observed with fracture toughness increases as much as two or three times values obtained in corresponding ceramics without such particles. In simplest terms, the volume change (≈4% dilatation) associated with the stress induced transformation of particles near a crack tip from a tetragonal to a monoclinic structure reduces the stress intensity at the tip. Details of the distribution of transformed particles are important, however. A cluster of transformed particles around a stationary crack has no net effect on the crack tip intensity. But as the crack advances (quasi-statically) and leaves behind a wake of transformed particles, the stress intensity at the crack tip becomes modified. Work on the mechanics of this interaction problem was initiated at last year's MRC session and has been pursued again this year now that more experimental evidence for the importance of the phenomena has accumulated.

With σ_C as the critical hydro-static tension required to induce the transformation and with θ_T as the stress-free, dilatational transformation strain of the particles, the relative reduction in the stress intensity factor at the crack tip is of the form:

$$\frac{\Delta K}{K} = .413(1+\nu)\lambda\ f(\lambda) \qquad (1)$$

where ν is Poisson's ratio and

$$\lambda = \frac{cE\theta_T}{9(1-\nu)\sigma_C} \qquad (2)$$

Here, c is the volume fraction of the Zirconia particles and E is Young's modulus. The function $f(\lambda)$ has not yet been computed except in the limit $\lambda = 0$ where $f(0) = 1$. This limit corresponds to the situation where the boundary of the transformed region is unperturbed by the transformation itself so that the boundary can be calculated from the untransformed near-tip stress field. We suspect that the above formula with $f(\lambda) \equiv 1$ will only be adequate for values of λ as large as .3 to .5, whereas actual values of λ can be larger than unity. To determine $f(\lambda)$ over the full range of interest a numerical solution will be necessary in which the perturbed shape of the transformed zone is obtained.

ACKNOWLEDGEMENT

This paper was written under the auspices of the DARPA Materials Research Council, Contract #MDA903-80-C-0505 with the University of Michigan.

EFFECTS OF RESIDUAL STRESS ON THE DIELECTRIC PROPERTIES OF FERROELASTIC MATERIALS

A. G. Evans and E. Cross

INTRODUCTION

Most ferroelastic materials undergo a phase transformation, accompanied by an unconstrained transformation strain, e^T_{ij}. The transformation strain induces residual stresses when the materials are prepared in polycrystalline form. The stresses affect the dielectric properties of the polycrystalline aggregate, in a manner associated with both the grain structure of the material and the propensity for forming 90° domain walls. In particular, fine grained materials not only contain fewer domain walls, but also exhibit appreciably enhanced dielectric properties. It has been inferred that the trend with grain size of both the domain structure and the dielectric properties can be attributed to the tendency for residual stress development at the phase transition. This issue is examined in the present paper.

The problem is addressed by firstly examining the conditions for forming 90° domains in materials of differing grain size, based on the premise that the domain spacing is associated with a minimum in the strain and domain wall energy changes that accompany the phase transition. This analysis predicts an equilibrium domain spacing (as a function of the grain size, the transformation strain and the domain wall energy), as well as a critical grain size for exclusion of 90° domain walls. The

results of the analysis are examined within the context of experimental information on grain size trends in the 90° domain wall propensity; a comparison which also permits estimation of the domain wall energy in $BaTiO_3$.

Subsequent to the analysis of domain formation, the stresses that develop within the grains are computed as a function of the domain density. These stresses are used to calculate changes in the dielectric constant, using determinations of the c/a ratio in the polycrystalline aggregate as an independent basis for assessing the validity of the stress analysis. Finally, a prediction of the change in dielectric constant with grain size is made.

DOMAIN FORMATION

The ferroelastic phase transformation is accompanied by a large change in the polarization energy, as well as smaller changes in the strain energy and 90° domain wall energy. The polarization energy is not influenced by the 90° domain structure of the material. It is thus reasonable to suppose that the domain spacing is dictated primarily by the strain and wall energies. For cases in which the domain walls exhibit a low critical initiation/propagation stress (or, equivalently, ready mobility in the presence of residual stress), the wall will propagate and/or readjust during (or after) the transformation, in order to mimimize the total strain and wall energies of the entire grain. Larger domain wall propagation stresses are likely to result in an individual domain spacings that minimize the

energy change in the partially transformed configurations that evolve during the transformation. The latter could involve dynamic contributions to the strain energy and the computation would require a knowledge of the transformation sequence.

The present calculations are based on 'end-point' energies for the entire grain, and thus pertain to conditions of minimal wall formation stresses. Consequently, the analysis is considered most appropriate for materials, such as $BaTiO_3$, which undergo twinning (90° wall formation) in the presence of modest external stresses. In general, however, the analysis provides an upper bound for the domain wall spacing (or, equivalently, an upper bound estimate of the wall energy).

The problem is addressed by examining the strain and wall energies of a twinned grain. The strain energy $\Delta\phi_e$ of a twinned sphere in an infinite isotropic elastic material is a function of the number of twin pairs, η, and of the unconstrained twinning shear strain e^T_{13}, as depicted in Fig. 1. An approximate analytic result appropriate to a large number of twin pairs is (for Poisson's ratio $\upsilon = 1/3$);

$$\frac{\Delta\phi_e}{\mu V(e^T_{13})^2} \approx \frac{2.6}{2.4+\eta} \qquad (1)$$

where V is the volume of the grain and μ is its shear modulus. Most of the strain that contributes to $\Delta\phi_e$ is confined to an interfacial zone of width ~d, the twin spacing. Interaction effect with neighboring grains are then minimal. Equation (1) can

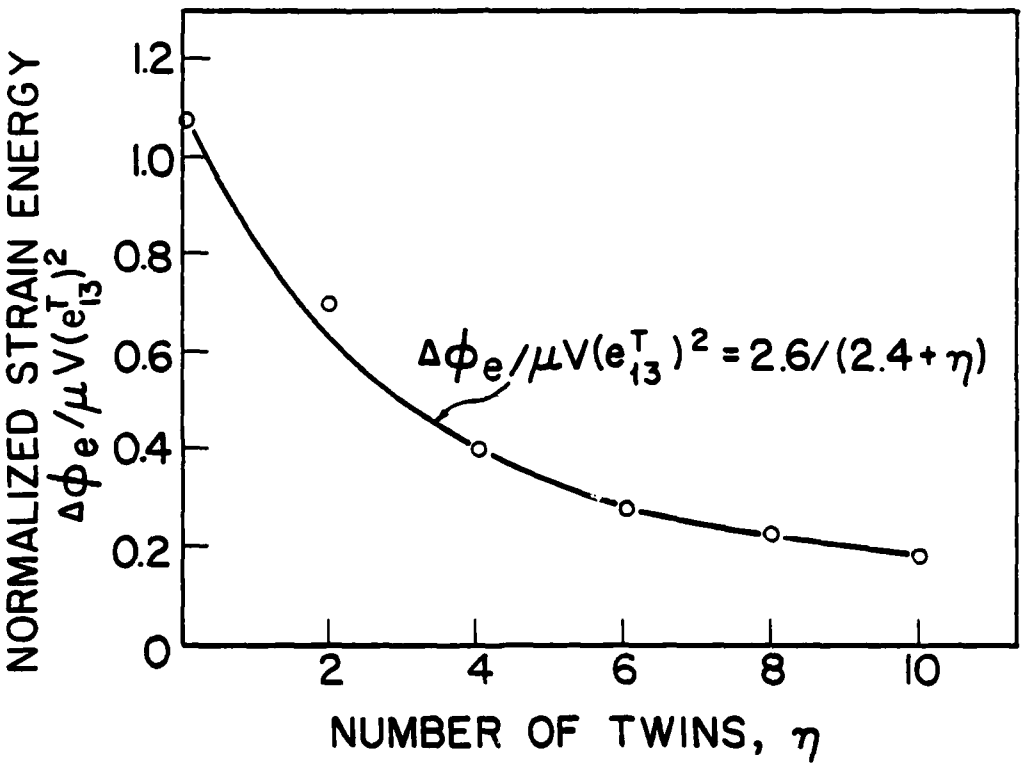
NORMALIZED STRAIN ENERGY
$\Delta\phi_e/\mu V(e_{13}^T)^2$
1.2
1.0
0.8
0.6
0.4
0.2
0
2
4
6
8
10
NUMBER OF TWINS, η
$\Delta\phi_e/\mu V(e_{13}^T)^2 = 2.6/(2.4+\eta)$

FIGURE 1.

thus be expected to provide a reasonable estimate of the strain energy of an individual grain within a polycrystalline aggregate.

The energy $\Delta\phi_S$ of the domain walls contained within a spherical grain is given by;

$$\Delta\phi_S = (2/3)\pi r^2[(\eta-1)(\eta+1)/\eta]\gamma \qquad (2)$$

where γ is the wall energy per unit area and r is the grain radius. The total increase in strain and wall energy during transformation is thus;

$$\Delta\phi \approx (2/3)\pi r^2 \left[\frac{5.2r\mu(e^T_{13})^2}{2.4+\eta} + \frac{(\eta^2-1)\gamma}{\eta}\right] \qquad (3)$$

This energy change exhibits a minimum with respect to the number of twin pairs contained within a grain of specified radius r. This minimum will determine the influence of the grain radius on the equilibrium number of twins. Differentiating Eq. (3) with respect to η, we obtain;

$$\frac{\partial\Delta\phi}{\partial\eta}\Big|r,e^T_{13} = (2/3)\pi r^2 \left\{\frac{(\eta^2+1)\gamma}{\eta^2} - \frac{5.2r\mu(e^T_{13})^2}{(2.4+\eta)^2}\right\} = 0 \qquad (4)$$

which becomes;

$$\frac{(\eta_c{}^2+1)(2.4+\eta_c)^2}{\eta_c^2} = \frac{5.2r\mu(e^T_{13})^2}{\gamma} \qquad (5)$$

The equilibrium number of twins η_c is plotted as a function of the parameter, $r\mu(e^T_{13})^2/\gamma$ in Fig. 2. This result pertains for

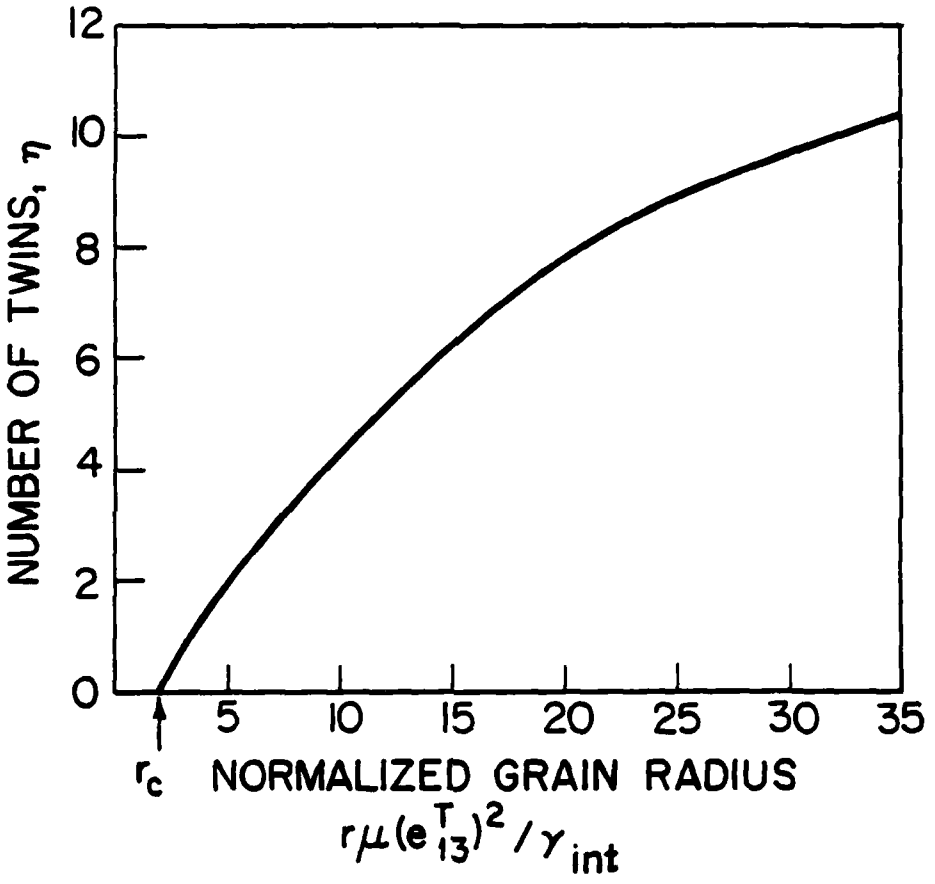
12
10
8
6
4
2
0
NUMBER OF TWINS, η
5
10
15
20
25
30
35
r_c
NORMALIZED GRAIN RADIUS
$r\mu(e^T_{13})^2/\gamma_{int}$

FIGURE 2.

$\eta_c > 1$. The condition associated with the formation of the first domain wall is most conveniently obtained by noting that there is a discrete strain energy decrease associated with this event. The strain energy decrease can be equated to the corresponding increase in domain wall energy in order to deduce a critical grain size for domain wall formation. This procedure gives (Fig. 2);

$$r_c \mu (e_{13}^T)^2 / \gamma = 2.1 \qquad (6)$$

The results expressed by Eqs. (5) and (6) and in Fig. 2 can be compared directly with experimental observations. For example, the "critical" grain size that fully excludes 90° domains in $BaTiO_3$ is ~0.7μm. Inserting this grain size into Eq. (6) and noting that $\mu \sim 5 \times 10^{10}$ Pa and $e_{13}^T \sim 4 \times 10^{-3}$ (at the phase transition) gives an estimate of the wall energy, $\gamma \approx 0.12$ Jm^{-2}. This estimate is within the range of typical twin boundary energies, but appreciably larger than the value calculated by Lawless.

Residual Stresses

The residual stresses within an untwinned grain can be readily calculated using the Eshelby procedure (as adapted to the determination of stresses induced by thermal expansion anisotropy). The stresses are singular adjacent to the facet corners, such that the concentrated stresses extend a distance ~$\ell/4$ from the corner (where ℓ is the facet length). The remainder of the grain is subject to an approximately uniform residual strain. The fraction of the grain volume exposed to the

concentrated strain is thus relatively small, $\sim\pi/16\sqrt{3}$. Hence, the volume average residual stress, which dictates the change in dielectric constant, is closely approximated by the uniform stress in the grain center.

Most ferroelastic materials do not experience a significant volume change during transformation. The residual stresses are thus primarily deviatoric in character. The deviatoric stresses at the grain center can be calculated directly from the results derived by Eshelby for the spherical inclusion. The constrained strains are related to the transformation strains by;

$$e^{C}_{ij} = \frac{2(4-5\nu)}{15(1-\nu)}\, e^{T}_{ij} \tag{7}$$

where ν is Poisson's ratio, and the residual stresses are given by;

$$p^{I}_{ij} = 2\mu(e^{C}_{ij}-e^{T}_{ij}) = -\frac{2(7-5\nu)}{15(1-\nu)}\,\mu e^{T}_{ij} \tag{8}$$

The tranformation strains e^{T}_{ij} depend upon the crystal structure change accompanying the transformation. For a cubic to tetragonal transformation, exemplified by $BaTiO_3$, the c/a ratio in the unconstrained tetragonal phase dictates e^{T}_{ij}. Specifically, in the absence of a volume change the tranformation strain change along the c-axis is,

$$e^{T}_{11} = (c/a)^{2/3} - 1 \tag{9a}$$

while the strain along the a-axes is;

$$e^{T}_{22} = e^{T}_{33} = (a/c)^{1/3} - 1 \tag{9b}$$

Hence, expressing c/a as;

$$c/a = \Delta c/a + 1 \tag{10}$$

the transformation strains become (for $\Delta c/a < 0.1$),

$$e^T_{11} = (2/3)\Delta c/a$$
$$e^T_{22} = e^T_{33} = -(1/3)\Delta c/a \tag{11}$$

The residual stresses are then,

$$p^T_{11} = -\frac{4(7-5\nu)}{45(1-\nu)}\left(\frac{\mu\Delta c}{a}\right)$$

$$p^I_{22} = p^I_{33} = \frac{2(7-5\nu)}{45(1-\nu)}\left(\frac{\mu\Delta c}{a}\right) \tag{12}$$

For $BaTiO_3$, with $\nu = 1/4$, $\mu \sim 5\times10^{10}$ Pa and $\Delta c/a \sim 8\times10^{-3}$, the stresses become: $p^I_{11} = -260$ MPa, $p^I_{22} = p^I_{33} = 130$ MPa.

The stresses in twinned grain are spatially more complex than those in the absence of twinning. For a high density of twins, the residual stresses are localized near the grain boundaries and the volume average residual stress is of negligible magnitude. For a small number of twin boundaries (1 to 3) a significant residual stresses may persist over the grain volume, but the volume average residual stress can only be accurately evaluated using numerical techniques. Such analyses are not considered in the present paper.

The average stress in the polycrystalline aggregate can be estimated from independent measurements of the average c/a ratio of the polycrystal, which provides a direct measure of the

average constrained strain. The problem is most conveniently posed by considering the polycrystal to consist of a number of twinned and untwinned grains, such that only the untwinned grains are subject to significant constraint. The constrained c/a ratio in the untwinned grain is then obtained from Eq. (7) as;

$$(\Delta c/a)_c = \frac{2(4-5\nu)}{15(1-\nu)} (\Delta c/a) \tag{13}$$

Hence, if f is the fraction of untwinned grains, the measured c/a ratio can be expressed as;

$$[2(4-5\nu)/15(1-\nu)]\ f(\Delta c/a) + (1-f)(\Delta c/a) = (\Delta c/a)^* \tag{14}$$

when $(\Delta c/a)^*$ is the measured value for the polycrystal.

If n is the ratio of c/a measured on the polycrystal to the unconstrained c/a (e.g. determined on powders or single crystals), Eq. (14) becomes;

$$f = \frac{15(1-n)(1-\nu)}{(7-5\nu)} \tag{15}$$

The average stress can now be obtained because (consistent with the above premise) only the untwinned grains contribute to residual stress. Hence,

$$\langle p^I_{22} \rangle = f\ p^I_{22} = (2/3)(1-n)\mu(\Delta c/a)$$
$$\langle p^I_{11} \rangle = -4/3(1-n)\mu(\Delta c/a) \tag{16}$$

The solution is exemplified by some results for a fine grained $BaTiO_3$ with n = 0.8. The average a-axis stress is then (for $\Delta c/a = 8x10^{-3}$), $\langle p^I_{22} \rangle$ = 53 MPa. A stress of this magnitude would change the dielectric constant.

ACKNOWLEDGEMENT

This paper was written under the auspices of the DARPA Materials Research Council, Contract #MDA903-80-C-0505 with the University of Michigan.

FERROBIELASTIC DOMAIN SWITCHING IN QUARTZ CRYSTALS

L. E. Cross

The macroscopic properties of ferroic materials depend strongly on their internal domain structure. This domain structure can be altered to suit specific needs by applying appropriate external fields or stresses, and the readjustment is primarily by the motion of walls which separates individual domains.

In ferromagnetic crystals the wall region is broad, extending over hundreds to thousands of unit cells. The energy required to translate the wall by one unit cell is then small compared to the total wall energy and smooth sideways motion occurs. There is a definite coercive magnetic field below which domain structure can not be altered, and for fields above this threshold, a wall mobility can be defined. For simple proper ferroelectrics in contrast, the walls are very narrow, only a few unit cells thick. The energy required to translate the wall by one lattice spacing is thus a large fraction of the total wall energy; and 'true' sideways motion does not occur. Switching in ferroelectrics is by nucleation and growth of new domains (most often on existing walls) making the switching process exponentially time dependent with no unique coercivity.

Data on the kinetics of domain wall motion are not available for any simple ferroelastics, or for any secondary ferroic crystals.

The objective of our research program is to provide such data and the models appropriate for some of their switching processes.

Quartz is a technologically important secondary ferroic which exhibits both ferrobielastic[1] and ferroelastoelectric[2] switching. Earlier studies in our laboratory have explored the acoustic emission, accompanying domain switching, suggesting that nucleation and growth probably underlie this mechanism of wall motion.

Recently, using a small hand operated stressing jig (Fig. 1) we have been making detailed observations of the slow isothermal switching under static fields. Figures 2 and 3 show the slow increase in the size of a bielastic domain under static stress. From such observations at different stress levels again the nucleation and growth model is supported. Most often new ferrobielastic domains appear at stress concentrations on the edges of the quartz samples. Figure 4 is a rare example of a switching twin initiated inside the crystal.

To study the shorter switching times under higher static stresses, we have constructed a simple jig which permits the application of stress in times less than 5 m seconds, and for which the switching is monitored by the change in the piezoelectrically generated charge. This system will permit a full exploration of the switching analagous to the earlier experiments by Merz[3] on ferroelectrics.

ACKNOWLEDGEMENT

This paper was written under the auspices of the DARPA Materials Research Council, Contract # DA903-80-C-0505 with the University of Michigan.

REFERENCES

1. T. L. Anderson, R. E. Newnham, L. E. Cross, "Coercive Stress for Ferrobielastic Switching in Quartz," Proc. 31st Ann. Freq. Control Symposium, pp. 171-177 (1977).

2. J. W. Laughner, R. E. Newnham, L. E. Cross, "Ferroelastoelectricity in Quartz," Phys. Stat. Sol. A56 K83, 1979.

3. W. J. Merz, "Polarization Reversal in $BaTiO_3$," Phys. Rev. 88, 421 (1952).

SOME PRELIMINARY IDEAS ON A DUCTILE-BRITTLE TRANSITION IN Fe-Si SINGLE CRYSTALS

R. Thomson and J. P. Hirth

Vehoff, Rothe and Neumann[1] have published some recent experiments which show that brittle behavior in Fe-2.6% Si single crystals can be induced by increasing the strain rate or by introducing H_2 into the environment. In the normal ductile crack configuration (Fig. 1) the crack advances by alternate slip on complementary slip planes which intersect the crack line (<110> crack line (100) cleavage plane) at an included angle α, of 71°.

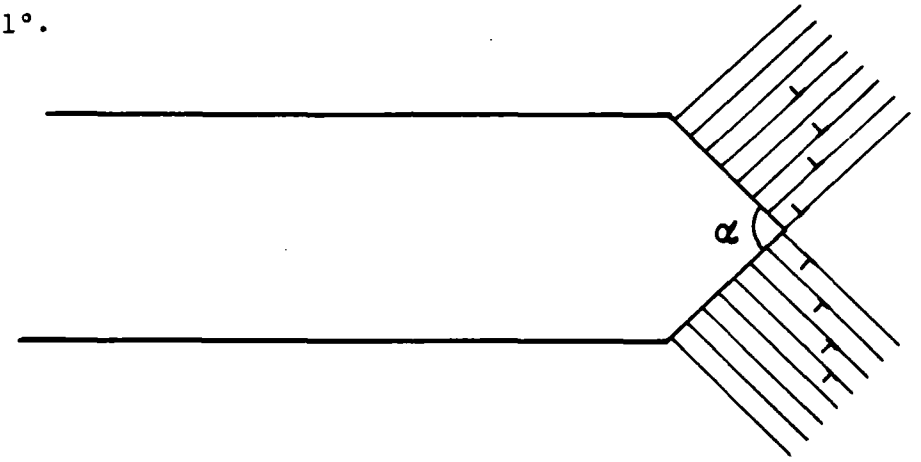

Fig. 1. Ductile fracture configuration in Fe-Si. <110> crack line, (100) slip plane, {112} slip planes.

With this configuration, the emission of a dislocation advances the crack by the ledge created by the dislocation as it comes through the surface at the tip.

Over a range of temperatures, in vacuum, the crack can be be induced to become fully brittle at a critical strain rate S_c has the form;

$$S_c = S_o \, e^{-E_1/kT} \qquad (1)$$

E_1 is the activation energy measured for plastic flow in this material.

If a crack is formed in the ductile range, and H_2 gas is injected into the chamber, the crack again becomes brittle, but in a gradual manner, with hydrogen pressure. Specifically, the angle, α, Fig. 2,

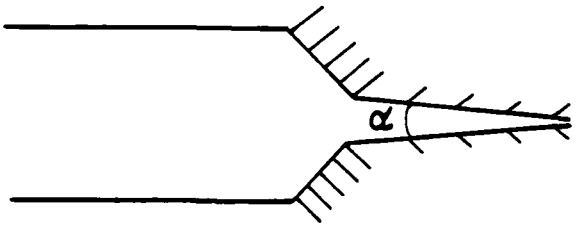

Figure 2. When hydrogen is present, the angle α sharpens over a range of T and P.

decreases with increasing H_2. Over a range of T and P, α is a function of P_{h2} and T, but not of the strain rate, S. The temperature dependence is given by the relation (if $\alpha = \alpha(T,P)$)

$$P = P_o(\alpha)e^{-E_2/kT} \qquad (2)$$

E_2 is the activation for hydrogen desorbtion from the surface.

These experiments throw a direct light on the mechanisms of dislocation emission from cracks in material, and the object of this paper is to discuss these implications in a preliminary and qualitative manner.

Rate Dependent Transition

Rice and Thomson[2] have published criteria for intrinsic dislocation emission from cracks which we write in the form;

$$K_{ductile} > \frac{\mu}{2\sqrt{\zeta_{core}}}$$

$$K_{cleavage} > \sqrt{4\gamma\mu} \qquad (3)$$

K is the crack stress infinity factor, μ the shear modulus, γ the intrinsic surface energy, and ζ_{core} the normalized core radius score = r_{core}/b. These equations state conditions on the stress intensity of the crack for the onset of cleavage or ductility. When $K_{ductile} < K_{cleavage}$, the material is an intrinsically ductile material, and vice-versa. However, at low stresses, ductile crack advance should be slow because the dislocation experience forces considerably lower than those exerted by stresses at the theoretical limit of the material, and the advance of the dislocation atmosphere is rate determining. However, if a sudden high external stress is applied, the crack stress intensity factor will exceed $K_{cleavage}$, and if the stress is sufficiently high, the crack will generate sonic speeds.

Under these high stress conditions, the force on the dislocation will be given by Fig. 4.

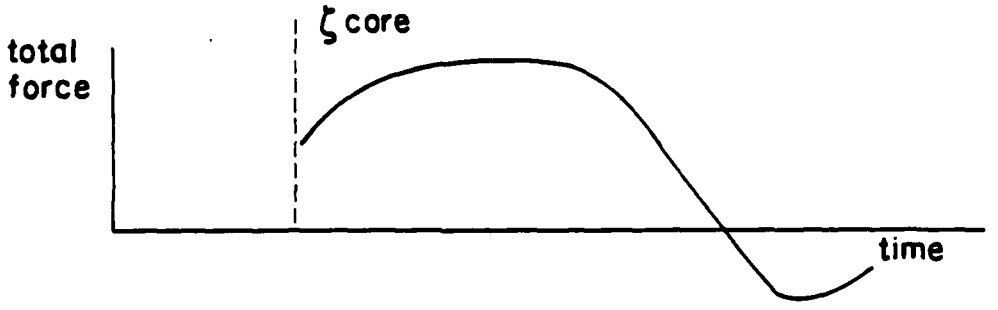

Figure 4. The force experienced by an emitted dislocation as a crack moves through the material at sonic speeds.

The force is approximately constant over much of its range because of the partial cancellation of the K-field repulsive force on the dislocation and the image force on the dislocation in the cleavage plane of the crack. Also, the force exerted on the dislocation is well below that to drive it to sonic speeds because of the same partial cancellation. Thus, provided the crack can move at sonic speeds, the dislocation is left after emission sitting at a position where it can easily be drawn back into the cleavage plane.

Quantitive results, however, will have to await a more adequate treatment including the effects of multiple dislocation emission and the reactions between the dislocations and the crack.

Hydrogen Effects

The most striking point relative to the hydrogen experiment is the fact that the embrittlement takes place over a range of hydrogen coverage which is nearly unity. Using a simple diatomic molecular dissociative process at the surface with a Langmuir isotherm, we find that $\theta/(1-\theta) > 10^5$ or $\theta \cong 1$. This fact means that one may not invoke models where the embrittlement is due to the gradual filling of the available sites on the surface.

However, we note that in the case $\theta \sim 1$, the Gibbs adsorbtion equation becomes

$$\gamma = \gamma_o - \frac{kT}{a_o^2} \int \frac{\theta}{P} \, dP = \gamma_o - \frac{kT}{a_o^2} \ln \frac{P}{P_o} \qquad (4)$$

If the fracture is modified by the chance in γ, then only if the ln P/P_o team can generate numbers of order 10 can γ be affected in a way fracture equilibrium can be sensitive to. However, this is precisely what is observed, because the angle varies over a pressure range of 10^{-1} to 10^{4} Pa. In Fig. 5, the straight portion of the γ plot is the one corresponding to embrittlement.

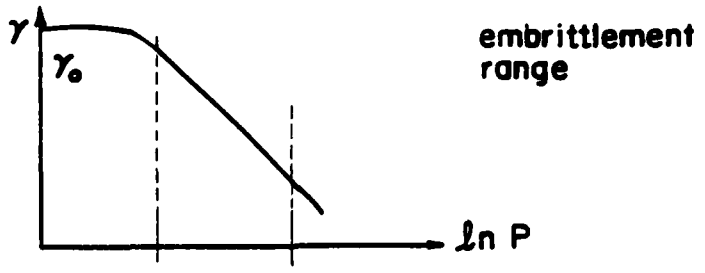

Figure 5. Gibbs isotherm showing range where $\theta/(1-\theta)$ is very large and embrittlement occurs.

With these clues, we assume that embrittlement is driven by thermodynamic forces, and that the crack grows under equilibrium conditions (a point already noted by Vehoff and Neumann[1]). Under these conditions we assume that the γ change is sufficient to reverse the ductility-cleavage order for Fe, and that under H_2, $K_{ductile} < K_{cleavage}$ in Eq. (3). We now assume that dislocations are emitted by thermal nucleation, and that the crack motion is also controlled by thermal fluctuations at the crack tip where the H adsorption occurs. From the theory of these processes [2,3], we find that

$$v_c = v_o\, e^{-(E(H)-K\lambda_c)kT}$$

$$v_d = v_o\, e^{-(E_o+b\delta\gamma-K\lambda_d)/kT} \qquad (5)$$

where v_o is the crack velocity, E(H) is the activation energy due to hydrogen reaction at the crack tip plus lattice trapping, K is the stress intensity factor measured from the Griffith value in the presence of hydrogen, and λ_c is the activation volume for crack growth. We expect E(H) to be essentially insensitive to hydrogen pressure in this range, because $\theta \cong 1$. In the second equation, E_o is the activation energy of dislocation nucleation in the absence of H_2 (essentially zero), $b\delta\gamma$ is the additional activation energy required to form a nucleus at the pressure of hydrogen, and λ_d is the activation volume for dislocation nucleation.

The ratio of the two expressions in (5) gives the angle of opening of the crack, α. Thus

$$\tan\alpha = \frac{v_d}{v_c} = \frac{v_o e^{(E(H)-E_o)/kT}\; e^{-b\delta\gamma/kT}\; e^{K(\lambda_d-\lambda_c)/kT}}{v_o} \qquad (6)$$

This equation has the desired character. The second term yields the basic relation between α and hydrogen pressure, and the tendency of λ_d and λ_c to cancel yields the result that α should be only weakly dependent on K (or strain rate), as observed.

These ideas are far from a complete theory, but seem to contain the basic physics of both types of ductile to brittle transition as observed by Vehoff, Rothe and Neumann.

ACKNOWLEDGEMENT

This paper was written under the auspices of the DARPA Materials Research Council, Contract #MDA903-80-C-0505 with the University of Michigan.

REFERENCES

1. H. Vehoff, W. Rothe and P. Neumann, Adv. Fract. Rsh., 1, 265, (1980); H. Vehoff and P. Neumann, Acta Met. 28, 265 (1979).

2. J. Rice and R. Thomson, Phil. Mag. 29, 73 (1974).

3. R. Thomson, Report of NATO Conference on Atomistics of Fracture, Ed. R. Latanision, 1981. Pergamon New York.

COMMENT ON A PROCEDURE FOR THERMOMECHANICAL ANALYSIS OF ELASTIC COMPOSITE MATERIALS

James R. Rice

ABSTRACT

A "homogenization" technique has been employed recently by Gurtman et al. (1981) to derive equations governing the macroscale static thermoelastic response of structures composed of a periodic composite material. The approach is outlined briefly here, and the identity of the effective thermoelastic properties, as they arise within the homogenization procedure, to those of the classical approach to overall properties of composites is demonstrated.

COMMENT ON A PROCEDURE FOR THERMOMECHANICAL ANALYSIS OF ELASTIC COMPOSITE MATERIALS

James R. Rice

Gurtman et al. (1981) investigate the equations governing static thermoelastic response of structures composed of fiber-reinforced, periodic composites by use of an elegant homogenization technique, based on multiscale asymptotic expansion, the fundamentals of which are referenced to Keller (1977) and Bensoussan et al. (1978). Basically , Gurtman et al. consider a boundary value problem for an elastic solid with periodic structure characterized by ε, where ε is a ratio of cell size to macroscopic dimension of the body. They embed the displacement field $\underline{u}(\underline{x},\varepsilon)$, where ε is regarded as a parameter, in the function $\underline{v}(\underline{x},\underline{\xi},\varepsilon)$ of two space variables $\underline{x}$ and $\underline{\xi}$, where

$$\underline{u}(\underline{x},\varepsilon) = \underline{v}(\underline{x},\underline{x}/\varepsilon,\varepsilon) \tag{1}$$

and where $\underline{v}$ $(\underline{x},\underline{\xi},\varepsilon)$ and its derivatives on $\underline{x}$ (macroscale) and $\underline{\xi}$ (microscale) are assumed to be analytic in the neighborhood of $\varepsilon = 0$. Thus

$$\underline{v} = \underline{v}^{(0)}(\underline{x},\underline{\xi}) + \varepsilon\underline{v}^{(1)}(\underline{x},\underline{\xi}) + \varepsilon^2\underline{v}^{(2)}(\underline{x},\underline{\xi}) + \ldots \tag{2}$$

where $\underline{v}^{(1)},\underline{v}^{(2)}$, ..., have a vanishing average on $\underline{\xi}$ over a unit cell.

Assuming that stress $\underline{\sigma}$ is related to displacement gradient $\partial\underline{u}/\partial\underline{x}$ and temperature change T by

$$\sigma_{ij} = C_{ijkl}\partial u_k/\partial x_l - \gamma_{ij}T \quad , \tag{3}$$

where $\underline{C}$ and $\underline{\gamma}$ are periodic (and hence regarded as functions of $\underline{\xi}$) and $\underline{C}$ is consistent with a positive definite strain energy, and by enforcing the equilibrium condition, $\partial\sigma_{ij}/\partial x_i = 0$, Gurtman et al. show that

$$v^{(0)}(\underline{x},\underline{\xi}) = \underline{v}^{(0)}(\underline{x}) \equiv \underline{u}^{o}(\underline{x}) \quad , \tag{4}$$

so that $u^o(x)$ can be interpreted as a cell-average displacement field (i.e., as the displacement field at the macroscale level), and that

$$\frac{\partial}{\partial \xi_i}\left(C_{ijkl}\partial v_k^{(1)}/\partial \xi_l\right) + \frac{\partial}{\partial \xi_i}\left(C_{ijkl}\right)\partial u_k^{(0)}/\partial x_l$$

$$- \frac{\partial}{\partial \xi_i}\left(\gamma_{ij}\right)T^{(0)} = 0 \tag{5}$$

where $T^o(x)$ is the macroscale temperature field. This differential equation for $\underline{v}^{(1)}$ is shown to have a solution, in the form

$$v_k^{(1)}(\underline{x},\underline{\xi}) = \phi_{klm}(\underline{\xi})\partial u_l^{(0)}(\underline{x})/\partial x_m - \Psi_k(\underline{\xi})T^o(\underline{x}) \tag{6}$$

(where $\underline{\phi}$ and $\underline{\Psi}$ are periodic, with zero means) only if the "forcing terms" $\underline{u}^{(0)}(\underline{x})$ and $T^{(0)}(\underline{x})$ satisfy the differential equations

$$C^{(e)}_{ijkl}\partial^2 u_k^{(0)}(\underline{x})/\partial x_l \partial x_i - \gamma^{(e)}_{ij}\partial T^{(0)}(\underline{x})/\partial x_i = 0 \tag{7}$$

where

$$C^{(e)}_{ijkl} = \langle C_{ijkl} \rangle + \langle C_{ijmn} \partial \phi_{mkl} / \partial \xi_n \rangle$$

$$\gamma^{(e)}_{ij} = \langle \gamma_{ij} \rangle + \langle C_{ijkl} \partial \Psi_k / \partial \xi_l \rangle \qquad (8)$$

and the brackets denote averages over a unit cell.

Plainly, Eqs. (7) are the equations of equilibrium for an elastic body of homogeneous properties, and thus $\underline{C}^{(e)}$ and $\underline{\gamma}^{(e)}$ can be regarded as the "effective" (or macroscale) elastic properties of the periodic composite.

It is perhaps obvious, but not remarked upon explicitly in the work of Gurtman et al., that at this point the homogenization procedure has led to results which are fully consistent with the classical literature (created, for example, during the 1960's and 1970's by Budiansky, Christensen, Hashin, Hill, Laws, Rosen, Walpole, Willis and others) on composite materials. This literature has been summarized in a review by Hashin (1970) and in a book by Christensen (1979).

The interpretation of the homogenization procedure in terms of the classical approach to effective properties can be illustrated in the following way. Consider a composite material of periodic structure subjected to the set of macroscopic displacement gradients $\underline{F}$ (with property $F_{ij} = \langle \partial u_i / \partial x_j \rangle$) and to temperature change T. Then the local displacement field within the composite can be written as

$$u_i(\underline{x}) = F_{ij} x_j + u'_i(x) \qquad (9)$$

where $\underline{u}'(\underline{x})$ is periodic. The stress field is therefore

$$\sigma_{ij} = C_{ijkl}(F_{kl} + \partial u'_k/\partial x_l) - \gamma_{ij}T \tag{10}$$

and, since $\partial\sigma_{ij}/\partial x_i = 0$,

$$\frac{\partial}{\partial x_i}(C_{ijkl}\partial u'_k/\partial x_l) + \frac{\partial}{\partial x_i}(C_{ijkl})F_{kl} - \frac{\partial}{\partial x_i}(\gamma_{ij})T = 0 \tag{11}$$

This has the same form as eq. (5) and if, analogously to Eq. (6), we denote its solution by

$$u'_i(\underline{x}) = \phi_{klm}(\underline{x})F_{lm} - \Psi_k(\underline{x})T \quad , \tag{12}$$

then σ_{ij} may be computed by substitution into eq. (10) and hence the macroscopic stress, equatable to $\langle\sigma_{ij}\rangle$ by the mean stress theorem, is given by

$$\langle\sigma_{ij}\rangle = \overline{C}_{ijkl}F_{kl} - \overline{\gamma}_{ij}T \tag{13}$$

where

$$\begin{aligned} \overline{C}_{ijkl} &= \langle C_{ijkl}\rangle + \langle C_{ijmn}\partial\phi_{mkl}/\partial x_n\rangle \\ \overline{\gamma}_{ij} &= \langle\gamma_{ij}\rangle + \langle C_{ijkl}\partial\Psi_k/\partial x_l\rangle \end{aligned} \tag{14}$$

By comparison of these equarions for $\underline{\overline{C}}$, $\underline{\overline{\gamma}}$ with those given previously, Eqs. (8), for $\underline{C}^{(e)}$, $\underline{\gamma}^{(e)}$, it is obvious that $\underline{C}^{(e)} = \underline{\overline{C}}$ and $\underline{\gamma}^{(e)} = \underline{\overline{\gamma}}$, and hence that the result of the homogenization approach is consistent fully with the classical approach to effective properties outlined in this paragraph.

ACKNOWLEDGEMENTS

The preparation of this note was supported by the DARPA Materials Research Council, Contract #MDA-903-80C-0505 with the University of Michigan. Discussions with B. Budiansky and D. C. Drucker concerning the literature on effective properties of composites have been very helpful.

References

Bensoussan, A., Lions, J. L., and Papanicolaou, G., Asymptotic Analysis of Periodic Structures, North-Holland, 1978.

Christensen, R. M. , Mechanics of Composite Materials, Wiley, 1979.

Gurtman, G. A., Rice, M. H. and Maewal, A., Systems, Science and Software draft final report SSS-R-81-4862 (title: Thermomechanical analysis of graphite/metal matrix composites) to DARPA, Contract DNA001-80-C-0129, Feb. 1981.

Hashin, Z., in Mechanics of Composite Materials (Proc. 5th ONR Symp. on Naval Struct. Mech., ed. F. W. Wendt et al.), Pergamon, 1970, p. 201.

Keller, J. B., in Statistical Mechanics and Statistical Methods in Theory and Application (ed. W. Landman), Plenum, 1977, p. 631.

STABILITY OF SHEAR IN PLASTIC MATERIALS WITH DIFFUSIVE TRANSPORT OF STATE PARAMETERS

James R. Rice

ABSTRACT

Shear of rate-dependent plastic materials is analyzed in cases for which some or all of the state parameters, on which the plastic response rate depends, are capable of both transport by diffusion and further generation by the plastic flow process itself. The first section of the paper establishes a general thermodynamic framework for such phenomena. The latter sections establish conditions for stability of isothermal shear in the simplified case of a single internal state parameter.

STABILITY OF SHEAR IN PLASTIC MATERIALS WITH DIFFUSIVE TRANSPORT OF STATE PARAMETERS

James R. Rice

INTRODUCTION AND GENERAL THEORY

Consider a layer of material which is being deformed in simple shear, Fig. 1. We consider the class of deformations for which displacement u (illustrated as a displacement in the x direction from P to P') and all state parameters depend only on the coordinate y perpendicular to the plane of the layer and time t. The following analysis applies whenever (i) the layer is constrained so that there is no displacement in the y direction, or (ii) there is no normal stress in the y direction; either of these assumptions, unessential to the results which follow, simplify matters by removing normal stress working terms from the energy equation.

Regarding y as a Lagrangian (or material) coordinate, a shear strain γ is defined by

$$\gamma = \partial u(y,t)/\partial y \tag{1}$$

Suppose that the state of the material is described, in a thermodynamic sense, by the strain γ, the "plastic strain" η (to be made precise later), temperature T, and a set of n internal state variables $\underline{\theta}$ $[=(\theta_1,\theta_2,\ldots,\theta_n)]$. The variables $\underline{\theta}$ are additional to the plastic strain and are in the form of concentrations per unit volume of reference state, e.g., of

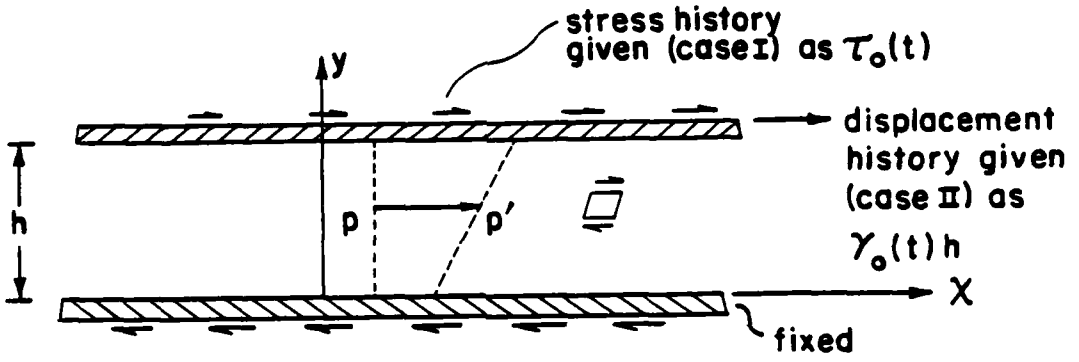

Figure 1. Layer deforming in shear.

dislocation line length (defining dislocation density), of numbers of dislocation loops or appropriate moments, of masses of mobile chemical species, etc. The possibility is allowed that, in general, the quantities denoted by $\underline{\theta}$ may be subject to diffusive transport as well as to evolution in time even in the absence of transport. For chemical concentrations, at least of species that do not participate in reactions, the latter evolution is absent. For dislocation concentrations, it is normally assumed that there is no diffusive transport, but only evolution in time owing to ongoing plastic flow and/or recovery processes. However, following a suggestion of Perzyna (1980), we consider here the possibility of diffusive transport associated with state variables representing dislocation or similar defect densities.

Thus, letting τ be the shear stress, q the energy flow in the y direction (consisting of heat flow plus the additional flow due to diffusive transport), and $\underline{J}[=(J_1,J_2,\ldots,Jn)]$ the set of diffusive fluxes in the y direction associated with the set $\underline{\theta}$, the governing equations are

<u>momentum</u>:

$$\partial\tau/\partial y = \rho\, \partial^2 u/\partial t^2 \tag{2}$$

<u>energy</u>:

$$\tau\, \partial\gamma/\partial t - \partial q/\partial y = \partial e/\partial t \tag{3}$$

(where e is the internal energy per unit reference volume), and

entropy production:

$$\partial(q/T)/\partial y + \partial s/\partial t - \partial(\underline{\mu} \cdot \underline{J}/T)/\partial y \geq 0 \qquad (4)$$

In the last expression s is entropy per unit reference volume and the set $\underline{\mu}$ [= $(\mu_1, \mu_2, \ldots, \mu_n)$] are the potentials associated with $\underline{\Theta}$.

Letting $\phi = \phi(\gamma-\eta, T, \underline{\Theta}) = e-Ts$ be the free energy per unit reference volume (the dependence on $\gamma-\eta$ serves to identify the plastic strain, η, if it is assumed that $\partial\phi/\partial\gamma = 0$ when $\gamma = \eta$), the stress τ, entropy s, and potentials $\underline{\mu}$ are

$$\tau = \frac{\partial}{\partial\gamma}\,\phi(\gamma-\eta, T, \underline{\Theta}), \quad s = -\frac{\partial}{\partial T}\,\phi(\gamma-\eta, T, \underline{\Theta}) \quad ,$$

and

$$\underline{\mu} = \frac{\partial}{\partial \underline{\Theta}}\,\phi(\gamma-\eta, T, \underline{\Theta}) \qquad (5)$$

Also, the total differential of ϕ is

$$\delta\phi = \tau\delta\gamma - \tau\delta\eta - s\delta T + \underline{\mu} \cdot \delta\underline{\Theta} = \delta e - T\delta s - s\delta T \qquad (6)$$

Now, when the energy equation is used to substitute for the term $\partial q/\partial y$ in the entropy production inequality there arises

$$-\frac{q-\underline{\mu}\cdot\underline{J}}{T}\,\frac{\partial T}{\partial y} - \underline{J} \cdot \frac{\partial \underline{\mu}}{\partial y}$$

$$+ \tau\,\frac{\partial\gamma}{\partial t} - \frac{\partial e}{\partial t} + T\,\frac{\partial s}{\partial t} - \underline{\mu} \cdot \frac{\partial \underline{J}}{\partial y} \geq 0 \quad ,$$

and by using the expression for $\delta\phi$ above this may be reduced to

$$-\frac{q-\underline{\mu}\cdot\underline{J}}{T}\,\frac{\partial T}{\partial y} - \underline{J} \cdot \frac{\partial \underline{\mu}}{\partial y} + \tau\,\frac{\partial\eta}{\partial t} - \underline{\mu} \cdot \left(\frac{\partial \underline{\Theta}}{\partial t} + \frac{\partial \underline{J}}{\partial y}\right) \geq 0 \qquad (7)$$

Through well known arguments, it is plausible to assume that the first two terms and the remaining terms sum separately to non-negative quantities, so that constitutive equations describing the non-elastic processes involved must satisfy

$$- \frac{q-\underline{\mu}\cdot\underline{J}}{T} \frac{\partial T}{\partial y} - \underline{J} \cdot \frac{\partial \underline{\mu}}{\partial y} \geq 0 \tag{8}$$

and

$$\tau \frac{\partial \eta}{\partial t} - \underline{\mu} \cdot \left(\frac{\partial \underline{\Theta}}{\partial t} + \frac{\partial \underline{J}}{\partial y}\right) \geq 0 \tag{9}$$

As a general framework, we may assume that the plastic strain rate $\partial\eta/\partial t$ and the rates of generation, $\partial\underline{\Theta}/\partial t + \partial\underline{J}/\partial y$, of quantities represented by the variables $\underline{\Theta}$ are functions of τ, T and $\underline{\Theta}$:

$$\partial\eta/\partial t = f(\tau, T, \underline{\Theta}) \tag{10}$$

$$\partial\underline{\Theta}/\partial t + \partial\underline{J}/\partial y = \underline{g}(\tau, T, \underline{\Theta}) \tag{11}$$

where, by Eq. (9), the functions must satisfy $\tau f - \underline{\mu} \cdot \underline{g} \geq 0$. Of course, for a variable Θ_k representing a fully conserved species, the corresponding g_k is zero; also, for a set of Θ's representing variables involved in a chemical reaction, the corresponding g's are constrained by linear relations to one another.

If we are concerned only with modest departures from spatial uniformity, the fluxes can be written as

$$q-\mu\cdot J = - TL_{00} \frac{\partial T}{\partial y} - T\underline{L}_{01} \cdot \frac{\partial \underline{\mu}}{\partial y} \tag{12}$$

$$J = - \underline{L}_{10} \frac{\partial T}{\partial y} - \underline{L}_{11} \cdot \frac{\partial \underline{\mu}}{\partial y} \tag{13}$$

where the composite n + 1 by n + 1 matrix

$$[L] = \left[\begin{array}{c|c} L_{00} & \underline{L}_{01} \\ \hline \underline{L}_{10} & \underline{\underline{L}}_{11} \end{array}\right]$$

is positive definite and, if assumptions appropriate for Onsagers relations are met, [L] is symmetric.

As a final note regarding the general formalism, observe that the energy equation may be re-written as

$$-\frac{\partial q}{\partial y} = \frac{\partial e}{\partial t} - \tau \frac{\partial \gamma}{\partial t} = \frac{\partial \phi}{\partial t} - \tau \frac{\partial \gamma}{\partial t} + s \frac{\partial T}{\partial t} + T \frac{\partial s}{\partial t} \quad ,$$

which can be rewritten by use of the above expression for $\delta\phi$ as

$$-\frac{\partial q}{\partial y} = T \frac{\partial s}{\partial t} - \tau \frac{\partial \eta}{\partial t} + \underline{\mu} \cdot \frac{\partial \underline{\Theta}}{\partial t} \tag{14}$$

By regarding s and all other state parameters as functions of γ, η, T and $\underline{\Theta}$, and then using Maxwell relations and denoting by c the specific heat at constant γ, η, and $\underline{\Theta}$, one has

$$\begin{aligned} \partial s/\partial t &= (\partial s/\partial \gamma)\partial\gamma/\partial t + (\partial s/\partial \eta)\partial\eta/\partial t + (\partial s/\partial T)\partial T/\partial t \\ &\quad + (\partial s/\partial \underline{\Theta}) \cdot \partial\underline{\Theta}/\partial t \qquad (15) \\ &= -(\partial\tau/\partial T)\ \partial(\gamma-\eta)/\partial t + (c/T)\partial T/\partial t - (\partial\underline{\mu}/\partial T) \cdot \partial\underline{\Theta}/\partial t \end{aligned}$$

Thus, with a further rearrangement of terms, the energy Eq. (14) may be written as

$$-T \frac{\partial}{\partial y} \frac{q-\underline{\mu}\cdot\underline{J}}{T} = c \frac{\partial T}{\partial t} - T \frac{\partial \tau}{\partial T} \frac{\partial(\gamma-\eta)}{\partial t} - T \frac{\partial \underline{\mu}}{\partial T} \cdot \frac{\partial \underline{\Theta}}{\partial t} - TZ \tag{16}$$

where

$$Z = [\tau \frac{\partial \eta}{\partial t} - \underline{\mu} \cdot (\frac{\partial \underline{\Theta}}{\partial t} + \frac{\partial \underline{J}}{\partial y}) - (\frac{q - \underline{\mu} \cdot \underline{J}}{T}) \frac{\partial T}{\partial y} - \underline{J} \cdot \frac{\partial \underline{\mu}}{\partial y}]/T \qquad (17)$$

is the total entropy production rate [compare to Eq. (7)].

For simplicity in what follows, it will be assumed that $\tau = G(\gamma - \eta)$, where the shear modulus G is independent of T and $\underline{\Theta}$. This implies that s and $\underline{\mu}$ are dependent only on the variables T and $\underline{\Theta}$ and, further, that the term $\partial\tau/\partial T$ above vanishes.

Although some attention has been given here to development of the energy equation, the subsequent sections are based on an assumption of high enough thermal conductivity that this equation may be disregarded.

Specialization to Isothermal Shear

To examine in the simplest case the possible effects of transport processes involving the Θ's on stability of a layer of material deformed in shear, assume that the boundaries of the layer are held at a constant temperature and that heat conduction is sufficiently fast that T is effectively constant. Further, consider the case in which there is a single state variable Θ, and all deformations are quasi-static (inertia term neglected in momentum equation). Then the system of governing equations is

$$\gamma = \partial u/\partial y \qquad (18)$$

$$\partial\tau/\partial y = 0 \qquad (19)$$

$$\tau = G(\gamma - \eta) \qquad (20)$$

$$\partial\eta/\partial t = f(\tau,\theta) \quad \text{(inelastic strain rate)} \tag{21}$$

$$\partial\theta/\partial t + \partial J/\partial y = g(\tau,\theta) \quad \text{(inelastic generation rate)} \tag{22}$$

$$J = -D\partial\theta/\partial y \tag{23}$$

In the last equation, $D = L\partial\mu/\partial\theta$ and since $L > 0$ by the entropy inequality, one has $D > 0$ if it is assumed (as seems plausible, and as we shall until further notice) that $\partial\mu/\partial\theta > 0$.

Let the upper boundary of the layer be displaced as an arbitrary function of time due either to prescription of a τ (case I) or a u (case II) history at $y = h$. Use the subscript "o" to denote the spatially uniform solution for deformation of the layer under these imposed conditions: $\gamma = \gamma_o(t)$, $\eta = \eta_o(t)$, $\theta = \theta_o(t)$, $\tau = \tau_o(t)$, $u = u_o(y,t) = \gamma_o(t)y$. Thus, if primes denote deviations from this uniform solution e.g., $\gamma = \gamma_o(t) + \gamma'(y,t)$, etc..., then the linearized equations satisfied by the primed quantities are

$$\partial\tau'/\partial y = 0 \quad , \tag{24}$$

$$\tau' = G(\partial u'/\partial y - \eta') \quad , \tag{25}$$

$$\partial\eta'/\partial t = f_{1o}\,\tau' + f_{2o}\,\theta' \quad , \tag{26}$$

$$\partial\theta'/\partial t - D_o\,\partial^2\theta'/\partial y^2 = g_{1o}\,\tau' + g_{2o}\,\theta' \quad . \tag{27}$$

Here

$$\begin{aligned} [f_1,\ g_1] &= \partial[f(\tau,\theta),\ g(\tau,\theta)]/\partial\tau \\ [f_2,\ g_2] &= \partial[f(\tau,\theta),\ g(\tau,\theta)]/\partial\theta \quad . \end{aligned} \tag{28}$$

The boundary conditions to be satisfied in two cases to be considered are for case I, $\tau' = 0$ at $y = 0, h$ and for case II, $u' = 0$ at $y = 0, h$ and (assuming no flux at the layer boundaries) $\partial\theta'/\partial y = 0$ for both cases I and II at $y = 0,h$. When $D_o = 0$ and $G = \infty$, these equations reduce to a system considered by Ruina (1980).

Observe that the stress perturbation must be constant through the layer, $\tau' = \tau'(t)$. Case I and case II are now considered in turn.

Case I: Stress Boundary Conditions in Isothermal Shear

For case I, $\tau' = 0$ at $y = 0, h$ and thus, since τ' is independent of y, $\tau' = 0$ everywhere. The remaining system of equations is

$$\partial\theta'/\partial t - D_o\, \partial^2\theta'/\partial y^2 = g_{2o}\, \theta' \tag{29}$$

$$\partial\eta'/\partial t = f_{2o}\, \theta' \tag{30}$$

$$\partial u'/\partial y = \eta' \tag{31}$$

Consistently with the boundary conditions on θ', one may assume that

$$\theta'(y,t) = \sum_{n=0}^{\infty} \phi_n(t) \cos\,(n\pi y/h) \tag{32}$$

where $\phi_n\,(0)$ are fourier coefficents of some small initial non-uniformity of state, so that

$$d\phi_n(t)/dt = (g_{2o} - n^2\pi^2 D_o/h^2)\, \phi_n(t),\ n=0,1,2,\ldots;$$

$$\phi_n(t) = \phi_n(0)\, \exp\,[\int_0^t (g_{2o} - n^2\pi^2 D_o/h^2)dt],\ n=0,1,2,\ldots \tag{33}$$

Hence, if $g_{2o} < 0$, all modes exhibit decay in time, and the homogeneous deformation state within the layer is stable. On the other hand if $g_{2o} > 0$, the mode n = 0 (independent of y) is unstable and exhibits exponential growth at rate g_{2o}. Higher modes, if any, that correspond to values of n for which

$$g_{2o} > n^2\pi^2 D_o/h^2 \tag{34}$$

also exhibit growth, but at a slower rate. However, it is evident that if $D_o > 0$, modes for sufficiently high n will be stable.

To interpret the stability condition, $g_{2o} < 0$, observe that in the absence of diffusion (which is, indeed, absent from the n = 0 mode since $\partial\theta/\partial y$ vanishes for that mode),

$$\partial\theta'/\partial t = g_{1o}\,\tau' + g_{2o}\,\theta' \tag{35}$$

Thus if there is no perturbation from the basic stress history $\tau_o(t)$, one has $\tau' = 0$ and

$$\partial\theta'/\partial t = g_{2o}\,\theta' \tag{36}$$

This shows that when $g_{2o} < 0$, any disturbance from the homogeneous deformation history tends to decay, whereas when $g_{2o} > 0$ such disturbances grow. The inequality $g_{2o} > n^2\pi^2 D_o/h^2$, on the other hand, shows that for high mode numbers, with their correspondingly higher diffusion, the diffusion of θ nonuniformities lends stability.

One observes that when $D_o = 0$ (i.e., when there is a negligibly small diffusivity), all modes exhibit growth when $g_{2o} > 0$. But when $D_o \neq 0$, only the lowest mode (n = 0) exhibits growth, with progressively more modes joining in the growth as g_{2o} increases.

As a final comment for case I, it is interesting to consider the possibility that beyond a certain θ, the potential μ ceases to increase and, rather, starts to decrease with θ, $\mu'(\theta) < 0$. Thus $D_o = L_o\mu'(\theta_o) < 0$ is negative, and now the inequality leading to instability, rewritten as

$$n^2\pi^2(-D_o)/h^2 > -g_{2o} \quad , \tag{37}$$

is always met for sufficiently large n, and the exponential growth rate of a given mode increases in proportion to n^2. This suggests a rapid localization of deformation.

Case II: Displacement Boundary Conditions in Isothermal Shear

For this case it is convenient to start by averaging all field quantities through the layer, with notation

$$\langle \text{function} \rangle = \frac{1}{h} \int_0^h (\text{function})\, dy \tag{38}$$

Noting that $\tau' = \tau'(t)$ so that $\langle \tau' \rangle = \tau'$, and observing that $u' = 0$ and $J' = -D_o\, \partial\theta'/\partial y = 0$ at $y = 0,h$, the averaged form of Eqs. (25) to (27) is

$$\tau' = -G\langle \eta' \rangle \tag{39}$$

$$d\langle \eta' \rangle/dt = f_{1o}\, \tau' + f_{2o}\langle \theta' \rangle \tag{40}$$

$$d\langle\theta'\rangle/dt = g_{1o}\,\tau' + g_{2o}\langle\theta'\rangle \tag{41}$$

This is a closed system of equations whose stability can be studied. What is interesting in this case is that the condition for overall stability of the layer (in the sense of averaged quantities of the preceding equations being stable) is not coincident with the condition, to be derived subsequently, for local stability.

To investigate overall stability, we substitute for τ' from the first of the previous equations and therefore write

$$\frac{d}{dt}\begin{Bmatrix}\langle\eta'\rangle\\ \langle\theta'\rangle\end{Bmatrix} = [M]\begin{Bmatrix}\langle\eta'\rangle\\ \langle\theta'\rangle\end{Bmatrix} \tag{42}$$

where

$$[M] = \begin{bmatrix} -G\,f_{1o} & f_{2o} \\ -G\,g_{1o} & g_{2o} \end{bmatrix}$$

The overall stability condition is therefore $Re(m) < 0$ where

$$m = \frac{1}{2}(g_{2o}-G\,f_{1o}) + \sqrt{\frac{1}{4}(g_{2o}-G\,f_{1o})^2 - G(g_{1o}f_{2o}-f_{1o}g_{2o})} \tag{43}$$

is, if real, the algebraically greatest eigenvalue of [M] and, if complex, one of the two complex conjugate eigenvalues of [M].

The instability condition $Re(m) > 0$, may therefore be stated as the condition that either

$$\Delta_o < 0 \tag{44a}$$

or that

$$\Delta_o > 0 \text{ and } g_{2o} > G\, f_{1o} \quad , \tag{44b}$$

where

$$\Delta_o = g_{1o}f_{2o} - f_{1o}g_{2o} \quad . \tag{45}$$

To interpret these conditions, it is convenient again to consider the form taken by the constitutive laws in the absence of diffusion:

$$d\eta'/dt = f_{1o}\,\tau' + f_{2o}\,\theta' \quad , \tag{46}$$

$$d\theta'/dt = g_{1o}\,\tau' + g_{2o}\,\theta' \quad . \tag{47}$$

These are usefully rearranged to the forms

$$\tau' = (d\eta'/dt)/f_{1o} - f_{2o}\theta'/f_{1o} \quad , \tag{48}$$

$$d\theta'/dt = g_{1o}(d\eta'dt)/f_{1o} - \Delta_o\theta'/f_{1o} \quad , \tag{49}$$

the first of which may be re-expressed as

$$\tau' = -g_{2o}(d\eta'/dt)/\Delta_o + f_{2o}(d\theta'/dt)/\Delta_o \quad . \tag{50}$$

Thus, if in the non-diffusive circumstances considered any one of the set

$$\tau, \dot{\eta}\ (=d\eta/dt),\ \theta,\ \dot{\theta}\ (=d\theta/dt)$$

is regarded as a function of any two of the other, we see that

$$1/f_1 = (\partial\tau/\partial\dot{\eta})|_{\theta=\text{const.}} \quad , \tag{51}$$

$$\Delta/f_1 = -(\partial\dot{\theta}/\partial\theta)|_{\dot{\eta}=\text{const.}} \quad , \tag{52}$$

$$g_2/\Delta = -(\partial\tau/\partial\dot{\eta})|_{\dot{\theta}=\text{const.}} \quad , \tag{53}$$

$$g_2 = (\partial\dot{\theta}/\partial\theta)|_{\tau=\text{const.}} \quad . \tag{54}$$

Evidently, Eq. (51) shows that $1/f_1$ is an incremental viscosity at constant state, and it seems reasonable to assume that this is generally positive, $f_1 > 0$. The other parameters Δ and g_2 are unlikely to be universally of one sign, although $\Delta > 0$ is plausible in the following sense: Suppose that for given $\dot{\eta}$, Θ tends to evolve towards a "steady state" value $\Theta_{ss}(\dot{\eta})$, so that $\dot{\Theta} = 0$ when $\Theta = \Theta_{ss}(\dot{\eta})$ and that $\dot{\Theta}$ decreases (increases) monotonically as Θ increases (decreases) from $\Theta_{ss}(\dot{\eta})$. In this case Eq. (52) shows that $\Delta/f_1 > 0$, so that $\Delta > 0$. Finally, if the partial derivative in Eq. (53) is evaluated for $\dot{\Theta} = 0$, it is equal to $-d\tau_{ss}(\dot{\eta})/d\dot{\eta}$, where τ_{ss} is the value of τ at a given $\dot{\eta}$ and at $\Theta = \Theta_{ss}(\dot{\eta})$. Thus, $g_2 < 0$ if $d\tau_{ss}(\dot{\eta})/d\dot{\eta} > 0$, and conversely.

The significance of the quantity denoted by g_2/Δ above, i.e., by $-(\partial\tau/\partial\dot{\eta})|_{\dot{\Theta} = \text{const.}}$, was first discovered and commented upon by Ruina (1980), in an analysis paralleling the present discussion but neglecting possible diffusion effects. One observes, also following Ruina, that so long as $\Delta_o > 0$, the mode of instability exhibited by the overall quantities is one of flutter type, i.e., oscillations of growing amplitude. This is because the eigenvalue m is pure imaginary at the critical condition $g_{2o} = G\, f_{1o}$ that results when $\Delta_o > 0$ [Eq. (44b)]. A consequence of an instability of this type is that a finite amplitude periodic solution for perturbations of the average quantities in the layer generally exists in a one-sided neighborhood of the critical point, a solution which may be stable (limit cycle) or unstable according to the side of the critical point

on which it occurs. (See theory of the Hopf bifurcation as discussed, e.g., by Howard, 1979).

Now, to consider stability based on local (versus overall, or average) field values, we may write

$$\theta' = \langle\theta'\rangle + \sum_{n=1}^{\infty} \phi_n(t) \cos(n\pi y/h) \qquad (55)$$

$$(\text{i.e., } \phi_o(t) = \langle\theta'\rangle) \quad .$$

In view of the equations satisfied by the average quantities [Eqs. (39) to (41)], the system of Eqs. (25) to (27) then leads to

$$\partial\eta'/\partial t - d\langle\eta'\rangle/dt = f_{2o}(\theta - \langle\theta'\rangle) \quad , \qquad (56)$$

$$\partial u'/\partial y = \eta' - \langle\eta'\rangle \qquad (57)$$

$$\partial\theta'/\partial t - d\langle\theta'\rangle/dt - D_o\, \partial^2\theta'/\partial y^2 = g_{2o}(\theta - \langle\theta'\rangle) \qquad (58)$$

The first two equations can be integrated directly to show that

$$\eta' = \langle\eta'\rangle + \sum_{n=1}^{\infty} \left(\beta_n + \int_0^t f_{2o}\phi_n dt\right) \cos(n\pi y/h) \quad , \qquad (59)$$

$$u' = \sum_{n=1}^{\infty} (h/n\pi) \left(\beta_n + \int_0^t f_{2o}\phi_n dt\right) \sin(n\pi y/h) \quad , \qquad (60)$$

where the constants β_1, β_2, ... are Fourier components for $n > 1$ of the initial non-uniformity of plastic strain, and the last equation requires that

$$d\phi_n/dt = (g_{2o} - n^2\pi^2 D_o/h^2)\, \phi_n, \quad n=1,2,\ldots,$$

and hence that

$$\phi_n(t) = \phi_n(0) \exp\left[\int_0^t (g_{2o} - n^2\pi^2 D_o/h^2)dt\right], \quad n=1,2,... \qquad (61)$$

This solution for ϕ_n is the same as given earlier for case I, of stress boundary conditions, except that in case I it applies for n = 0 also, whereas in the present case it applies only for $n \geq 1$. Hence, assuming that $\partial\mu/\partial\theta > 0$, so that $D_o > 0$, the condition for local instability is

$$g_{2o} < \pi^2 D_o/h^2 \qquad (62)$$

(mode n = 1 is most critical). [The case $\partial\mu/\partial\theta < 0$ again leads to instability at any g_{2o} for sufficiently large mode number, with rate of growth increasing with n^2].

If $D_o = 0$, the local instability condition of Eq. (62), then reducing to $g_{2o} > 0$, will be met before the overall instability condition [namely, that $g_{2o} > G\, f_{1o}$, as in Eq. (44b)] at least if one assumes that $\Delta_o > 0$ and that g_{2o} increases from negative to positive values during the history of deformation. On the other hand, if the diffusivity D_o is sufficiently large and positive, the situation will be reversed and the overall instability will occur before local instability. The possibility of such a reversal of order is greater for thinner layers, since the local instability condition of Eq. (62) involves $1/h^2$. Both conditions are met simultaneously (again, assuming $\Delta_o > 0$) if $h^2 = \pi^2 D_o/G\, f_{1o}$; this results from equating the critical conditions of Eqs. (44b) and (62).

ACKNOWLEDGEMENT

The work was done under support of the DARPA Materials Research Council, Contract #MDA903-80-C-0505 with the University of Michigan. D. C. Drucker, J. W. Hutchinson and A. Ruina are thanked for helpful discussions.

References

Howard, L. N., in Lecture Notes in Applied Mathematics, Vol. 17 (Utah Symp.), Amer. Math Soc., 1979.

Perzyna, P., presentatuion at 15th Int. Congr. Theoretical and Appl. Mech., Toronto, 1980 (Proceedings published by North-Holland, editors F. P. J. Rimrott and B. Tabarrok, 1980).

Ruina, A. L., Ph.D. thesis, Brown University, 1980.

DARPA SOLID LUBRICANTS PROGRAM

J. L. Margrave

The DARPA/AFWAL solid lubricants program was reviewed for the Materials Research Council by Michael N. Gardos of Hughes Aircraft.[1] Current efforts are directed to the development of (1) small gyro bearings in which selected solid lubricants, hard coats for balls and races and various design parameters can be tested and, (2) a cruise missile bearing for operation at 600°F. The Ga/In/WSe_2 composite developed by Westinghouse and various doped transition metal dichalcogenides (MoS_2, $GeTaS_2$, $CuNbS_2$, $AgNbS_2$, $CuNbSe_2$ and $AgNbSe_2$) are being evaluated. TiC, CrC-TiC and TiN hard coats have been successfully prepared on steel, Co-bonded WC and Ni/Mo-bonded TiC balls by CVD at 1000°C. TiN has also been reaction sputtered at ~500°C.

Experimental testing at elevated temperatures with a ball-on-disc/inner race apparatus and a new concentrated contact traction apparatus is providing useful performance information. Wear equations are being evaluated for various self-lubricated bearing systems.

Future plans include extended tests of CVD hardcoats, sputtered MoS_2, mixed dichalcogenides and the Westinghouse compact in gyro bearings. Efforts to identify the vulnerable phase in the Westinghouse material will be continued and solid lubricants/hardcoats for the high-temperature cruise missile bearing will be selected. The 3-D weave carbon fiber materials

and parameters relating to their uses in self-lubricating bearing systems are under examination. The fluorocarbon solid lubricant, (CFX), has not been evaluated because of the difficulty of applying it in the form of a film or getting adherent layers by CVD or sputtering techniques.

ACKNOWLEDGEMENT

This paper was written under the auspices of the DARPA Materials Research Council, Contract #MDA903-80-C-0505 with the University of Michigan.

REFERENCES

1. "Solid Lubricated Rolling Element Bearings, "Report No. FR81-76-661, M.N. Gardos, Hughes Aircraft Co., Culver City, California, March 15, 1981.

NEW METHODS FOR PREPARATION OF CFX

J. L. Margrave

The solid fluorocarbon, CFX, has well-known uses as a solid lubricant and as an electrochemical material in Li/CFX batteries.[1] Its wide utilization has been limited by the fact that only one practical synthesis has been devised:

$$2\ C(\text{graphite}) + F_2(\text{gas}) = 2\ CFX(\text{solid})$$

Elemental fluorine is expensive and only produced electrochemically. In addition, the CFX (solid) is always formed as a fine powder which has little tendency to cohere to itself or adhere to surfaces. A pressed CFX tablet is friable and can be crushed between the fingers. A surface layer of CFX on a graphite block can be scratched off with a fingernail. The material does not melt or sublime at high temperatures but disproportionates to CF_4 and amorphous carbon.

Techniques for producing CFX by using HF or some easily derived fluoride instead of F_2 are badly needed. Three possible reactions which could produce CFX economically are:

I. $C(\text{graphite}) + HF(\text{gas}) + 1/2\ Cl_2(\text{gas}) = CF(\text{solid}) + HCl(\text{gas})$

$$\begin{aligned} \Delta H_{500} &= -5000 \text{ cal mole}^{-1} \\ \Delta S_{500} &= -23 \text{ cal mole}^{-1} \text{ deg}^{-1} \\ \Delta G_{500} &= +6500 \text{ cal mole}^{-1} \\ \log K_{500} &= -2.8 \end{aligned} \qquad (1)$$

II. $C(graphite) + HF(gas) + Cl(gas)^* = CF(solid) + HCl(gas)^*$

$$\Delta H_{500} = -34{,}000 \text{ cal mole}^{-1}$$
$$\Delta S_{500} = -25 \text{ cal mole}^{-1} \text{ deg}^{-1}$$
$$\Delta G_{500} = -21{,}500 \text{ cal mole}^{-1} \quad (2)$$
$$\log K = 10^{+9.4}$$

*(Use UV light to produce Cl-Atoms)

III. $C(Solid) + CuF(solid) = CF(solid) + Cu(solid)$

$$\Delta H_{500} \approx -2000 \text{ cal mole}^{-1}$$
$$\Delta S_{500} \approx 0$$
$$\Delta G_{500} = -2000 \text{ cal mole}^{-1} \quad (3)$$
$$\log K_{500} = 10^{+0.87}$$

Finally, there is interest in techniques for producing adherent CFX films on carbon shapes or on metal objects. RF resistive heating to provide a hot surface for chemical vapor deposition of CFX should be possible for these reactions:

(a) $CH_4 + SF_6 \overset{?}{\rightarrow} CFX + HF + S_x$

(b) $CH_4 + NF_3 \overset{?}{\rightarrow} CFX + HF + N_2$

(c) $C_2H_2 + F_2 \overset{?}{\rightarrow} CFX + HF$

(d) $F_3\text{-}\underset{H}{\overset{H}{C}}\text{-}\underset{H}{\overset{H}{C}}\text{-}C\text{-}CF_3 \overset{?}{\rightarrow} 2\ CF + 4\ HF + 2C$

(e) $F_3\text{-}\underset{H}{\overset{H}{C}}\text{-}C{=}C\text{-}CF_3 \overset{?}{\rightarrow} 4\ CF + 2\ HF$

Exothermic and spontaneous reactions which could yield CFX deposits if carefully controlled include:

(a) $C + NF_3 \overset{?}{\rightarrow} CFX + N_2$

(b) $B_4C + F_2 \overset{?}{\rightarrow} CFX + BF_3$

(c) $SiC + F_2 \overset{?}{\rightarrow} CFX + SiF_x$

(d) $TiC + F_2 \overset{?}{\rightarrow} CFX + TiF_x$

In all these cases, a runaway exothermic reaction will produce CF_4 instead of CFX.

ACKNOWLEDGEMENT

This paper was written under the auspices of the DARPA Materials Research Council, Contract #MDA903-80-C-0505 with the University of Michigan.

REFERENCES

1. J. L. Margrave & P. Kamarchik, Accts. Chem. Res. 11, 296 (1978).

HEAT CAPACITIES OF LIQUID METALS ABOVE 1500 K

J. L. Margrave

Experimental heat capacity measurements for liquid metals by both the levitation and exploding wire techniques have shown that Cp values in the range 2000-5000°K may approach 10R cal $mole^{-1}$ deg^{-1} and thus, significantly enhance the importance of liquid metals as heat sinks during nuclear excursions, laser irradiations or high current pulses.[1,2] The excess heat capacities can be related to other thermophysical properties through the equation

$$C_p - C_v = C_{electronic} + \alpha^2 VTB_T$$

where $C_{electronic} = \gamma T$; α = the thermal expansion coefficient; V = the molar volume; and B_T = the bulk modulus. $C_v \approx 3R$ for all liquid metals at T > 1500 K. Thus,

$$C_p(T) = 3R + \gamma T + \alpha^2 VTB_T$$

and often can be described by a general equation

$$C_p^l = a + bT + cT^2 + \ldots$$

There seems to be little experimental support for the suggestion by Hoch et al[3] that Cp's for liquid metals fit an equation like

$$C_p^l = a + bT + cT^{-2}$$

which describes a few low-melting metals over temperature ranges of a few hundred degrees.

Unfortunately, there is a paucity of experimental data for α, V or B_T at high temperatures for solids and only a few investigators have studied liquid metals. For example, there are Cartesian Diver density determinations for a few liquid metals by Kirschenbaum, Cahill and Grosse.[4] There are a few density measurements for liquid metals by suspended drop techniques;[5] and a few photographic density determinations on levitated liquid metal drops.[6] In most cases the measurements are within a few hundred degrees of the melting points. Gathers, Shaner, et al.[2] have used the exploding wire technique supplemented by fast photographic observations and fast multicolor optical pyrometry to obtain values for liquid metal densities and for liquid metal expansion coefficients over the range 500-5000°K for V, Fe, Nb, Mo, Ta, Ir, W, Pb and U.

There seem to be few experimental determinations of bulk moduli over ranges of temperatures, although one has the intuitive feeling that they should decrease as temperature increases. Again, the exploding wire studies[2] which yield equations of state as well as other thermodynamic properties offer a unique source of experimental values for B_T and for α_T in the 2000-7000°K range.

The electronic contributions to Cp are expected to be given by γT where γ is the well-known coefficient derivable from low-temperature Cp-measurements. γT-contributions at low temperatures may be enhanced by electon-phonon interactions but this should not be important in high temperature liquids. Typical

values for γ from low temperature studies are in the range 10^{-3} to 10^{-4} cal mol^{-1} K^{-2}.

By collecting these ideas and utilizing both levitation and exploding wire data for liquid transition metals, one can estimate the Cp-values listed in Table I.

Since Cp (5000) falls in the range 8R to 10R for many liquid metals, one can more confidently assign heat loads and predict structure survival during extreme temperature excursions caused by nuclear, laser or particle irradiation.

ACKNOWLEDGEMENT

This paper was written under the auspices of the DARPA Materials Research Council, Contract #MDA903-80-C-0505 with the University of Michigan.

TABLE I

CP's for Liquid Transition Metals

Cp in Cal $mole^{-1}$ deg^{-1}

Element	MP K	Near MP	3000 K	4000 K	5000 K	HT Avg.
Sc	1812	(10)	(12)	(14)	(16)	
Ti	1933	11.1-L	(14)	(17)	(22)	
V	2190	11.2-L;11.3-E	14.6-E	16.6-E	(22)	(15.8)-E
Cr	2176	(9.4)	(12)	(14)	(16)	
Mn	1517	(11)	(13)	(15)	(17)	
Fe	1809	11.1-L	(14)	(17)	(22)	
Co	1768	12.0-L	(15)	(18)	(23)	
Ni	1725	9.4-L	(13)	(15)	(17)	
Cu	1357	8.3-L	(12)			
Zn	693	7.5-D				
Y	1803	10.3-D	(12)	(14)	(16)	
Zr	2125	9.7-L	15.3-L	(17)	(20)	
Nb	2740	9.7-L	(10)	(13)	(16)	(13.6)-E
Mo	2892	9.0-L	(12)	(16)	(20)	(17.0)-E
Tc		(9)	(10)	(12)	(15)	
Ru	2700	(8.5)	(10)	(13)	(17)	
Rh	2239	(10)	(12)	(15)	(18)	
Pd	1823	9.9-L	(12)	(15)	(18)	
Ag	1234	(7.3)	(10)			
Cd	594	7.1-D				

Cp in Cal $mole^{-1}$ deg^{-1}

Element	MP K	Near MP	3000 K	4000 K	5000 K	HT Avg.
La	1193	(8.3)	(11)	(13)	(15)	
Hf	2500	(9.5)	(12)	(15)	(18)	
Ta	3269	(10.5)		(13)	(18)	(16.6)-E
W	3680	(10)		(13)	(16)	(13.4)-E
Re	3453	(10.8)		(13)	(16)	
Os	3300	(8.6)		(12)	(15)	
Ir	2727	7.2-E	(8)	10.1-E	11.1-E	(11.4)-E
Pt	2043	9.3-L	(11)	(13)	(15)	
Au	1336	9.0-D	(9.0)	(10.0)		
Hg	234	6.8-D				
Th	1968	(12)	(16)	(18)	(22)	
U	1405	11.3-L;11.5-E	16.2-E	17.5-E	23.1-E	(11.8)-E

L = Levitation Measurements
E = Exploding Wire Measurements
D = Drop Calorimetry Measurements
( )= Estimated Values

REFERENCES

1. (a) J. L. Margrave, High Temp-High Press. 2, 583-6 (1970).

   (b) J. A. Treverton and J. L. Margrave, Proc. 5th Symp. Thermophys. Prop., New York, 1970, pp. 489-494.

   (c) A. K. Chaudhuri, D. W. Bonnell, L. A. Ford and J. L. Margrave, High Temp. Sci. 3, 203 (1970).

   (d) B. Ya. Chekovskoi and A. E. Sheindlin, High Temp. Sci. 4, 478-85 (1972).

   (e) V. Ya. Chekhovskoi, in "Methods of Thermophysical Measurements," Ed. by K. D. Maglic, to be published, 1982.

   (f) J. L. Margrave, Symp. on Thermophysical Properties, Washington, D.C., June, 1981.

2. (a) G. R. Gathers, J. W. Shaner and D. A. Young, Phys. Rev. Lett. 33, 70 (1974).

   (b) J. W. Shaner, C. R. Gathersland and C. Minichino, High Temp-High Press. 8, 425 (1976).

   (c) G. R. Gathers, J. W. Shaner and R. L. Brier, Rev. Sci. Instr. 47, 471 (1976).

   (d) J. W. Shaner, G. R. Gathers and C. Minichino, UCRL-79344, Lawrence Livermore Laboratory, 1977.

   (e) J. W. Shaner and G. R. Gathers, UCRL-79586, Lawrence Livermore Laboratory, 1977.

3. (a) M. Hoch, Rev. Int. Hautes Temp et Refract. 12, 8-11 (1975).

   (b) M. Hoch and T. Vernardkis, ibid. 13, 75-82 (1976).

   (c) M. Hoch and T. Vernardkis, High Temp-High Press. 8, 241-6 (1976).

   (d) M. Hoch, Symp. on Thermophysical Properties, Washington, D.C., June, 1981.

4. A. Kirschembaum, J. Cahill and A. V. Grosse, J. Inorg. Nucl. Chem. 22, 33 (1961).

5. Yu. N. Ivashchenko and P. S. Martsenyuk, High Temp. (USSR, Translation) 11, 1146 (1973); Teplofiz. Vys. Temp. 11, 1255 (1973).

6. (a) T. Saito, Y. Shiraishi and Y. Sakuma, Trans. Iron Steel Inst. Japan 9, 118 (1969).

   (b) T. Saito and Y. Sakuma, Nippon Kinzoku Gakkai 31, 1140, Oct., 1967.

7. (a) C. Kittel, "Introduction to Solid State Physics," Third Edition, (J. Wiley, New York), 1965, pp. 209-214.

   (b) R. Hultgren, R. L. Orr, P. D. Anderson and K. K. Kelley, "Thermodynamic Properties of Metals and Alloys," J. Wiley, New York), 1963.

8. JANAF Thermochemical Tables, D. R. Stull and H. Prophet, Editors, U.S. Govt. Printing Office, Washington, D.C., 1971.

NEW REACTIONS OF ASTROCHEMICAL INTEREST

J. W. Kauffman, R. H. Hauge, M. M. Konarski,
W. E. Billups and J. L. Margrave

As radio astronomers have surveyed the various emissions and absorptions of electromagnetic radiation from space with more sensitivity and resolution over wider ranges of wave length, it has become clear that many chemical processes are proceeding in that mix of atoms, ions, electrons and molecules. The ultraviolet radiation from the sun provides an initiating process which keeps a supply of high energy species, both neutral and charged, available for reaction. We have discovered several new chemical processes in the laboratory which, if duplicated in the space environment could provide it with a potential for chemical systhesis almost as rich as on earth, including good yields of complex molecules under appropriate conditions.[1] Other recent papers have discussed ion-molecule type reactions and shown that such processes can account for the presence of simple organic molecules.[2,3] Residual organic species in meteorite samples have been reported by many investigators.

In space one has fairly low effective translational temperatures, various sorts of radiation environments and very low density gases, with occasional "dust" particles. Since these "dust" particles are being exposed to ultraviolet or x-radiation under relatively high vacuum conditions, it seems probable that some of them are in fact metallic in nature and, of course, there is a wide distribution of sizes from a few

hundred or thousand Angstroms in dimension up to a few microns, and even a few macroscopic chunks. Such metallic clusters would represent ideal spots for the same kinds of catalytic chemistry which have been observed in our laboratory matrix isolation experiments. A close encounter of a water molecule or a methanol molecule or an ammonia molecule with a small metallic cluster (M, M_2,...M_x) should result in the formation of a neutral adduct, stable at low temperatures. When this adduct is activated by an ultraviolet photon, the oxidative insertion process shown below occurs:

$$M_x + H_2O = (M_x{:}OH_2) = HM_xOH$$

Some metals (Al and Si, for example) react spontaneously to form the insertion product. Obviously, if there is excess metal one might get products like HM_xOM_xH, e.g., if the clusters break off in dimeric or trimeric units, one might find species like HM_2OM_2H or HM_3OM_3H. Several of these types of molecules have been observed under laboratory conditions in matrix isolation studies and infrared absorption frequencies, isotope shift data, etc., have been recorded for identification purposes.

Specifically, we have observed in the laboratory a large number of spontaneous low temperature interactions of metal atoms with water, with ammonia, with methane, with CO, with alcohols, with ethers and with a variety of other Lewis bases.[4,5,6] These processes not only provide ways for utilizing the low concentration of metal atoms in space for catalytic purposes but also can provide possibilities for creating a great

variety of organic and inorganic materials, including alkenes, alkynes and long chain saturated hydrocarbons, as well as oxides, hydroxides, amines, etc. The presence of metal atoms in space environments is now well-documented and the chemistry which it makes possible is extremely extensive. Our work establishes the generality of metal atom interactions with Lewis bases across the Periodic Table; Fig. 1 shows in a general way some interactions which have been observed between metal atoms or diatomic molecules of the metal and water molecules, either themselves monomeric or dimeric, depending upon pressure and concentration. Some metals form the adduct at 10K but undergo further reaction on annealing or with UV-irradiation. Certain elements are especially active and undergo unique reactions. The very active metals--aluminum, scandium, titanium, vanadium, etc., undergo spontaneous reactions with water even at very low temperatures, 10K, and form hydrido-hydroxides or even oxides.

As one forms such species there are several kinds of questions. (1) How general is the phenomenon? (2) How stable are the adducts and insertion products? (3) What further chemistry can result after adduct formation and/or oxidative insertion has occurred?

To answer these questions we have concentrated our efforts on certain metal atoms and studied their reactions with a variety of Lewis bases. For example, iron atoms have been reacted with the isoelectronic sequence CH_4, NH_3, OH_2 and FH as well as with the organo-analogs of water--CH_3OH, CH_3OCH_3,

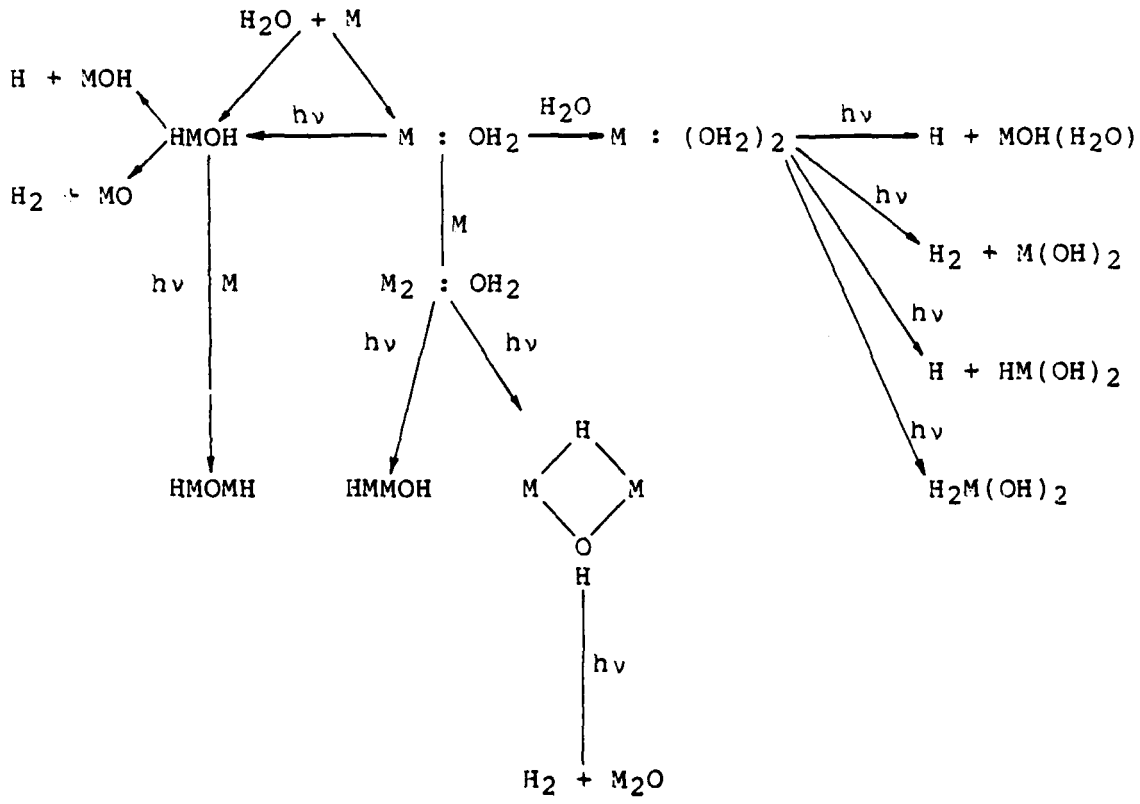

Figure 1. Reactions of metal atoms with water at low temperatures.

$CH_3OC_2H_5$, $C_2H_5OC_2H_5$, etc.[7,8] The results of such studies indicate that iron atoms can be inserted with the aid of an ultraviolet photolysis step into the CH bond, the NH bond, the OH bond and the HF bond to yield the products $HFeCH_3$, $HFeNH_2$, HFeOH, and HFeF, respectively. These are all new molecular species and are capable of undergoing a variety of further chemical reactions. Mn, Co, Ag, Cu, As and Au behave similarly and studies with Si, Ge, Sn and Pb-atoms are in progress.[8] When one reacts iron or certain other transition metals with methanol the insertion product CH_3FeOH and the products CH_3OFeH are both formed. These adducts can be warmed to room temperature and recovered as grayish powders, somewhat pyrophoric and very hydrolytically sensitive. With CH_3OCH_3 and Fe-atoms, one forms CH_3FeOCH_3 after ultraviolet photolysis. This product is recoverable as a grayish crystalline powder and can be hydrolyzed with the formation of appreciable quantities of C_5H_{12}, C_6H_{14}, C_7H_{16}, as well as lighter alkanes, alkenes and alkynes.[7] When calcium, strontium or barium are co-deposited with dimethyl ether one produces adducts which primarily form alkenes and alkynes with a minimum of alkanes on hydrolysis.[6]

It seems clear that a new set of chemical processes which could play an important role in interpreting astrochemical phenomena has been identified through this work. The availability in space of simple reactive species like water, ammonia, methane, CH_3OH, etc., has been demonstrated by various spectroscopic measurements. The existence of metallic clusters, some

in the range of a few hundred to a few thousand square Angstroms in cross section while others are micron size ranges, is also well-documented. The interaction of simple molecules and metallic surfaces which are probably quite clean after degassing in vacuum for long periods along with the ultraviolet radiation, should make formation of the chemical molecules in space which we have described in this work not only straightforward but totally plausible. From such adducts and insertion products one can develop all of the areas of organic and organometallic chemistry, hydrocarbon chemistry, and nitrogen chemistry (including the possibility of forming amines, amides and amino acids) as well as specific ways to create unique chemical reducing agents like metal alkyl hydrides and ultimately, inorganic species like oxides, hydroxides, nitrides, etc.

ACKNOWLEDGEMENT

This paper was written under the auspices of the DARPA Materials Research Council, Contract # MDA903-80-C-0505 with the University of Michigan. The laboratory studies on which the paper is based were done at Rice University, Houston, Texas, with support from the Robert A. Welch Foundation and the National Science Foundation.

REFERENCES

1. (a) 1. "Matrix Isolation IR and EPR Studies of Reaction Intermediates: Lithium Metal Reactions with H_2O, CH_3OH, and NR_3", Proc. Berlin Symp. on Matrix Isolation Spectroscopy, West Berlin, Germany, June 21-24 (1977), J. L. Margrave, R. H. Hauge and P. F. Meier (Abstract in Berichte der Bunsengesellschaft, Physikalische Chemie, 82, 102 (1978)).

   2. "Reactions of Small Hydrocarbons in Fluorine Matrices", Proc. Berlin Symp. on Matrix Isolation Spectroscopy, West Berlin, Germany, June 21-24 (1977), J. L. Margrave, with R. H. Hauge, S. Gransden and J. L. F.Wang. (Abstract in Berichte der Bunsengesellschaft, Physikalische Chemie, 82, 104 (1978)).

   (b) "Electron Spin Resonance Studies of the Reaction of Lithium Atoms With Lewis Bases in Argon Matrices: Formation of Reactive Intermediates with Water and Ammonia", J. Am. Chem. Soc., 100, 2108 (1978), J. L. Margrave, P. F. Meier and R. H. Hauge.

   (c) C. N. Krishnan, Ph.D. Thesis, Rice University, 1972.

   (d) P. F. Meier, Ph.D. Thesis, Rice University, 1977.

   (e) M. M. Konarski, Ph.D. Thesis, Rice University, August, 1980.

   (f) J. W. Kauffman, Ph.D. Thesis, Rice University, June, 1981.

   (g) M. Douglas, Ph.D. Thesis, Rice University, in preparation.

2. "Laboratory Studies of Ion-Neutral Reactions in Interstellar Regions: Gas Phase Equilibria Between NCN and NH_3 in Dense Clouds," Astrophys. J. 208, 237-244 (1976), W. T. Huntress, Jr. and V. G. Anicich.

3. (a) "An Ioncyclotron Resonance Study of Reactions of Some Atomic and Simple Polyatomic Ions with Water," Chem. Phys. Lett. 59, 84-86 (1978), Z. Karpas, V. S. Anicich and W. T. Huntress, Jr.

   (b) "Interstellar Synthesis of the Cyano-Polyynes and Related Molecules," Astrophys. J. 233, 102-108 (1979), G. F. Mitchell, W. T. Huntress, Jr. and S. S. Prasad.

4. "Infrared Matrix-Isolation Studies of the Interactions and Reactions of Group IIIA Metal Atoms with Water:, J. Am. Chem. Soc., 102, 19, 6005-6011 (1980), J. L. Margrave, R. H. Hauge and J. W. Kauffman.

5. "Carbon-Carbon Bond Formation in the Reaction of Calcium Atoms with Ethers", J. Am. Chem. Soc., 102, 3649 (1980), J. L. Margrave, W. E. Billups, M. M. Konarski and R. H. Hauge.

6. "Activation of Dimethyl Ether with Transition Metal Atoms", Tetrahedron Letters, 21, 3861-3864 (1980), J. L. Margrave, W. E. Billups, M. M. Konarski and R. H. Hauge.

7. "Activation of Methane with Photo-excited Metal Atoms", J. Am. Chem. Soc., 102, 7393 (1980), J. L. Margrave, W. E. Billups, M. M. Konarski and R. H. Hauge.

8. J. P. Bell, Work in Progress, Rice University, 1981.

PYROELECTRIC COMPOSITES FOR LOW TEMPERATURE APPLICATIONS

L. E. Cross

Initial work has been concentrated on the antimony sulpho-iodide (SbSI) family, using Br substitution for I and As substitution for Sb to reduce the ferroelectric curie point. Composites on the scale suitable for pyroelectric point and image detectors are being fabricated by directed recrystallization of SbSI glasses in very high thermal gradients. The glass ceramics show a good separation in the maxima of pyroelectric coefficient ρ_3 and permitivity ε_3 so that the figure of merit ρ/ε can be optimized.

Future work will be extended to include compositions in the potassium ferrocyanide and the colemanite families of ferroelectric crystals. Composites in the Fresnoite and barium titanium germonate families which show increasing ρ down to 80°K will be characterized in the 4.2 to 80°K temperature range.